STUDIES ON CARBON DIOXIDE FIXATION CATALYZED BY RUTHENIUM COMPLEXES

(ルテニウム錯体触媒による二酸化炭素固定反応に関する研究)

HITOSHI ISHIDA

OSAKA UNIVERSITY

1989

Preface

The work of this thesis were mainly carried out under the guidance of Professor Toshio Tanaka at Department of Applied Chemistry, Faculty of Engineering, Osaka University; a part of the work at Department of Applied Chemistry, Faculty of Engineering, Kumamoto University.

Hitoshi Ishida

Department of Applied Chemistry,
Faculty of Engineering,
Kumamoto University,
Kurokami, Kumamoto,
Kumamoto 860,
Japan

November, 1989.

List of Publications

(1) "The Electrochemical Reduction of CO_2 Catalyzed by Ruthenium Carbonyl Complexes"
Hitoshi Ishida, Koji Tanaka, and Toshio Tanaka
Chemistry Letters, **1985**, 405.

(2) "Isolation of Intermediates in the Water Gas Shift Reactions Catalyzed by $[Ru(bpy)_2(CO)Cl]^+$ and $[Ru(bpy)_2(CO)_2]^{2+}$"
Hitoshi Ishida, Koji Tanaka, Masaru Morimoto, and Toshio Tanaka
Organometallics, **1986**, 5, 724.

(3) "Electrochemical CO_2 Reduction Catalyzed by $[Ru(bpy)_2(CO)_2]^{2+}$ and $[Ru(bpy)_2(CO)Cl]^+$. The Effect of pH on the Formation of CO and $HCOO^-$"
Hitoshi Ishida, Koji Tanaka, and Toshio Tanaka
Organometallics, **1987**, 6, 181.

(4) "Selective Formation of $HCOO^-$ in the Electrochemical CO_2 Reduction Catalysed by $[Ru(bpy)_2(CO)_2]^{2+}$ (bpy = 2,2'-bipyridine)"
Hitoshi Ishida, Hiroaki Tanaka, Koji Tanaka, and Toshio Tanaka
J. Chem. Soc., Chem. Commun., **1987**, 131.

(5) "Electrochemical Reaction of CO_2 with Me_2NH to Afford N,N-Dimethylformamide, Catalyzed by $[Ru(bpy)_2(CO)_2]^{2+}$ (bpy = 2,2'-

bipyridine)"
Hitoshi Ishida, Hiroaki Tanaka, Koji Tanaka, and Toshio Tanaka
Chemistry Letters, **1987**, 597.

(6) "Photoreduction of CO_2 in the $[Ru(bpy)_2(CO)_2]^{2+}$ / $[Ru(bpy)_3]^{2+}$ or $[Ru(phen)_3]^{2+}$ / Triethanolamine / N,N-Dimethylformamide System"
Hitoshi Ishida, Koji Tanaka, and Toshio Tanaka
Chemistry Letters, **1987**, 1035.

(7) "Photochemical CO_2 Reduction by an NADH Model Compound in the presence of $[Ru(bpy)_3]^{2+}$ and $[Ru(bpy)_2(CO)_2]^{2+}$ (bpy = 2,2'-bipyridine) in H_2O / DMF"
Hitoshi Ishida, Koji Tanaka, and Toshio Tanaka
Chemistry Letters, **1988**, 339.

(8) "Photochemical CO_2 Reduction Catalyzed by $[Ru(bpy)_2(CO)_2]^{2+}$ Using Triethanolamine and 1-Benzyl-1,4-dihydronicotinamide as an Electron Donor"
Hitoshi Ishida, Tohru Terada, Koji Tanaka, and Toshio Tanaka
Inorg. Chem. in press.

(9) "Ligand Effects of the Ruthenium 2,2'-Bipyridine and 1,10-Phenanthroline Complexes on Electrochemical CO_2 Reductions"
Hitoshi Ishida, Katsuyuki Fujiki, Koji Tanaka, Tohru Terada,

Toshio Tanaka, and Katsutoshi Ohkubo
J. Chem. Soc., Dalton Trans. in contribution.

(10) "N,N-dimethylformamide Generation from Electrochemical CO_2 Reduction Catalyzed by $[Ru(bpy)_2(CO)_2]^{2+}$"
Hitoshi Ishida, Tomoyuki Ohba, Katsuyuki Fujiki, Hiroaki Tanaka, Koji Tanaka, Toshio Tanaka, and Katsutoshi Ohkubo
in preparation.

List of Supplementary Papers

(1) "Highly Efficient Enantioselectivite Hydrolysis of Short Chain N-Acetyl Amino Acid p-Nitrophenyl Esters Catalysed by Esterase Models"
Katsutoshi Ohkubo, Masahiko Kawata, Takashi Orito, and Hitoshi Ishida
J. Chem. Soc., Perkin Trans. 1, **1989**, 666.

(2) "Stereoselective Dioxygenation of a Racemic Tryptophan Derivative Catalysed by Chiral Manganese Porphyrins"
Katsutoshi Ohkubo, Takashi Sagawa, Mutsuo Kuwata, Tsuguru Hata, and Hitoshi Ishida
J. Chem. Soc., Chem. Commun., **1989**, 352.

(3) "Stereoselective Dioxygenation of a Tryptophan Derivative

Catalyzed by a Manganese Porphyrin Included in Bovine Serum Albumin"
Katsutoshi Ohkubo, Hitoshi Ishida, and Takashi Sagawa
J. Mol. Cat., **1989**, 53, L5.

(4) "Photoinduced Enantioselective and Catalytic Reduction of $Co(acac)_3$ with a Chiral Ruthenium Photosensitizer"
Katsutoshi Ohkubo, Taisuke Hamada, Tohru Inaoka, and Hitoshi Ishida, Inorg. Chem., **1989**, 28, 2021.

(5) "Micellar Effects on Reduction of Tris(acetylacetonato)-cobalt(III) by 1-Benzyl-1,4-dihydronicotinamide with Ionic Surfactants"
Kohichi Yamashita, Hitoshi Ishida, and Katsutoshi Ohkubo
J. Chem. Soc., Perkin Trans. 2 in press.

(6) "Enantioselective Electron Transfer Reaction Catalyzed by a Novel Photosensitizer, $[Ru(S(-)$ or $R(+)\text{-}PhEt^{*}bpy)_3]^{2+}$"
Katsutoshi Ohkubo, Hitoshi Ishida, Taisuke Hamada, and Tohru Inaoka
Chemistry Letters, **1989**, 1545.

Contents

General Introduction

Almost all the organic compounds on the earth are derived from substances produced by photosynthesis, in which the CO_2 fixation is performed by using electrons obtained from H_2O. Chemists have long dreamed of imitating this reaction in a test tube, because the artificial photosynthesis is expected to solve the problem of shortage of fuel, resources and energy. Especially, the increase of carbon dioxide concentrations in air becomes one of the recent social problems.

Although a number of organic synthesis with carbon dioxide as a starting material have been developed, carbon dioxide has been employed only for industrial use of urea synthesis, and on a small scale, of the Kolbe-Schmitt reaction until now. In laboratories, the reaction between Grignard reagents and carbon dioxide is practically important in the synthesis of carboxylic acid. In the development of organotransition metal chemistry, there have been numerous papers which report the reactions of a transition metal alkyls and hydrides with carbon dioxide to give the corresponding carboxylic acids and formic acid, respectively. However, catalytic fixation of carbon dioxide by transition metal complexes has scarcely been reported.

The objects of this thesis are to search the efficient catalysts for CO_2 reduction, and to clarify catalytic properties and mechanisms of the reaction. Other objects are to convert carbon dioxide to more useful organic molecules, and to develop

photochemical CO_2 reductions as artificial photosyntheses.

Chapter 1 describes the Water Gas Shift (WGS) reaction catalyzed by ruthenium complexes as the reverse reaction of CO_2 reduction, especially, the isolation and properties of reaction intermediates. It is described in chapter 2 that $[Ru(bpy)_2(CO)_2]^{2+}$ and $[Ru(bpy)_2(CO)Cl]^{+}$, which are catalysts for the WGS reactions, catalyze electrochemical CO_2 reductions to afford CO and $HCOO^-$ in aqueous DMF solutions with low and high pH, respectively. In chapter 3, selective $HCOO^-$ formation in the electrochemical CO_2 reductions with organic acids having low pK_a values in anhydrous acetonitrile is discussed. Chapter 4 describes ligand effects of the ruthenium catalysts on the electrochemical CO_2 reduction in connection with the reduction potentials and the equilibrium reactions with OH^-. Chapter 5 describes electrochemical preparation of N,N-dimethylformamide from CO_2 and dimethylamine, catalyzed by $[Ru(bpy)_2(CO)_2]^{2+}$. It is discussed in chapter 6 that photochemical CO_2 reduction has been performed by irradiation of visible light to the CO_2-saturated N,N-dimethylformamide / triethanolamine solutions containing $[Ru(bpy)_3]^{2+}$ and $[Ru(bpy)_2(CO)_2]^{2+}$, giving selective $HCOO^-$ formation. Chapter 7 describes photochemical CO_2 reduction with 1-benzyl-1,4-dihydronicotinamide, a model compound of NADH, which acts as electron donor in the photosynthetic systems.

CHAPTER 1

Water Gas Shift Reaction Catalyzed by Ruthenium Complexes; Mechanism and Isolation of the Reaction Intermediates

1-1 Introduction

The water gas shift (WGS) reaction, in which carbon monoxide is oxidized by water to give carbon dioxide and dihydrogen (eq. 1-1), is the reverse reaction of CO_2 reduction. One possibility

$$CO + H_2O \longrightarrow CO_2 + H_2 \qquad (1\text{-}1)$$

of catalytic CO_2 reduction is to cause the reverse reaction of WGS reaction by using transition metal catalysts. Therefore, the study on catalysts for the WGS reaction is important also for the CO_2 reduction.

Since the homogeneous WGS reaction catalyzed by transition metal complexes was reported in 1977[1], a number of homogeneous WGS reactions under mild conditions have been studied by employing mono- and polynuclear transition metal carbonyl complexes,[2,3] of which ruthenium carbonyl clusters have attracted much attention as active catalysts for the WGS reaction.[4] The WGS reaction catalyzed by transition metal complexes in alkaline media at elevated temperatures has been suggested to involve the

following key steps: (i) a nucleophilic attack of OH^- or H_2O on the carbon atom of CO coordinated to transition metals, giving a hydroxycarbonyl complex (eq. 1-2),[5, 6] (ii) thermal decarboxylation of the hydroxycarbonyl complex to afford CO_2 and a metal hydride (eq. 1-3), and (iii) H_2 evolution by the reaction

$$M\text{-}CO + OH^- \longrightarrow M\text{-}COOH \qquad (1\text{-}2)$$

$$M\text{-}COOH \longrightarrow M\text{-}H + CO_2 \qquad (1\text{-}3)$$

of the metal hydride with protons or water. However, few hydroxycarbonyl, hydride, and aquo intermediates involved in each step have been confirmed mechanistically so far. This chapter describes the WGS reaction catalyzed by $[Ru(bpy)_2(CO)Cl]^+$ (bpy = 2,2'-bipyridine) which is a catalyst precursor in aqueous alkaline solutions, as well as mechanisms of the reaction, based on systematic isolation of all the possible intermediates.

1-2 Experimental Section

Materials. Bis(2,2'-bipyridine)dichlororuthenium(II), $Ru(bpy)_2Cl_2$,[7] tris(2,2'-bipyridine)ruthenium(II) dichloride, $[Ru(bpy)_3]Cl_2$,[8] and bis(2,2'-bipyridine)carbonylhydrido-ruthenium(II) hexafluorophosphate, $[Ru(bpy)_2(CO)H](PF_6)$[9] were prepared according to the literatures. A C_2H_5OH/H_2O (1:1 v/v, 50 cm^3) solution containing both $Ru(bpy)_2Cl_2 \cdot 2H_2O$ (420 mg, 0.81

mmol) and $Na_2MoO_4 \cdot 2H_2O$ (200 mg, 0.82 mmol) was stirred in a sealed tube at 120°C for 18 h. The solution was cooled to room temperature to give a black precipitate of $(bpy)_2Ru\text{-}O\text{-}Mo\text{-}O(O)_2$, which was collected by filtration, washed with water, ethanol, and then diethyl ether, and dried in vacuo, 51% yield; mp 150°C (dec.). Anal. Calcd for $C_{20}H_{16}N_4MoO_4Ru$: C, 41.90; H, 2.81; N, 9.77%. Found: C, 41.42; H, 2.89; N, 9.83%.

Preparation of $[Ru(bpy)_2(CO)Cl](PF_6)$. An ethylene glycol solution (100 cm^3) containing $Ru(bpy)_2Cl_2 \cdot 2H_2O$ (137 mg, 0.26 mmol) and a catalytic amount of $Ru(bpy)_2O_2MoO_2$ (12 mg, 0.02 mmol) was refluxed for 6 h, during which time the color of the solution changed from purple to reddish brown. After cooled to room temperature, the solution was evaporated to about a quarter volume in vacuo, followed by the addition of water (50 cm^3). The resulting solution was filtered, and the filtrate was mixed with an aqueous (5 cm^3) solution of NH_4PF_4 (200 mg, 1.2 mmol) to afford an orange precipitate, which was filtered and the filtrate was chromatographed on alkaline alumina using CH_3CN/C_6H_6 (1:1 v/v) as an eluent, and then recrystallized from CH_3CN/C_6H_6, 80% yield; mp. 290°C (dec.), $\nu(C{\equiv}O)$ 1960 cm^{-1}. Anal. Calcd for $C_{21}H_{16}ClF_6N_4OPRu$: C, 40.56; H, 2.59; N, 9.01%. Found: C, 40.27; H, 2.64; N, 9.16%.

Preparation of $[Ru(bpy)_2(CO)_2](PF_6)_2$. An aqueous (15 cm^3) suspension of $[Ru(bpy)_2(CO)Cl](PF_6)$ (354 mg, 0.57 mmol) under 10

kg/cm^2 of CO in a stainless-steel bomb was stirred magnetically at 150°C for 20 h. After the bomb was cooled to room temperature, the CO pressure was released. The resulting colorless solution was filtered. To the filtrate was added NH_4PF_6 (810 mg, 5.0 mmol) dissolved in a small amount of water (5 cm^3) to yield a white precipitate, which was collected by filtration and crystallized from CH_3CN/C_6H_6 (1:1 v/v), 70% yield; mp. 280°C, $\nu(C\equiv O)$ 2040, 2085 cm^{-1}. Anal. Calcd for $C_{22}H_{16}F_{12}N_4O_2P_2Ru$: C, 34.80; H, 2.12; N, 7.38%. Found: C, 34.98; H, 2.29; N, 7.65%.

Preparation of $[Ru(bpy)_2(CO)(H_2O)][B(C_6H_5)_4]_2 \cdot H_2O$. An aqueous acidic solution (400 cm^3) of $[Ru(bpy)_2(CO)H](PF_6)$ (50 mg, 0.085 mmol) at pH 4.0 (adjusted with 1.0 N HCl) was stirred for 1 h at room temperature and then concentrated to about a half volume under reduced pressures. To the resulting solution was added $NaB(C_6H_5)_4$ (120 mg, 0.35 mmol) dissolved in a small amount of water (5 cm^3) at pH 4.0 to afford a yellow precipitate, which was collected by filtration and recrystallized from CH_3OH/H_2O (pH 4.0), 50% yield; mp. 120°C (dec.), the amount of H_2O solvated was determined by ^1H nmr in CD_3CN, $\nu(C\equiv O)$ 1990 cm^{-1}, $\nu(O-H)$ 3040 cm^{-1}. Anal. Calcd for $C_{69}H_{60}B_2N_4O_3Ru$: C, 73.05; H, 5.51; N, 4.94%. Found: C, 72.76; H, 5.34; N, 5.30%.

Preparation of $[Ru(bpy)_2(CO)(OH)](PF_6) \cdot H_2O$. An aqueous acidic solution (100 cm^3) of $[Ru(bpy)_2(CO)H](PF_6)$ (51 mg, 0.087 mmol) at pH 4.0 (adjusted with 1.0 N HCl) was stirred for 1 h at

room temperature, and 1.0 N NaOH was then added to adjust the pH of the solution to 9.5. The resulting solution was filtered, and the filtrate was concentrated to about a quarter volume under reduced pressures, followed by adjusting the pH value to 11 to produce an orange precipitate, which was collected by filtration and dried in vacuo, 30% yield; mp. 200°C (dec.), the amount of H_2O solvated was determined by ^1H nmr in CD_3CN, $\nu(C\equiv O)$ 1980 cm^{-1}, $\nu(O-H)$ 3050 cm^{-1}. Anal. Calcd for $C_{21}H_{19}F_6N_4O_3PRu$: C, 40.59; H, 3.08; N, 9.01%. Found: C, 40.32; H, 2.84; N, 8.87%.

Preparation of $[Ru(bpy)_2(CO)C(O)OH](PF_6)\cdot 1/2H_2O$. An aqueous solution (300 cm^3) of $[Ru(bpy)_2(CO)_2](PF_6)_2$ (144 mg, 0.19 mmol) at pH 9.5 (adjusted with 0.2 N NaOH) was concentrated to ca. 20 cm^3 under reduced pressures, and the pH value was adjusted to 10 to produce a yellow precipitate, which was collected by filtration, washed with ether, and dried in vacuo, 20% yield; mp. 155°C (dec.), the amount of H_2O solvated was determined by ^1H nmr in CD_3CN, $\nu(O-H)$ 3070 cm^{-3}, $\nu(C\equiv O)$ 1960 cm^{-1}, $\nu(C=O)$ 1587 cm^{-1}, $\nu(C-O)$ 1140 cm^{-1}. Anal. Calcd for $C_{22}H_{18}F_6N_4O_{3.5}PRu$: C, 41.26; H, 2.83; N, 8.75%. Found: C, 41.08; H, 2.82; N, 8.87%.

Preparation of $[Ru(bpy)_2(CO)C(O)OCH_3](PF_6)\cdot 1/2CH_2Cl_2$. An anhydrous CH_3OH (50 cm^3) solution containing $[Ru(bpy)_2(CO)_2](PF_6)_2$ (77 mg, 0.10 mmol) and CH_3ONa (0.29 mmol) was stirred for 1 h under N_2 atmosphere at room temperature. The resulting solution was evaporated to dryness under reduced pressures. The

crude product thus obtained was dissolved in CH_2Cl_2 (90 cm^3), and the solution was dried with Na_2SO_4. The resulting solution was filtered, and the filtrate was evaporated to ca. 5 cm^3, giving a yellow solid, 80% yield; mp. 110°C (dec.), the amount of CH_2Cl_2 solvated was determined by ^1H nmr in CD_3CN, ν(C≡O) 1960 cm^{-1}, ν(C=O) 1605 cm^{-1}, ν(C-O) 1045 cm^{-1}. Anal. Calcd for $C_{23.5}H_{20}ClF_6N_4O_3PRu$: C, 41.03; H, 2.93; N, 8.14%. Found: C, 41.02; H, 3.28; N, 7.86%.

General Procedure for the WGS Reaction Studies. The WGS reaction was carried out in a stainless-steel bomb (65 cm^3) containing a glass tube in which a ruthenium catalyst (0.05 mmol) and an aqueous KOH solution (0.21 mol dm^{-3}, 15 cm^3) were placed. After degassed by three 10 kg/cm^2 pressurization/depressurization cycles with CO, the bomb was pressurized with 3-20 kg/cm^2 of CO and kept at the reaction temperature for 20 h with stirring magnetically. After the bomb was cooled to room temperature, gaseous products in the vapor phase were sampled with a gas syringe through a septum cap attached to the exit of the tap and analyzed with a Shimadzu GC-7A gas chromatograph equipped with TCD using a 60/80 mesh Unibeads 1S under N_2 carrier gas. A Shimadzu Chromatopack C-E1B digital integrator was used to integrate the output from the gas chromatograph.

Physical Measurements. Electronic and infrared spectra were measured with Union SM-401 and Hitachi 215 spectrophotome-

ters, respectively. ^{1}H nmr spectra were recorded on a JEOL PS-100 spectrometer. pH Values of the reaction mixture were determined with a Toa Denpa Model GS-135 pH electrode. Equilibrium constants were determined by electrophotometry or potentiometric titration at 25°C. The kinetic measurement for the nucleophilic attack of OH^- to $[Ru(bpy)_2(CO)_2](PF_6)_2$ was carried out in H_2O under the pseudo-first-order conditions with at least 5-fold excess amounts of $[Ru(bpy)_2(CO)_2](PF_6)_2$ (2.63×10^{-4} mol dm^{-3}) in an aqueous KOH solution. The rate of reaction was measured by monitoring the absorbance at 440 nm due to $[Ru(bpy)_2(CO)C(O)OH]^+$ and $[Ru(bpy)_2(CO)(COO^-)]^+$ in the reaction mixture, using a Union RA-413 stopped-flow spectrophotometer equipped with a 2 mm length quartz cell in a cell holder thermostated within 25.0 $\pm$ 0.2°C. Pseudo-first-order rate constants were obtained from the slope of plots of $\log|A_t - A_\infty|$ against time, which was found to be linear for at least 3 half-lives, where A_t and A_∞ are absorbances at a time t and the end of the reaction, respectively.

1-3 Results and Discussion

Catalytic Reactions and the Isolation of $[Ru(bpy)_2(CO)_2](PF_6)_2$. It has already been reported that $[Ru(bpy)_2(CO)Cl]Cl$ and $[Ru(phen)_2(CO)Cl]Cl$ (phen = 1,10-phenanthroline) catalyze the photochemical WGS reaction in aqueous solutions under mild conditions (1 - 3 kg/cm^2 of CO, 100 - 160°C).[10] We have found, however, that $[Ru(bpy)_2(CO)Cl](PF_6)$ is still active for the WGS

reaction without irradiation in aqueous alkaline solutions, as shown in Table 1-I. Although the turnover number for the H_2 formation in the present study using $[Ru(bpy)_2(CO)Cl](PF_6)$ as a catalyst in the presence of KOH (3.2 mmol) was only 3.8 for 20 h under a pressure of 3 kg/cm^2 of CO at 100°C (entry 1, Table 1-I), it increases with increasing the reaction temperature and the CO pressure (compare entry 1 with 2, entries 3 and 4 with 5, and entry 2 with 4, Table 1-I). The maximum turnover number in the present study was 502 under 20 kg/cm^2 of CO at 150°C (entry 5, Table 1-I), while the theoretical one expected from the volume of the bomb used in this study is 800 under the initial pressure of 20 kg/cm^2 of CO. No further attempt to increase the turnover number has been performed, since the purposes of this work are to explore the active species in the WGS reaction and to clarify the mechanisms.[11]

The discrepancy in the amounts of H_2 and CO_2 evolved in the gas phase (Table 1-I) may result from the higher solubility of CO_2 than H_2 in addition to the formation of the carbonate ion in alkaline solutions as suggested previously.[12] In fact, the amount of CO_2 dissolved in the final solutions obtained after releasing the pressures in the bomb was determined as 20 - 30 wt% of that in the gas phase by gas chromatography. The $[Ru(bpy)_2(CO)Cl](PF_6)$ complex was gradually decomposed in the course of the WGS reaction for 20 h, finally giving a solution of $[Ru(bpy)_3]^{2+}$, as confirmed from the electronic absorption spectrum, with a pale green precipitate. The catalytic activity of [Ru-

Table 1-I. The Water Gas Shift Reaction

Entry	Catalyst[a]	Temp °C	CO kg cm^{-2}	KOH[b] mmol	Gaseous product[c] H_2	Gaseous product[c] CO_2
1	$[Ru(bpy)_2(CO)Cl]^+$	100	3	3.2	3.8	
2	$[Ru(bpy)_2(CO)Cl]^+$	100	10	3.2	165	95
3	$[Ru(bpy)_2(CO)Cl]^+$	150	5	3.2	112	46
4	$[Ru(bpy)_2(CO)Cl]^+$	150	10	3.2	197	75
5	$[Ru(bpy)_2(CO)Cl]^+$	150	20	3.2	502	203
6	$[Ru(bpy)_2(CO)Cl]^+$	150	10	0	1.1	0.7
7	$[Ru(bpy)_2(CO)_2]^{2+}$	70	10	3.2	4.1	1.1
8	$[Ru(bpy)_2(CO)_2]^{2+}$	100	3	3.2	10.8	0.4
9	$[Ru(bpy)_2(CO)_2]^{2+}$	100	10	3.2	147	82.7
10	$[Ru(bpy)_2(CO)_2]^{2+}$	150	10	3.2	198	75
11	$[Ru(bpy)_3]^{2+}$ [d]	150	20	3.2	16	15

[a] PF_6^- salt, 0.05 mmol in H_2O (15 cm^3). [b] Quantity of KOH initially added. [c] Mol/(mol of catalyst, 20 h). [d] Cl^- salt.

$(bpy)_3]Cl_2$ in the WGS reaction, however, is much lower than that of $[Ru(bpy)_2(CO)Cl](PF_6)$ (compare entry 5 with 11, Table 1-I), suggesting that $[Ru(bpy)_3]^{2+}$ is not the actual catalyst in the WGS reaction.

In the absence of KOH, the WGS reaction catalyzed by $[Ru(bpy)_2(CO)Cl](PF_6)$ is slow even under 10 kg/cm^2 of CO at 150°C for 20 h (entry 6, Table 1-I); an almost colorless solution of the Ru(II) salt was obtained without any decomposition after the reaction for 20 h. The addition of NH_4PF_6 to the resulting colorless solution afforded a known dicarbonyl complex, $[Ru(bpy)_2(CO)_2](PF_6)_2$,[13] in a 70% yield. This complex isolated also catalyzes the WGS reaction under similar conditions (entries 7 - 10, Table 1-I); the turnover numbers at 100 and 150°C are essentially the same as those in the case with $[Ru(bpy)_2(CO)Cl](PF_6)$ (compare entries 9 and 10 with 2 and 4, respectively, Table 1-I), indicating that $[Ru(bpy)_2(CO)Cl]^+$ may be converted to $[Ru(bpy)_2(CO)_2]^{2+}$ under CO pressure in an alkaline solution.

Solvolysis of $[Ru(bpy)_2(CO)Cl]^+$ to Give $[Ru(bpy)_2(CO)(H_2O)]^{2+}$. It has been suggested that $[Ru(bpy)_2(CO)Cl]^+$ undergoes thermal and photochemical solvolyses in H_2O to give $[Ru(bpy)_2(CO)(H_2O)]^{2+}$ (eq. 1-4) and $[Ru(bpy)_2(H_2O)Cl]^+$ (eq. 1-5),

$$[Ru(bpy)_2(CO)Cl]^+ + H_2O \xrightarrow{\Delta} [Ru(bpy)_2(CO)(H_2O)]^{2+} + Cl^- \quad (1\text{-}4)$$

$$[Ru(bpy)_2(CO)Cl]^+ + H_2O \xrightarrow{h\nu} [Ru(bpy)_2(H_2O)Cl]^+ + CO \quad (1\text{-}5)$$

respectively.[14] However, there is no difference between the electronic absorption spectra of aqueous solutions of $[Ru(bpy)_2(CO)Cl](PF_6)$ after irradiation with a 500 W Xe lamp ($\lambda > 360$ nm) at room temperature for 10 h and after refluxing for 1h. In addition, the spectra coincided with that of $[Ru(bpy)_2(CO)(H_2O)]^{2+}$ formed in the reaction of $[Ru(bpy)_2(CO)H](PF_6)$ with H_3O^+ in water (pH 4.0) for 1 h at room temperature (eq. 1-6).[9] In

$$[Ru(bpy)_2(CO)H]^+ + H_3O^+ \longrightarrow [Ru(bpy)_2(CO)(H_2O)]^{2+} + H_2 \quad (1\text{-}6)$$

fact, the addition of $NaBPh_4$ to the solution after the hydrolysis of $[Ru(bpy)_2(CO)Cl]^+$ afforded $[Ru(bpy)_2(CO)(H_2O)](BPh_4)_2$ as a yellow precipitate. Thus, $[Ru(bpy)_2(CO)Cl]^+$ is subject to a thermal solvolysis in water to give $[Ru(bpy)_2(CO)(H_2O)]^{2+}$, which may undergo the substitution of CO under CO pressures, yielding $[Ru(bpy)_2(CO)_2]^{2+}$.

Interconversion between $[Ru(bpy)_2(CO)(H_2O)]^{2+}$ and $[Ru(bpy)_2(CO)(OH)]^+$ in Weak Alkaline Solutions. The addition of an aqueous KOH solution to a weak acidic solution of $[Ru(bpy)_2(CO)(H_2O)]^{2+}$ resulted in the disappearance of electronic absorp-

tion bands of $[Ru(bpy)_2(CO)(H_2O)]^{2+}$ (λ_{max} 259, 304, 314, and 390 nm); instead of new bands appeared at 292, 350, and 444 nm with isosbestic points at 270, 304, and 340 nm, as shown in Figure 1-1. At pH values higher than 11, a limiting spectrum was obtained. In addition, the pH dependence of the spectra is reversible. Thus, an equilibrium may exist between $[Ru(bpy)_2(CO)(H_2O)]^{2+}$ and $[Ru(bpy)_2(CO)(OH)]^{+}$ (eq. 1-7). The

$$[Ru(bpy)_2(CO)(H_2O)]^{2+} + OH^- \overset{K_7}{\rightleftharpoons} [Ru(bpy)_2(CO)(OH)]^{+} + H_2O \quad (1\text{-}7)$$

equilibrium constant (K_7) calculated from the change of the absorbance at 260 nm was 5.06×10^5 mol^{-1} dm^3 at 25°C. The rate of the equilibrium reaction (eq. 1-7), however, is too fast to be determined by the stopped-flow method probably because of a diffusion controlled reaction. The existence of the equilibrium (eq. 1-7) is compatible with the fact that $[Ru(bpy)_2(CO)(OH)](PF_6)$ has been isolated on the addition of excess NH_4PF_6 to a concentrated aqueous alkaline solution of $[Ru(bpy)_2(CO)(H_2O)]^{2+}$.

Nucleophilic Attack of OH^- to CO Coordinated to $[Ru(bpy)_2(CO)_2]^{2+}$. The electronic absorption spectrum of an aqueous solution of $[Ru(bpy)_2(CO)_2](PF_6)_2$ also changed reversibly depending on the pH value. The spectrum of $[Ru(bpy)_2(CO)_2]^{2+}$ in an acidic solution shows two absorption maxima at 253 and 307 nm,

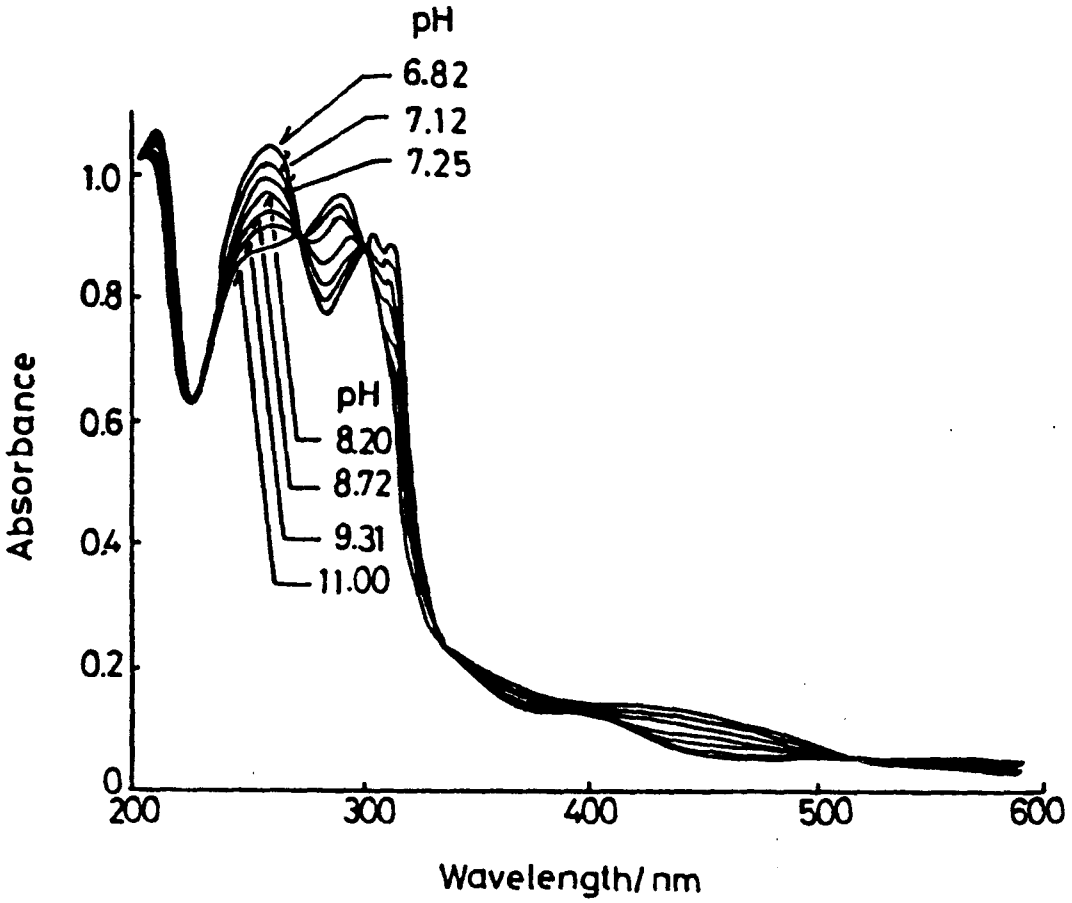

Figure 1-1. Electronic absorption spectra of $[Ru(bpy)_2(CO)(H_2O)]^{2+}$ (1.0×10^{-4} mol dm^{-3}) in H_2O at various pH values (25°C).

whose intensities gradually decrease upon the addition of an aqueous KOH solution; instead four new bands at 248, 274, 344, and 430 nm occur with three isosbestic points at 260, 302, and 329 nm, as shown in Figure 1-2a. It should be noted, however, that in a weak alkaline medium there appears a weak shoulder at 400 nm, which is concealed by an absorption at 430 nm occurring at pH values higher than 9.0 (Figure 1-2b). The 430 nm band attained a maximum intensity around pH 11.0 and was almost unchanged at the higher pH values. Moreover, $[Ru(bpy)_2(CO)_2](PF_6)_2$ (5.15×10^{-4} mol dm^{-3}) in H_2O behaves as a dibasic acid upon titration with an aqueous KOH solution (0.20 mol dm^{-3}), as shown in Figure 1-3. Thus, there may exist two successive equilibria in an aqueous alkaline solution of $[Ru(bpy)_2(CO)_2]^{2+}$.

When an aqueous solution of $[Ru(bpy)_2(CO)_2](PF_6)_2$ with pH 9.5 ± 0.5 was concentrated under reduced pressures, the ruthenium hydroxycarbonyl complex $[Ru(bpy)_2(CO)C(O)OH](PF_6)$ was obtained as a yellow precipitate, suggesting that the nucleophilic attack of OH^- on CO of $[Ru(bpy)_2(CO)_2](PF_6)_2$ takes place in weak alkaline media. Thus, $[Ru(bpy)_2(CO)_2]^{2+}$ may exist as an equilibrium mixture with $[Ru(bpy)_2(CO)C(O)OH]^+$ in weak alkaline solutions (eq. 1-8).

$$[Ru(bpy)_2(CO)_2]^{2+} + OH^- \underset{k_{-8}}{\overset{k_8}{\rightleftharpoons}} [Ru(bpy)_2(CO)C(O)OH]^+ \qquad (1\text{-}8)$$

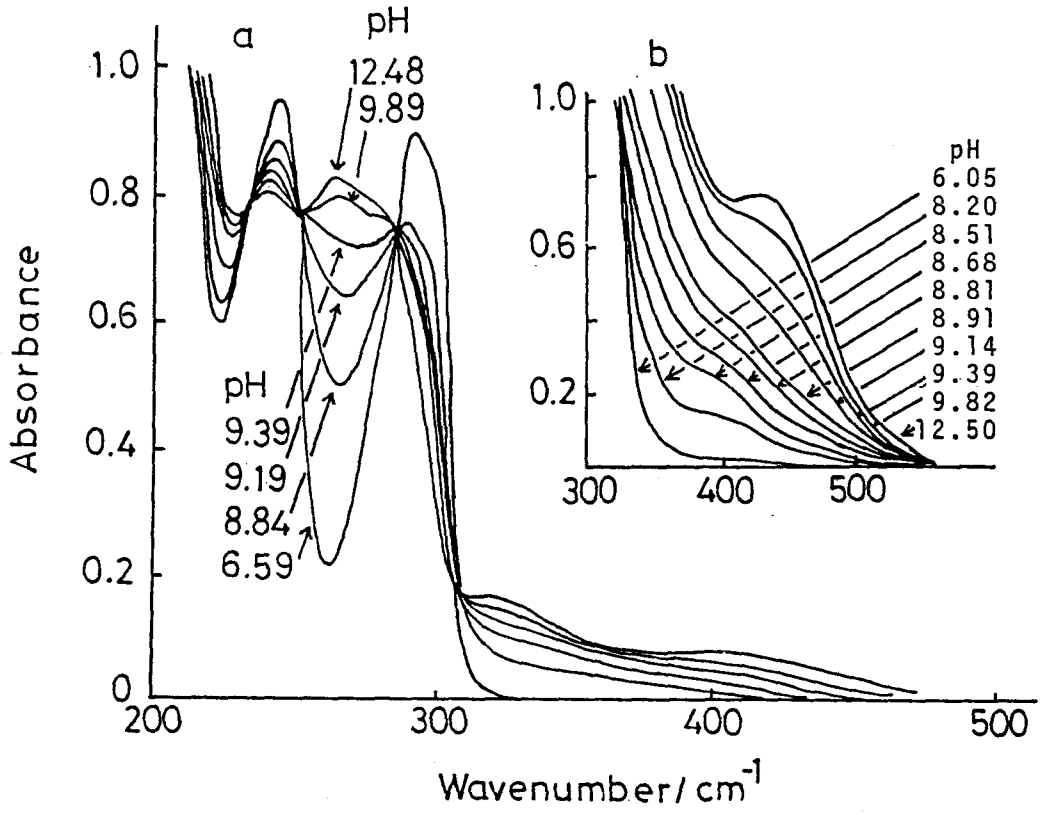

Figure 1-2. Electronic absorption spectra of $[Ru(bpy)_2(CO)_2]^{2+}$, ((a) 2.84 x 10^{-5} mol dm^{-3} and (b) 2.84 x 10^{-4} mol dm^{-3}) in H_2O at various pH values (25°C).

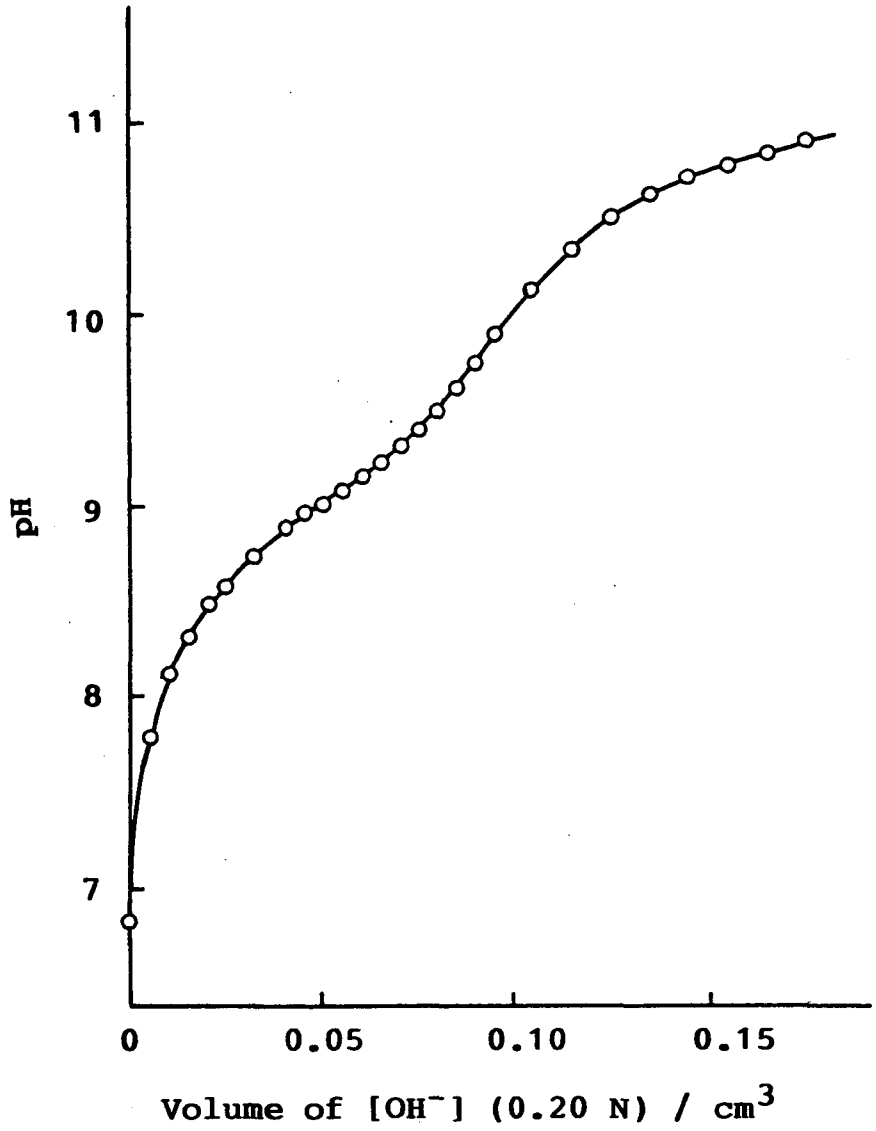

Figure 1-3. Titration of $[Ru(bpy)_2(CO)_2](PF_6)_2$ (1.03×10^{-5} mol) in H_2O (20 cm^3) by an aqueous KOH solution (0.2 mol dm^{-3}) at 25°C.

The formation of the monohydroxycarbonyl complex from $[Ru(bpy)_2(CO)_2]^{2+}$ in alkaline solutions (eq. 1-8) may be consistent with the fact that the reaction of $[Ru(bpy)_2(CO)_2](PF_6)_2$ with $NaOCH_3$ in dry CH_3OH afforded a monomethoxycarbonyl derivative, $[Ru(bpy)_2(CO)C(O)OCH_3](PF_6)$, whose ^1H nmr spectra shown in Figure 1-4 reveal that $[Ru(bpy)_2(CO)C(O)OCH_3](PF_6)$ readily undergoes hydrolysis in the presence of a small amount of water to give CH_3OH and $[Ru(bpy)_2(CO)_2]^{2+}$. Thus, $[Ru(bpy)_2(CO)C(O)OCH_3]^+$ and $[Ru(bpy)_2(CO)_2]^{2+}$ may exist as an equilibrium mixture in solution, as expressed by eq. 1-9. A similar equilibrium is known for $[Ru_3(CO)_{11}C(O)OCH_3]^-$, which partly dissociates into $Ru_3(CO)_{12}$ and CH_3O^- in methanol.[15]

$$[Ru(bpy)_2(CO)_2]^{2+} + CH_3O^- \rightleftharpoons [Ru(bpy)_2(CO)C(O)OCH_3]^+ \quad (1\text{-}9)$$

The hydroxycarbonyl complex formed in eq. 1-8 is known to undergo deprotonation reactions in strong alkaline solutions.[16] Another equilibrium existing in alkaline solutions may, therefore, be expressed by eq. 1-10. The existence of the equilibria shown by eq. 1-8 and 1-10 may be consistent with the fact that the reaction of $[PtH(CO)(P(\underline{i}\text{-}Pr)_3)_2]^+$ with an excess KOH in a mixture of THF and H_2O gives $PtH(COOK)(P(\underline{i}\text{-}Pr)_3)_2$.[16]

$$[Ru(bpy)_2(CO)C(O)OH]^+ + OH^- \overset{K_{10}}{\rightleftharpoons} [Ru(bpy)_2(CO)(COO^-)]^+ + H_2O \quad (1\text{-}10)$$

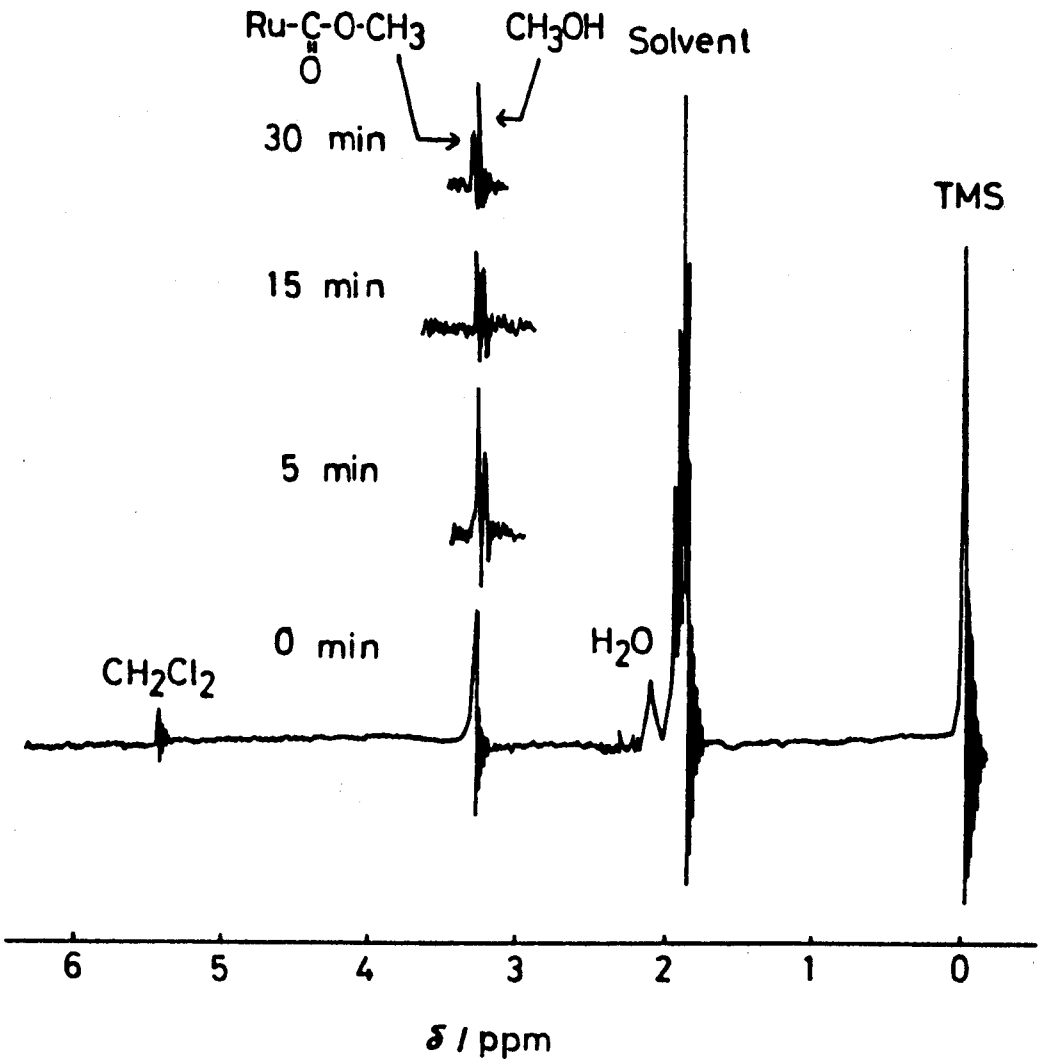

Figure 1-4. Time dependence of the ^1H nmr spectrum of $[Ru(bpy)_2(CO)C(O)OCH_3](PF_6)$ after dissolved in CD_3CN containing a small amount of H_2O at 25°C. A CH_2Cl_2 signal may be due to solvated molecules.

The equilibrium constants of eq. 1-8 ($K_8 = k_8/k_{-8}$) and 1-10 (K_{10}) were determined as 1.32×10^5 and 2.27×10^4 mol^{-1} dm^3, respectively, by the potentiometric method.[17] The rate of the reaction of $[Ru(bpy)_2(CO)_2](PF_6)_2$ with KOH at 25°C, k_{obsd}, is plotted against the concentration of KOH, as shown in Figure 1-5, which indicates a linear relation between those quantities with a small nonzero intercept. The forward rate constant (k_8) of eq. 1-8 determined from the slope of the plot is 2.3×10^4 s^{-1} mol^{-1} dm^3. The backward rate constant (k_{-8}) was calculated as 0.17 s^{-1} from K_8 and k_8, since the intercept of the plot (Figure 1-5) is too small to determine this value accurately. The reaction rate of eq. 1-10 has not been determined by the stopped-flow technique owing to a diffusion-controlled reaction.

Distribution of the Ruthenium Species in Water. In the WGS reaction under aqueous alkaline conditions, CO readily reacts with OH^- quantitatively to form a formate ion, which may function as a buffer to some extent, adjusting the pH of the initial solution around 8.5.[12] However, the pH value of the solution is lowered gradually to about 7.5 due to the formation of carbonate ion arising from CO_2 evolved in the course of the WGS reaction.[12] Thus, the reaction in alkaline media actually proceeds in the pH range 7.5 - 8.5. The distribution of several Ru(II) species at various pH, calculated from the equilibrium constants K_7, K_8, and K_{10}, are shown in Figure 1-6, which indicates that the Ru(II) species existing in the pH range of the present reaction (pH 7.5

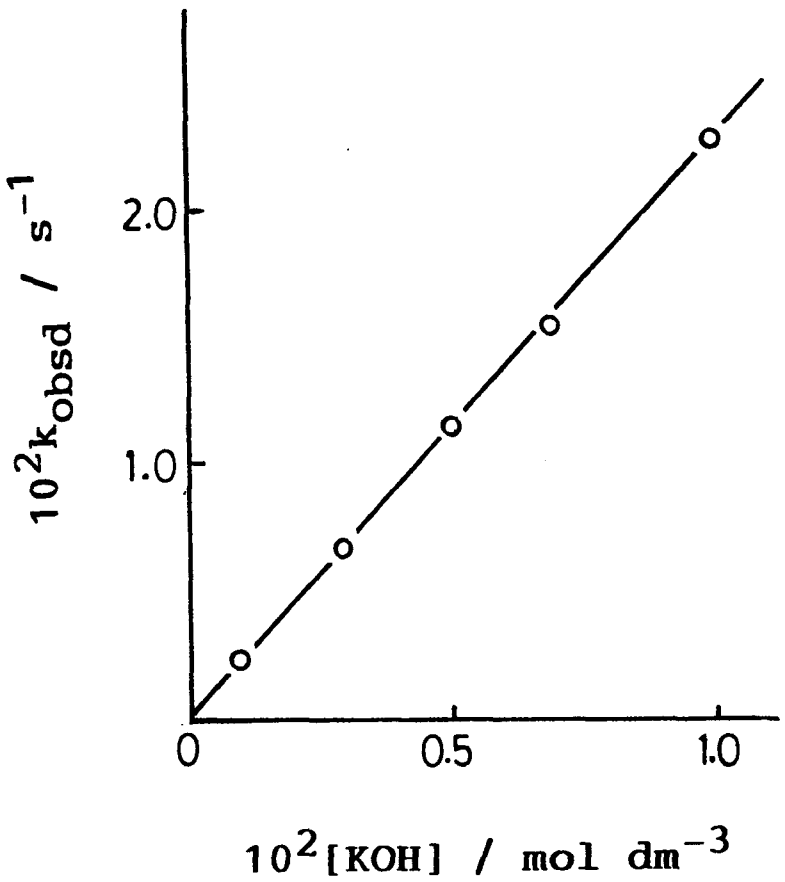

Figure 1-5. A plot of k_{obsd} vs. [KOH] for the reaction of $[Ru(bpy)_2(CO)_2](PF_6)_2$ with KOH in H_2O at 25°C.

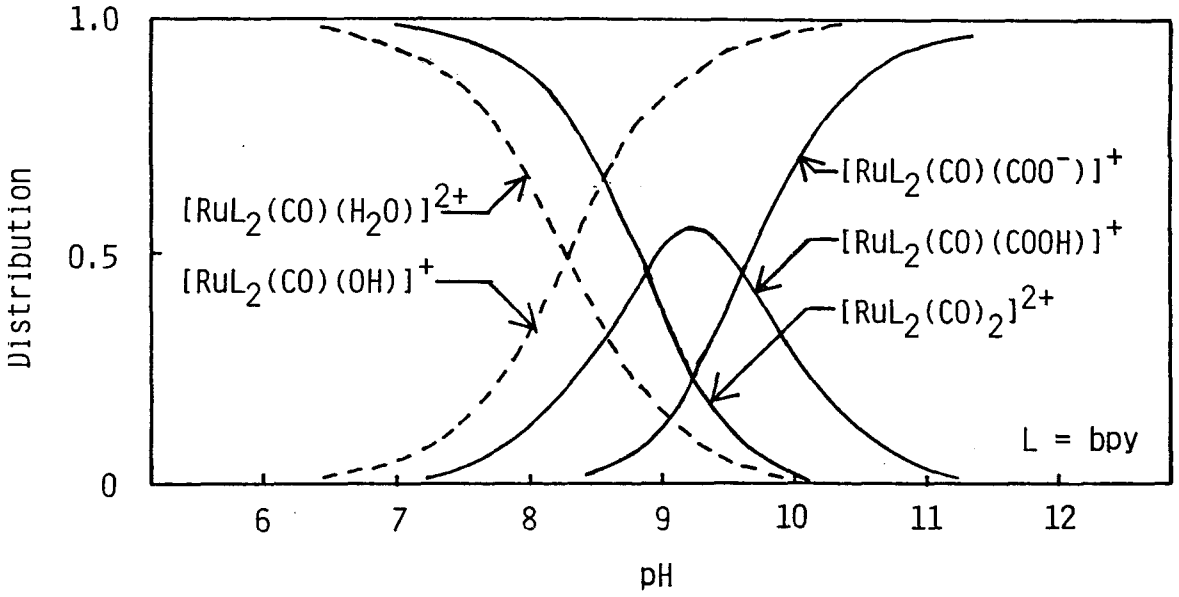

Figure 1-6. Distribution of the ruthenium species in H_2O at various pH at 25°C.

- 8.5) are $[Ru(bpy)_2(CO)_2]^{2+}$, $[Ru(bpy)_2(CO)C(O)OH]^+$, $[Ru(bpy)_2(CO)(H_2O)]^{2+}$, and $[Ru(bpy)_2(CO)(OH)]^+$. Although a hydroxyplatinum complex, $Pt(CH_3)(OH)L$ (L = bis(tertiary phosphine)), has been reported to undergo an insertion reaction of CO, affording the hydroxycarbonyl derivatives $Pt(CH_3)(C(O)OH)L$,[18] a substitution reaction of CH_3CN, but not CO, for the hydroxy group of $[Ru(bpy)_2(CO)(OH)](PF_6)$ occurred when the hydroxyruthenium(II) complex was heated in CH_3CN under 10 kg/cm^2 of CO at 100°C.

The Decarboxylation of $[Ru(bpy)_2(CO)C(O)OH]^+$. When an aqueous solution of $[Ru(bpy)_2(CO)_2](PF_6)_2$ at pH 8.09 ($KOH-H_3BO_3$ buffer) was kept at 100°C for 2 h under 10 kg/cm^2 of N_2 in a bomb, CO_2 and H_2 were evolved. To the resulting solution was added an aqueous solution of $NaBPh_4$ to precipitate all the cationic ruthenium species[19] as the BPh_4^- salt. After collected by filtration, washed with water, and dried in vacuo, the precipitate in Nujol mulls exhibits four IR bands at 1910 (s), 1960 (m), 1980 (s), and 1990 (sh) cm^{-1} due to $\nu(C\equiv O)$, as shown in Figure 1-7. The former two bands are assigned to $[Ru(bpy)_2(CO)H](BPh_4)$ and $[Ru(bpy)_2(CO)C(O)OH](BPh_4)$, respectively, by comparing the frequencies with those of the authentic samples. Of the latter two, the intense band is associated with $[Ru(bpy)_2(CO)(H_2O)](BPh_4)_2$ and the shoulder is assignable to $[Ru(bpy)_2(CO)(OH)](BPh_4)$, based on the infrared spectra of the authentic samples. On the other hand, no appreciable thermolysis of $[Ru(bpy)_2(CO)(COO^-)]^+$ has taken place when an aqueous solution (pH

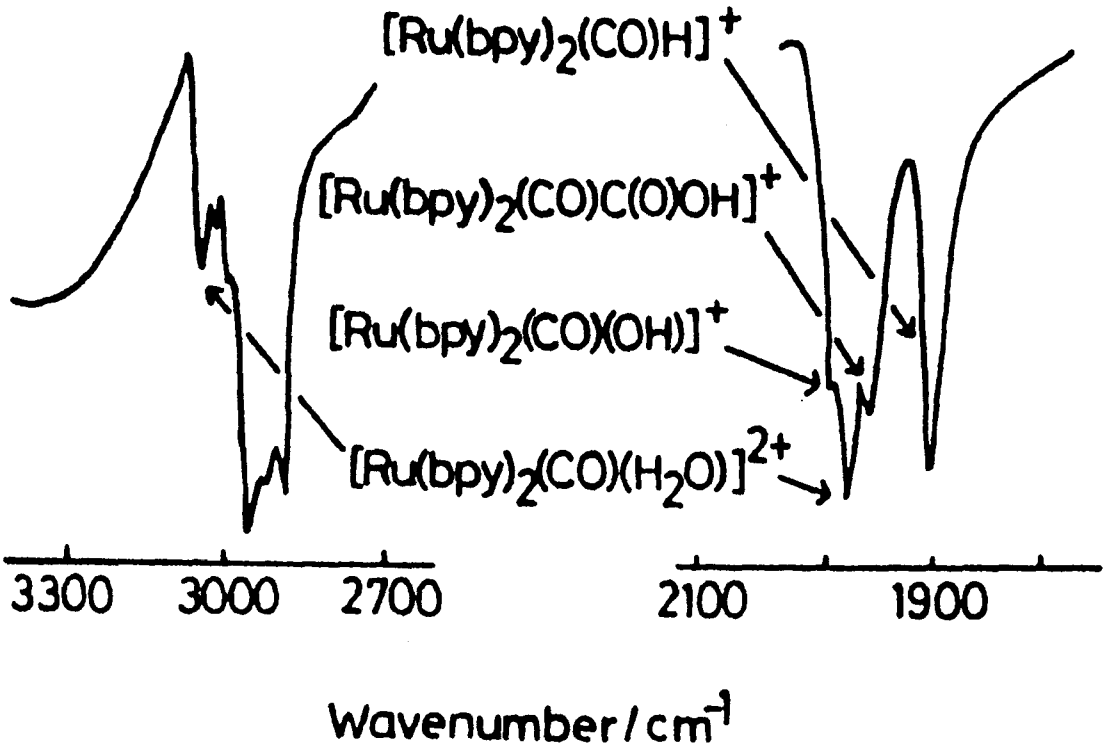

Figure 1-7. Infrared absorption spectra of the thermolysis products of $[Ru(bpy)_2(CO)_2](PF_6)_2$ in H_2O (pH 8.09) at 100°C.

11.0, KOH-H_3PO_4 buffer) of $[Ru(bpy)_2(CO)_2](PF_6)_2$ was heated at 100°C for 2 h under 10 kg/cm^2 of N_2.[20] These results indicate that $[Ru(bpy)_2(CO)C(O)OH]^+$ existing as an equilibrium mixture with $[Ru(bpy)_2(CO)_2]^{2+}$ in a weak aqueous alkaline solution undergoes decarboxylation to give $[Ru(bpy)_2(CO)H]^+$ (eq. 1-11), which

$$[Ru(bpy)_2(CO)C(O)OH]^+ \longrightarrow [Ru(bpy)_2(CO)H]^+ + CO_2 \quad (1\text{-}11)$$

further reacts with H_3O^+ to produce H_2 and $[Ru(bpy)_2(CO)(H_2O)]^{2+}$ (eq. 1-6), as described in the previous section. In fact, the hydrolysis of $[Ru(bpy)_2(CO)H](PF_6)$ in water at pH 8.05 (KOH-H_3BO_3 buffer) under 10 kg/cm^2 of N_2 at 100°C has evolved H_2. The reaction of $[Ru(bpy)_2(CO)H]^+$ with H_2O in place of H_3O^+ may also produce H_2 together with $[Ru(bpy)_2(CO)(OH)]^+$, though the contribution of this reaction to the H_2 formation has not been evaluated because of a rapid equilibrium between $[Ru(bpy)_2(CO)(H_2O)]^{2+}$ and $[Ru(bpy)_2(CO)(OH)]^+$ in weak alkaline solutions. However, $[Ru(bpy)_2(CO)H]^+$ may be one of the actual catalyst in the reaction, since $[Ru(bpy)_2(CO)H](PF_6)$ as a catalyst in the presence of KOH under 10 kg/cm^2 of CO at 100°C for 20 h gave the turnover number 179, which is essentially the same value as that with $[Ru(bpy)_2(CO)Cl](PF_6)$ under the same conditions (entry 2 in Table 1-I).

The WGS Reaction Using $Ru(bpy)_2Cl_2$ as a Catalyst Precursor. It has been reported that $Ru(bpy)_2Cl_2$ in CH_2Cl_2 under CO

pressures at 80°C is converted to $[Ru(bpy)_2(CO)_2]^{2+}$.[13] The same reaction occurred also when $Ru(bpy)_2Cl_2$ (0.05 mmol) was allowed to stand under 10 kg/cm^2 of CO at 100°C in water (15 cm^3) for 20 h.[21] As expected from this result, a large turnover number (243) was obtained in the WGS reaction using $Ru(bpy)_2Cl_2$ (0.05 mmol) as a catalyst precursor in the presence of KOH (3.2 mmol) under 10 kg/cm^2 of CO at 100°C for 20 h. It should be noted that the turnover number is considerably larger than that obtained in the reaction using the PF_6^- salt of $[Ru(bpy)_2(CO)Cl]^+$ or $[Ru(bpy)_2(CO)_2]^{2+}$ (see entry 2 or 9, Table 1-I). On the other hand, the addition of NH_4PF_6 (0.10 mmol) to an aqueous solution containing $Ru(bpy)_2Cl_2$ (0.05 mmol) and KOH (3.2 mmol) under 10 kg/cm^2 of CO at 100°C has decreased the turnover number of the reaction to 149. This result may be interpreted by a weak poisoning effect of PF_6^- on the WGS reaction.

Catalytic Cycle of the WGS Reaction. The WGS reaction catalyzed by some metal carbonyls, $M(CO)_6$ (M = Cr, Mo, W), in alkaline media has been reported to proceed preferentially by decomposition of the formate ion (eq. 1-12) which is produced at

$$HCOO^- + H_2O \xrightarrow{M(CO)_6} H_2 + CO_2 + OH^- \qquad (1\text{-}12)$$

the beginning of the reaction.[22-24] For example, $HCOO^-$ reacts with $M(CO)_5$ resulting from the dissociation of a CO ligand of

$M(CO)_6$ to afford $M(CO)_5OC(O)H^-$, which undergoes decarboxylation to generate $M(CO)_5H^-$, as proposed by King et al.[23,25,26] A similar thermal decarboxylation has been reported for $[Ru(bpy)_2(CO)OC(O)H]^+$ in 2-methoxyethanol, giving $[Ru(bpy)_2(CO)H]^+$.[27,28] Therefore, we have examined the H_2 evolution arising from the decomposition of $HCOO^-$ in the presence of the Ru(II) complexes. The thermal decomposition of HCOOH (13 mmol) in the presence of $[Ru(bpy)_2(CO)X](PF_6)$ (X = H, Cl) (0.05 mmol) in H_2O at pH 8.0 - 9.0 (KOH-HCOOH buffer) evolved 0.5 - 1.0 mmol of H_2 under 10 kg/cm^2 of N_2 at 100°C for 20 h. The amount of H_2 evolved, however, was much smaller than that in the WGS reaction at 100°C (see entries 2 and 9 in Table 1-I), despite the presence of a large amount of $HCOO^-$ in the solution. Thus, the decomposition of HCOOH may be no main pathway for the H_2 evolution in the present WGS reaction.

A plausible catalytic cycle of the reaction is depicted in Scheme 1-I; $Ru(bpy)_2Cl_2$ in an aqueous KOH solution under CO pressures at elevated temperatures may be converted to $[Ru(bpy)_2(CO)_2]^{2+}$ probably through $[Ru(bpy)_2(CO)Cl]^+$ and $[Ru(bpy)_2(CO)(H_2O)]^{2+}$ successively, followed by the substitution reaction by CO. The nucleophilic attack of OH^- to one of the coordinated CO of $[Ru(bpy)_2(CO)_2]^{2+}$ at pH 8.0 - 9.0 affords $[Ru(bpy)_2(CO)C(O)OH]^+$, which undergoes the decarboxylation to give $[Ru(bpy)_2(CO)H]^+$. The hydride complex thus formed reacts with H_3O^+ to evolve H_2 with regenerating $[Ru(bpy)_2(CO)(H_2O)]^{2+}$, while the reaction of $[Ru(bpy)_2(CO)H]^+$ with H_2O may participate into the

Scheme 1-I

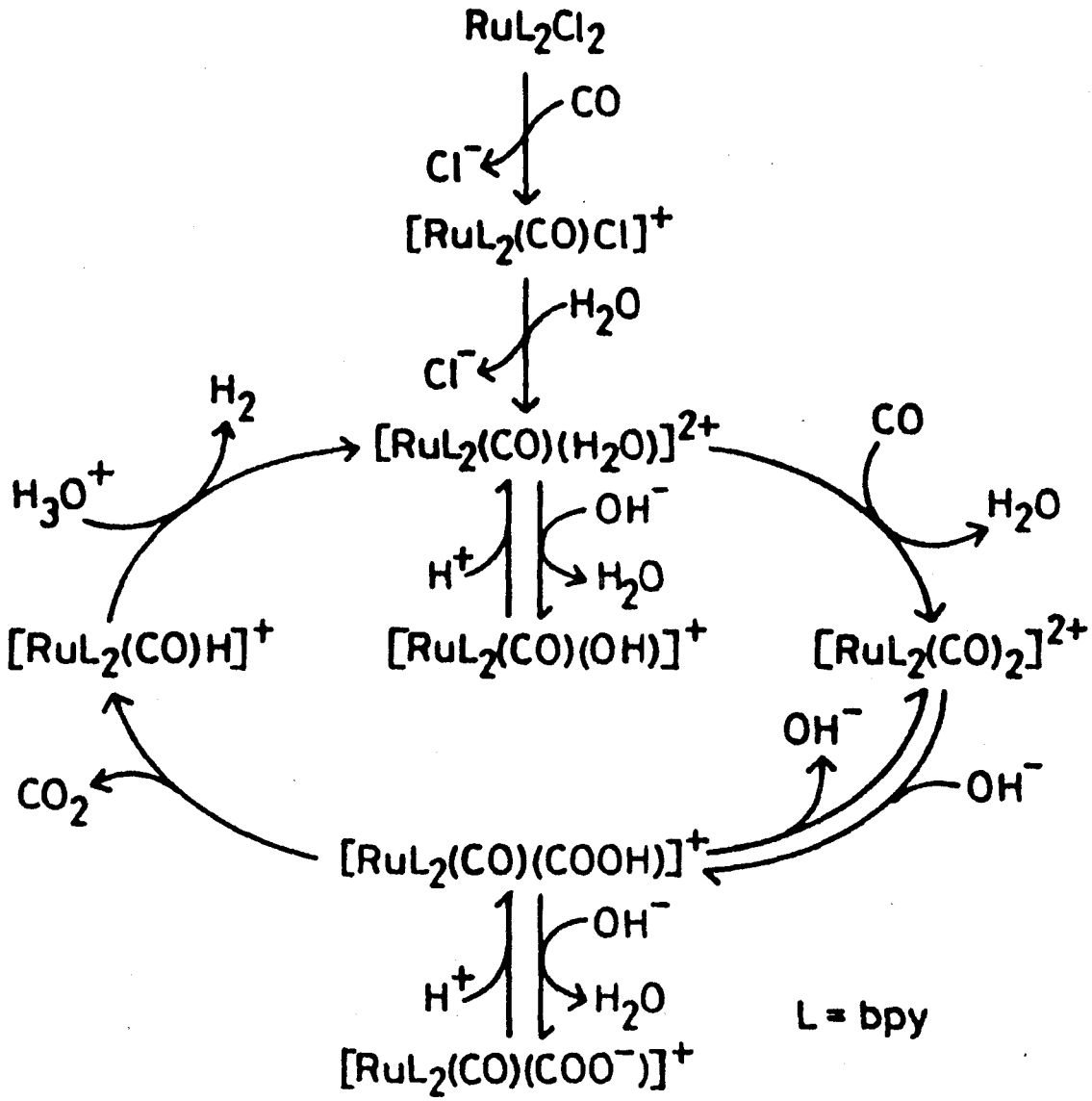
RuL2Cl2
CO
Cl-
[RuL2(CO)Cl]+
H2O
Cl-
[RuL2(CO)(H2O)]2+
H2
H3O+
CO
H2O
OH-
H+
H2O
[RuL2(CO)H]+
[RuL2(CO)(OH)]+
[RuL2(CO)2]2+
OH-
OH-
CO2
[RuL2(CO)(COOH)]+
OH-
H+
H2O
L = bpy
[RuL2(CO)(COO-)]+

production of H_2 to some extent. These reaction pathways are strongly supported by the isolation or characterization of all the intermediates.

1-4 References

(1) (a) Laine, R. M.; Rinker, R. G.; Ford, P. C. J. Am. Chem. Soc., **1977**, 99, 252. (b) Cheng, C. H.; Hendriksen, D. E.; Eisenberg, R. J. Am. Chem. Soc., **1977**, 99, 2791. (c) Kang H.; Mauldin, C. H.; Cole, T.; Slegeir, W.; Cann, K.; Pettit R. J. Am. Chem. Soc., **1977**, 99, 8323.

(2) (a) Ford, P. C. Acc. Chem. Res., **1981**, 14, 31 and the refe ences cited therein. (b) Darensbourg, D. J.; Rokicki, A. Organometallics, **1982**, 1, 1685. (c) Pearson, R. G.; Mauermann, H. J. Am. Chem. Soc., **1982**, 104, 500. (d) Yoshida, T.; Okano, T. Ueda, Y.; Otsuka, S. J. Am. Chem. Soc., **1981**, 103, 3411. (e) Baker, E. C.; Hendriksen, D. E Eisenberg, R. J. Am. Chem. Soc., **1980**, 102, 1020. (f) Nuzzo, R. G.; Feitler, D.; Whitesides, G. M. J. Am. Chem. Soc., **1979**, 101, 3683. (g) Cheng, C. H.; Eisenberg, R. J. Am. Chem. Soc., **1978**, 100, 5968. (h) King, R. B.; Fraizer C. C.; Hanes, R. M.; King, A. D., Jr. J. Am. Chem. Soc., **1978**, 100, 2925.

(3) Sato, S.; White, J. M. J. Am. Chem. Soc., **1980**, 102, 7206.

(4) (a) Inkrott, K. E.; Shore, S. G. J. Am. Chem. Soc., **1978**, 100, 3954. (b) Ford, P. C.; Rinker, R. G.; Ungermann, C.;

Laine, R. M.; Landis, V.; Moya, S. A. J. Am. Chem. Soc., **1978**, 100, 4595. (c) Laine, R. M. J. Am. Chem. Soc., **1978**, 100, 6451. (d) Inkrott, K. E.; Shore, S. G. Inorg. Chem., **1979**, 18, 2817. (e) Ungermann, C.; Landis, V.; Moya, S. A.; Cohen, H.; Walker, H.; Pearson, R. G.; Rinker, R. G.; Ford, P. C. J. Am. Chem. Soc., **1979**, 101, 5922. (f) Nagel, C. C.; Shore, S. G. J. Chem. Soc., Chem. Commun., **1980**, 530. (g) Nagel, C. C.; Bricker, J. C.; Alway, D. G.; Shore, S. G. J. Organomet. Chem., **1981**, 219, C9. (h) Bhattacharyya, A. A.; Nagel, C. C.; Shore, S. G. Organometallics, **1983**, 2, 1187. (i) Bhattacharyya, A. A.; Shore, S. G. Organometallics, **1983**, 2, 1251. (j) Bricker, J. C.; Nagel, C. C.; Bhattacharyya, A. A.; Shore, S. G. J. Am. Chem. Soc., **1985**, 107, 377. (k) Gross, D. C.; Ford, P. C. J. Am. Chem. Soc., **1985**, 107, 585.

(5) (a) Darensbourg, D. J.; Froelich, J. A. J. Am. Chem. Soc., **1977**, 99, 5940. (b) Lane, K. R.; Lee, R. E.; Sallans, L.; Squires, R. R. J. Am. Chem, Soc., **1984**, 106, 5767. (c) Trautman, R. J.; Gross, D. C.; Ford, P. C. J. Am. Chem. Soc., **1985**, 107, 2355.

(6) Tanaka, K.; Morimoto, M.; Tanaka, T. Chem. Lett., **1983**, 901.

(7) Sullivan, B. P.; Salmon, D. J.; Meyer, T. J. Inorg. Chem., **1978**, 17, 3334.

(8) Burstall, F. H. J. Chem. Soc., **1936**, 173.

(9) Kelly, J. M.; Vos, J. G. Angew. Chem., Int. Ed. Engl., **1982**, 21, 628.

(10) (a) Choudhury, D.; Cole-Hamilton, D. J. J. Chem. Soc., Dalton Trans., **1982**, 1885. (b) Cole-Hamilton, D. J. J. Chem. Soc., Chem. Commun., **1980**, 1213.

(11) Gas sampling in the course of WGS reactions has affected the turnover numbers significantly owing to small volume of the bomb. Therefore, no kinetic study for the WGS reaction has been performed.

(12) King, A. D., Jr.; King, R. B.; Yang, D. B. J. Am. Chem. Soc., **1980**, 102, 1028.

(13) Choudhury, D.; Jones, R. F.; Smith, G.; Cole-Hamilton, D. J. J. Chem. Soc., Dalton Trans., **1982**, 1143.

(14) Clear, J. M.; Kelly, J. M.; O'Connel, C. M.; Vos, J. G.; Cardin, C. J.; Costa, S. R.; Edwards, A. J. J. Chem. Soc., Chem. Commun., **1980**, 750.

(15) Gross, D. C.; Ford, P. C. Inorg. Chem., **1982**, 21, 1702.

(16) Yoshida, T.; Ueda, Y.; Otsuka, S. J. Am. Chem. Soc., **1978**, 100, 3941.

(17) Speakman, J. C. J. Chem. Soc., **1940**, 855.

(18) Appleton, T. G.; Bennett, M. A. J. Organomet. Chem., **1973**, 55, C88.

(19) No precipitate has been obtained by adding a large amount of $NaPF_6$ dissolved in H_2O.

(20) The final solution was treated with HCl to regenerate $[Ru(bpy)_2(CO)_2]^{2+}$, which was confirmed by the electronic absorption spectrum.

(21) A crude product obtained by evaporation of the solvent water

was $[Ru(bpy)_2(CO)_2]^{2+}$ contaminated with a small amount of $[Ru(bpy)_2(CO)(H_2O)]^{2+}$, as confirmed by the infrared spectrum.

(22) King, A. D., Jr.; King, R. B.; Yang, D. B. J. Am. Chem. Soc., **1981**, 103, 2699.

(23) King, A. D., Jr.; King, R. B.; Sailers, E. L., III J. Am. Chem. Soc., **1981**, 103, 1867.

(24) Weiler, B. H.; Liu, J.-P.; Grant, E. R. J. Am. Chem. Soc., **1985**, 107, 1595.

(25) Slegeir, W. A. R.; Sapienza, R. S.; Rayford, R.; Lam, L. Organometallics, **1982**, 1, 1728.

(26) Darensbourg, D. J.; Fischer, M. B.; Schmidt, R. E., Jr.; Baldwin, B. J. J. Am. Chem. Soc., **1981**, 103, 1297.

(27) Caspar, J. V.; Sullivan, B. P.; Meyer, T. J. Organometallics, **1983**, 2, 551.

(28) Sullivan, B. P.; Caspar, J. V.; Johnson, S. R.; Meyer, T. J. Organometallics, **1984**, 3, 1241.

Chapter 2

Electrochemical CO_2 Reduction Catalyzed by Ruthenium Complexes; the Effect of pH on the Formation of CO and $HCOO^-$

2-1 Introduction

Effective utilization of CO_2 being an ultimate oxidation product of organic molecule has become one of the most important subjects in the field of chemistry to cope with a predictable oil shortage in near future and the recent problem of increasing CO_2 concentration in air. Along this line, electrochemical,[1-10] photochemical,[11-16] and thermal[17-21] reductions of CO_2 have been studied by using homogeneous catalysts. Of these, the electrochemical reduction of CO_2 seems to have a bright prospect compared with other methods, since the reaction can easily be controlled by changing the applied potentials.

Electrochemically direct reduction of CO_2 giving $CO_2^{\cdot-}$ requires more negative potentials than -2.10 V vs. SCE (eq. 2-1).[10] However, CO_2 can be reduced at more positive potentials

$$CO_2 + e^- \longrightarrow CO_2^{\cdot-} \qquad (E^0 = -2.10\ V) \quad (2\text{-}1)$$

when protons participate in the reduction. The equilibrium potentials of the redox reactions affording HCOOH and CO (eq. 2-2

and 2-3, respectively) are -0.85 and -0.76 V vs. SCE, respectively, in water at pH 7.0.[11] These values are somewhat more negative than the redox potential of the H_2/H^+ couple at pH 7.0 (eq. 2-4).[11] In order to depress the evolution of H_2 in the

$$CO_2 + 2H^+ + 2e^- \longrightarrow HCOOH \quad (E^0 = -0.85\ V) \quad (2\text{-}2)$$

$$CO_2 + 2H^+ + 2e^- \longrightarrow CO + H_2O \quad (E^0 = -0.76\ V) \quad (2\text{-}3)$$

$$2H^+ + 2e^- \longrightarrow H_2 \quad (E^0 = -0.65\ V) \quad (2\text{-}4)$$

course of reduction of CO_2, therefore, it is desirable to use any catalysts which have a strong affinity for CO_2 even in the presence of protons. Of a number of transition-metal complexes as catalysts for the reduction of CO_2, nickel, rhenium, and ruthenium complexes have especially been of much interest from the viewpoint of efficiency for the formation of CO, $HCOO^-$, or both.

This chapter describes the electrochemical CO_2 reduction catalyzed by $[Ru(bpy)_2(CO)_2]^{2+}$ and $[Ru(bpy)_2(CO)Cl]^+$ which are catalysts for WGS reactions, in H_2O/DMF mixtures with different pH values.

2-2 Experimental Section

Materials. $[Ru(bpy)_2(CO)Cl](PF_6)$,[22] $[Ru(bpy)_2(CO)_2]$-

$(PF_6)_2$,[22] and $Ru(bpy)_2Cl_2 \cdot 2H_2O$,[23] were prepared according to the literatures. Commercially available guaranteed reagent grades of LiCl, NaOH, H_3PO_4, $NaHCO_3$, Na_2CO_3, and NBu^n_4OH were used without further purification. $NBu^n_4ClO_4$ prepared by the reaction of NBu^n_4Br with $HClO_4$ in water was recrystallized five times from diethyl ether/acetone. N,N-Dimethylformamide (DMF) was purified by refluxing with CaO for 24 h, followed by distillation under reduced pressure, and stored under an N_2 atmosphere. Mercury used as a working electrode was washed with aqueous HCl and aqueous $NaBH_4$ successively, and then distilled under reduced pressures.

Physical Measurements. Electrochemical measurements were carried out in a pyrex cell (30 or 100 cm^3) equipped with a hanging mercury drop electrode (HMDE, Metrohm Model E-410), a Pt auxiliary electrode, a saturated caromel electrode (SCE), and a nozzle for bubbling N_2 or CO_2. Cyclic voltammograms were obtained by the use of a Hokuto Denko HA-301 potentiostat, a Hokuto Denko HB-107A function generator, and a Yokogawa Electric Inc. 3077 X-Y recorder. The surface area of the HMDE was maintained at 2.22 ± 0.07 mm^2 throughout the work. Electronic absorption spectra were measured with a Union SM-401 spectrophotometer. Spectroelectrochemical experiments were carried out by the use of an optically transparent thin-layer electrode (OTTLE) cell, consisting of a Pt-gauze electrode in a 0.5 mm quartz cuvette, a Pt-wire auxiliary electrode, and a saturated

calomel reference electrode (SCE).[24]

Electrochemical Reduction of CO_2. The reduction of CO_2 in a CO_2-saturated H_2O/DMF mixture containing $[Ru(bpy)_2(CO)_2]^{2+}$ or $[Ru(bpy)_2(CO)Cl]^+$ was carried out by the controlled potential electrolysis at -1.50 V *vs.* SCE on an Hg electrode. The electrolysis cell[25] as depicted in Figure 2-1 was consisted of three compartments; one for an Hg working electrode (3.1 cm^2), the second separated from the working electrode cell by a glass frit for a platinum auxiliary electrode (*ca.* 3 cm^2), and the third for an SCE reference electrode. The volume of these compartments were 35, 25, and 8 cm^3, respectively, and the former two were connected with volumetric flasks with stainless tubes (I. D. = 0.4 mm). CO_2-saturated H_2O/DMF solutions containing $[Ru(bpy)_2(CO)_2]^{2+}$ or $[Ru(bpy)_2(CO)Cl]^+$ (0.50 mmol dm^{-3}, 50 cm^3) were prepared by mixing a CO_2-saturated DMF solution containing either the Ru(II) complex (0.025 mmol, 5 - 45 cm^3) with CO_2-saturated water (pH 6.0 or 9.5, 5 - 45 cm^3) buffered with H_3PO_4-NaOH (ionic strength is 0.05). After a stream of CO_2 was passed from the working electrode compartment to the volumetric flask for 30 min to displace the air in the electrolysis cell, the CO_2-saturated H_2O/DMF solution (40 cm^3) containing $[Ru(bpy)_2(CO)_2]^{2+}$ or $[Ru(bpy)_2(CO)Cl]^+$ was injected through a septum cap attached to the top of the working electrode compartment by a syringe technique. Then, the electrolysis cell was placed in a thermostat at 30 $\pm$ 0.1°C and the solution was stirred magnetically for 1 h. Attain-

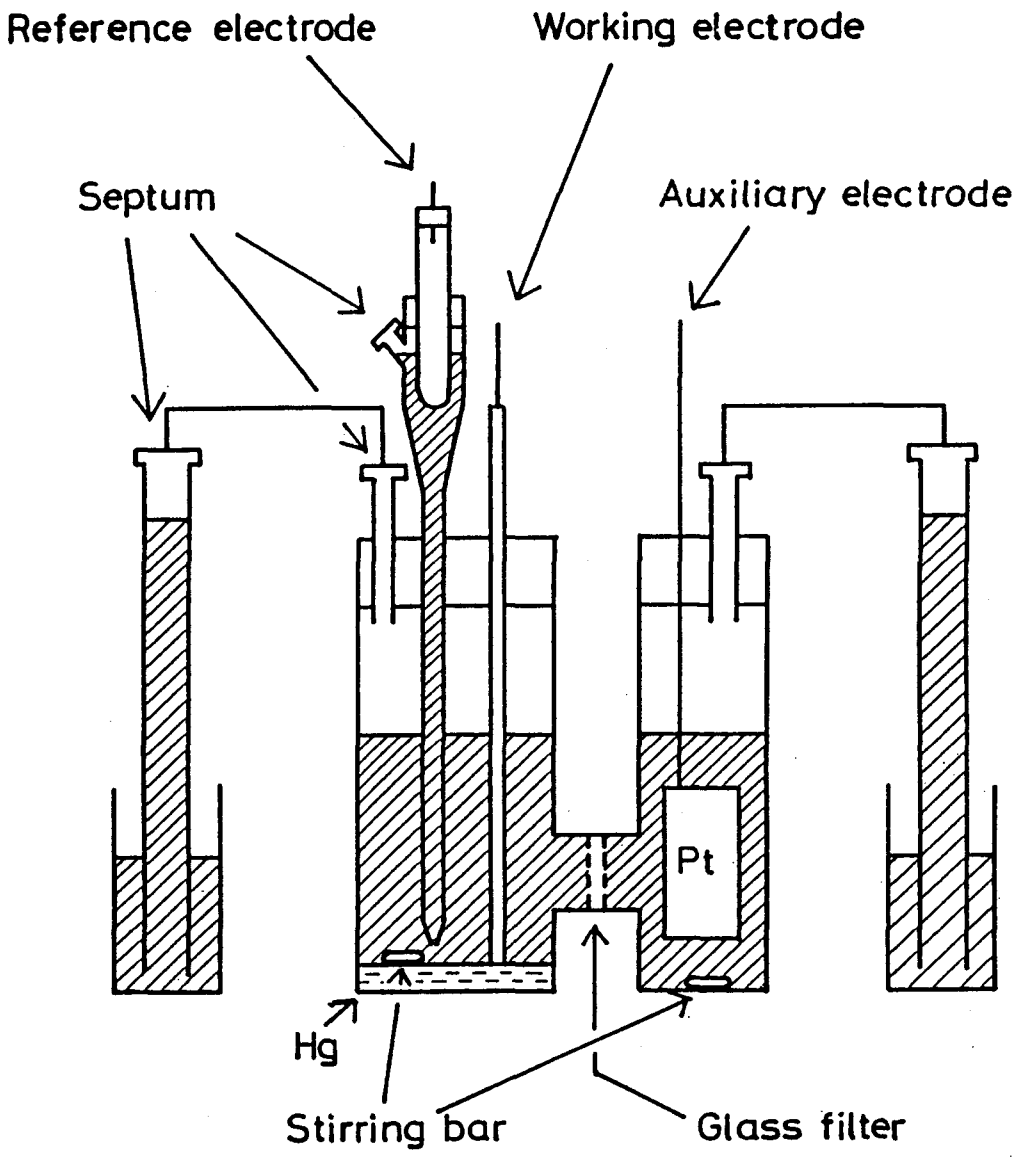

Figure 2-1. The electrolysis cell.

ment of the thermal equilibrium of CO_2 between the gaseous and liquid phase in the cell was confirmed from a constant height of the meniscus of CO_2-saturated water in the volumetric flasks connected with the working and auxiliary electrode compartments. The reduction of CO_2 was started by applying a given electrolysis potential to an Hg working electrode with a potentiostat, and the number of coulombs consumed in the reduction was measured with a Hokuto Denko Model HF-201 coulomb meter.

Product Analysis. At a fixed interval of coulombs consumed in the reduction, each 0.1 cm^3 portion of gas was sampled from the gaseous phases both of the working electrode compartment and of the volumetric flask with a pressure-locked syringe (Precision Sampling). Gaseous products were analyzed on a Shimadzu GC-3BT gas chromatograph equipped with a 2 m column filled with Molecular Sieve 13X using He as a carrier gas (for the determination of CO) and on a Shimadzu GC-7A gas chromatograph equipped with a 2 m column filled with Unibeads 1S using N_2 as a carrier gas (for the determination of H_2 and CO_2). The volume of the gas evolved in the reduction was determined by change of the meniscus in the volumetric flask connected with the working electrode compartment. The analysis of the solution was perfomed by sampling each 0.1 cm^3 portion from the working electrode compartment through a septum cap by a syringe technique at a fixed interval of coulombs consumed. The amount of $HCOO^-$ produced in the solution was determined with a Shimadzu Isotacho-

phoretic Analyzer IP-2A using aqueous $Cd(NO_3)_2$ (6.0 mmol dm^{-3}) and caproic acid (10.0 mmol dm^{-3}) solutions as leading and terminal electrolytes, respectively.

2-3 Results and Discussion

Cyclic Voltammetry of the Ruthenium Bipyridyl Complexes. Figure 2-2 shows the cyclic voltammograms of $[Ru(bpy)_2(CO)Cl]^+$ and $[Ru(bpy)_2(CO)_2]^{2+}$ by using a hanging mercury drop electrode (HMDE) with the surface area of 2.22 ± 0.07 mm^2 in DMF under N_2 and CO_2 atmospheres. The cyclic voltammogram of $[Ru(bpy)_2(CO)Cl]^+$ in an N_2-saturated DMF solution shows two redox couples in the potential range -0.50 V to -1.60 V *vs.* SCE. (a solid line in Figure 2-2a). The peak separations between the cathodic and anodic waves of the redox reactions at $E_{1/2}$ = -1.21 and -1.41 V *vs.* SCE are 60 mV and 90 mV, respectively, at the sweep rate 0.10 V s^{-1}. The peak potential of the former couple was independent of the sweep rate in the range 0.50 to 0.05 V s^{-1}. On the other hand, the anodic wave of the latter couple almost disappeared at the sweep rate 0.05 V s^{-1}, while the corresponding cathodic wave still observed clearly at -1.48 V *vs.* SCE. Thus, $[Ru(bpy)_2(CO)Cl]^+$ undergoes two successive one-electron reductions; one is reversible reduction at -1.24 V and the other essentially an irreversible reduction around -1.48 V *vs.* SCE, confirming that the two-electron reduction of $[Ru(bpy)_2(CO)Cl]^+$ is followed by a slow chemical reaction.

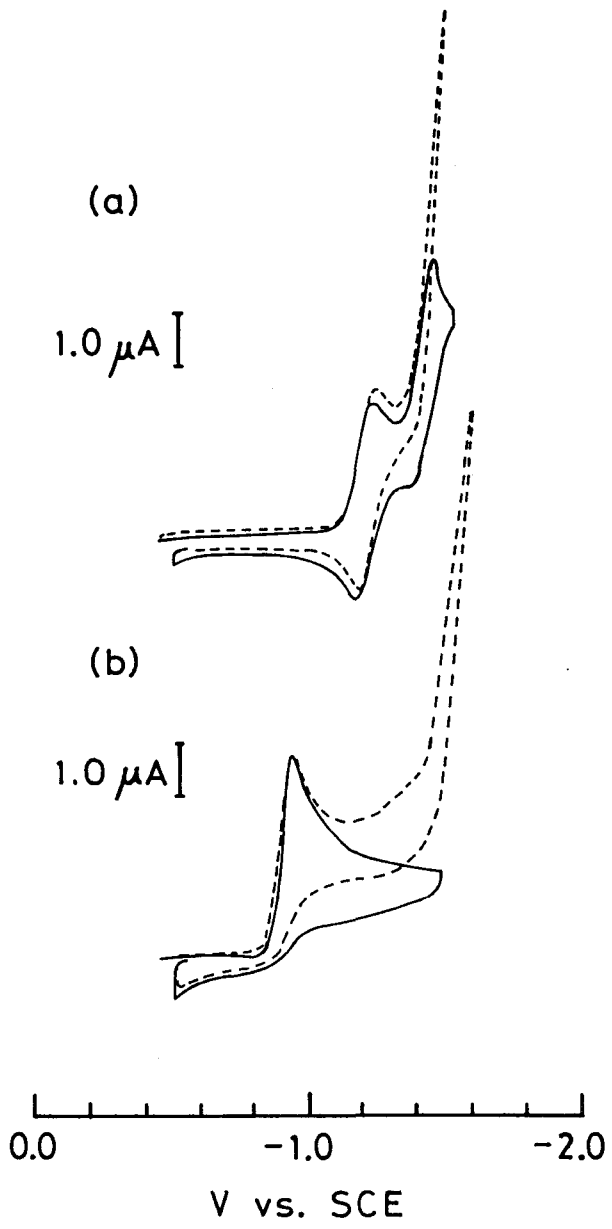

Figure 2-2. Cyclic voltammograms of (a) $[Ru(bpy)_2(CO)Cl]^+$ and (b) $[Ru(bpy)_2(CO)_2]^{2+}$ (5.0×10^{-4} mol dm^{-3}) in DMF containing $NBu^n{}_4ClO_4$ (0.10 mol dm^{-3}) as a supporting electrolyte under N_2 (———) and CO_2 (– – –) atmosphere, using an Hg electrode (sweep rate = 0.10 V s^{-1}).

The cyclic voltammogram of $[Ru(bpy)_2(CO)_2]^{2+}$ under N_2 atmosphere shows an irreversible cathodic wave at -0.95 V *vs.* SCE at the sweep rate 0.10 V s^{-1} (a solid line in Figure 2-2b). If one assumes that the diffusion constant of $[Ru(bpy)_2(CO)_2]^{2+}$ is essentially identical with that of $[Ru(bpy)_2(CO)Cl]^{+}$ on the basis of their similar structures, the number of electrons consumed in the irreversible cathodic wave of $[Ru(bpy)_2(CO)_2]^{2+}$ at -0.95 V can be determined by using the diffusion constant of $[Ru(bpy)_2(CO)Cl]^{+}$ calculated from the reversible cathodic wave at -1.24 V *vs.* SCE. The diffusion constant of an electroactive species which undergoes a reversible redox reaction can be correlated with its peak current (i_p) in the cyclic voltammogram at 25°C as expressed by eq. 2-5,[26]

$$i_p(rev) = (2.69 \times 10^5)\, n^{3/2}\, A\, D_0^{1/2}\, v^{1/2}\, C_0^{*} \qquad (2\text{-}5)$$

where n, A, D_0, v, and C_0^{*} are the number of electrons consumed in the redox reaction, the surface area (cm^2) of an electrode, the diffusion constant ($cm^2\ s^{-1}$) of an electroactive species, a voltage sweep rate (V s^{-1}), and the bulk concentration (mol cm^{-3}) of an electroactive species, respectively. Thus, the diffusion constant of $[Ru(bpy)_2(CO)Cl]^{+}$ is determined as 3.0×10^{-6} $cm^2\ s^{-1}$ from the peak current 2.3×10^{-6} A of the one-electron reversible cathodic wave at the sweep rate 0.20 V s^{-1}.[27] On the other hand, the relationship between the peak current $i_p(irr)$ and the diffusion constant D_0 of an electroactive species which undergoes a

totally irreversible redox reaction, can be expressed by eq. 2-6,[28]

$$i_p(irr) = (2.99 \times 10^5)\, n \left(\frac{47.7}{|E_p - E_{p/2}|} \right)^{1/2} \cdot A \cdot D_0^{1/2} \cdot v^{1/2} \cdot C_0^* \quad (2\text{-}6)$$

where E_p and $E_{p/2}$ are the peak potential (mV) of an irreversible wave and the potential (mV) at $i_{p/2}$, respectively. The values of $|E_p - E_{p/2}|$ and $i_p(irr)$ of the irreversible cathodic wave of $[Ru(bpy)_2(CO)_2]^{2+}$ at the sweep rate 0.20 V s^{-1} were calculated as 60 mV and 4.5×10^{-6} A, respectively. Substitution of these values in eq. 2-6 yields n = 1.96. Thus, $[Ru(bpy)_2(CO)_2]^{2+}$ undergoes an irreversible two-electron reduction around -0.95 V.

The cyclic voltammograms of $[Ru(bpy)_2(CO)Cl]^+$ and $[Ru(bpy)_2(CO)_2]^{2+}$ in CO_2-saturated DMF (dashed lines in Figures 2-2a and 2b, respectively) are essentially the same as those of the corresponding complexes in N_2-saturated DMF, except that strong cathodic currents begin to flow around -1.40 V vs. SCE in CO_2-saturated DMF (compare solid lines and dashed lines in Figures 2-2a and 2b). Removal of CO_2 from CO_2-saturated DMF solutions of $[Ru(bpy)_2(CO)Cl]^+$ and $[Ru(bpy)_2(CO)_2]^{2+}$ by bubbling N_2 through the solution for 1 h resulted in complete disappearance of the strong cathodic currents to give the cyclic voltammograms of those complexes in N_2-saturated DMF solutions. Thus, in the presence of $[Ru(bpy)_2(CO)Cl]^+$ or $[Ru(bpy)_2(CO)_2]^{2+}$, CO_2 can be reduced at -1.40 V vs. SCE.

Electrochemical Reduction of CO_2. The controlled potential electrolysis of a CO_2-saturated anhydrous DMF solution containing $NBu^n_4ClO_4$ as a supporting electrolyte and $[Ru(bpy)_2(CO)_2]^{2+}$ as a catalyst at -1.50 V vs. SCE has resulted in decomposition of the complex to yield a black precipitate with liberation of only about 10% on the basis of the amount of $[Ru(bpy)_2(CO)_2]^{2+}$.[29] However, the same electrolysis of a CO_2-saturated H_2O/DMF (1:1, v/v) solution containing LiCl (0.10 mol dm^{-3}) as a supporting electrolyte and $[Ru(bpy)_2(CO)_2]^{2+}$ (5.0×10^{-4} mol dm^{-3}) catalytically produces $HCOO^-$ and CO (eqs. 2-2 and 2-3) together with a little amount of H_2 (eq. 2-4), as shown in Figure 2-3. This result is in contrast to the catalytic reduction of CO_2 by the electrochemically (-1.50 V vs. SCE) reduced species $Re(bpy)(CO)_3Cl$ in CO_2-saturated CH_3CN, where the reduction of CO_2 takes place according to eq. 2-7.[2] Thus, the present CO_2 reduction does not result from an oxide transfer reaction shown in eq. 2-7.

$$2CO_2 + 2e^- \longrightarrow CO + CO_3^{2-} \qquad (2\text{-}7)$$

As shown in Figure 2-3, the amount of CO formed increases linearly with the number of coulombs consumed in the reaction of CO_2 up to 60 coulombs, and thereafter the rate of CO evolution gradually decreases. On the other hand, the amount of $HCOO^-$ formed slowly increases during the consumption of initial 60 coulombs and thereafter rapidly increases. The turnover numbers

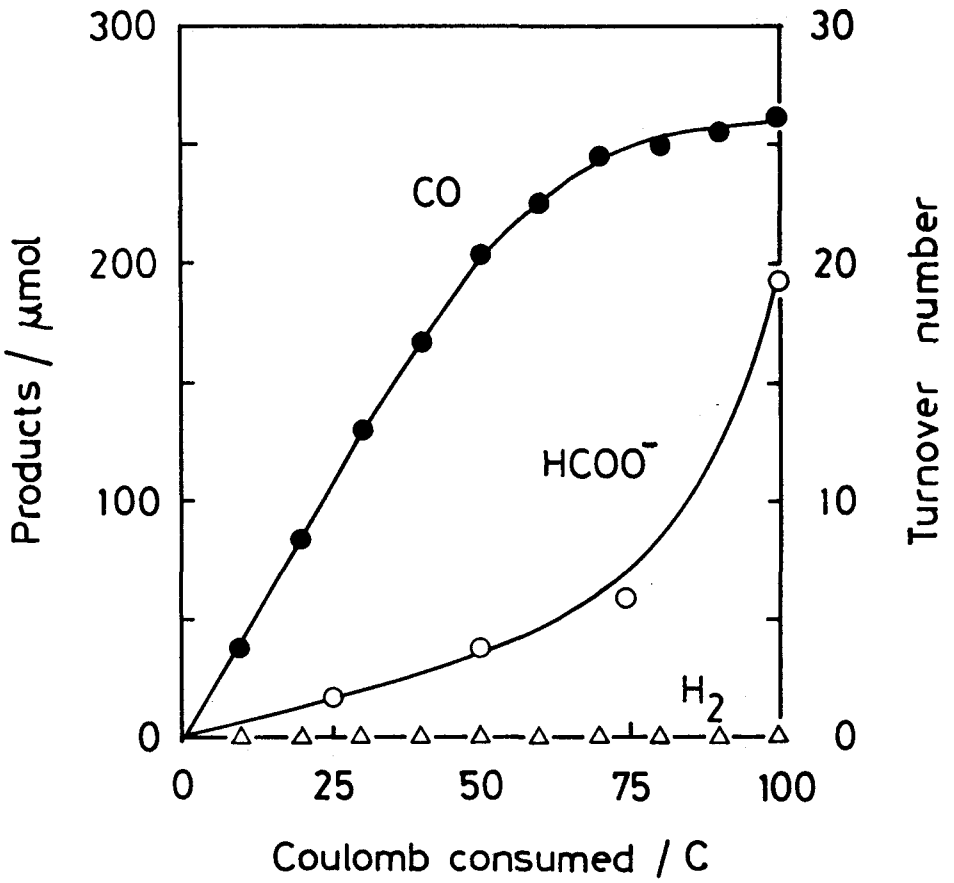

Figure 2-3. Plots of the amounts of products vs. the coulomb number consumed in the electrolysis (-1.50 V vs. SCE) of CO_2-saturated H_2O/DMF (1:1 v/v) solution containing $[Ru(bpy)_2(CO)_2](PF_6)_2$ (5.0×10^{-4} mol dm^{-3}) and LiCl (0.10 mol dm^{-3}) as a supporting electrolyte at 30°C.

for the formation of CO and $HCOO^-$ based on $[Ru(bpy)_2(CO)_2]^{2+}$ are 26.2 and 18.2, respectively, when the reduction consumed 100 coulombs, as summarized in entry 1 in Table 2-I. A similar result was obtained also in the reduction of CO_2 by $[Ru(bpy)_2(CO)Cl]^+$ under the same electrolysis conditions (entry 6 in Table 2-I). An increase and a decrease of the rates for the formation of $HCOO^-$ and CO, respectively, with a lapse of time may be associated with a decrease of the proton concentration due to the consumption of protons with the progress of the reactions shown by eqs. 2-2 and 2-3. In accordance with this, the electrolysis of a CO_2-saturated H_2O (pH 6.0 buffered with H_3PO_4-NaOH)/DMF mixture (9:1 v/v) containing $[Ru(bpy)_2(CO)_2]^{2+}$ produces only CO and H_2, both of which increase in the amount linearly with time, as shown in Figure 2-4a; no $HCOO^-$ has been detected in solution even after the reduction consumed 100 coulombs (entry 2 in Table 2-I). This is the case with $[Ru(bpy)_2(CO)Cl]^+$ used as a catalyst, as shown in Figure 2-4b. Similar results were obtained also in the reduction of CO_2 in CO_2-saturated water at pH 6.0 and in a CO_2-saturated H_2O (pH 6.0)/DMF (1:1 v/v) mixture (entries 3 and 4, respectively, in Table 2-I). It is worthwhile to note that the amount of H_2 evolved in the reduction of CO_2 conducted in water at pH 6.0 is much larger than in H_2O (pH 6.0)/DMF (1:1 v/v) (compare entries 3 with 4 in Table 2-I). This is suggestive of the competitive reductions of CO_2 and protons taking place. In fact, the amounts of CO and H_2 formed increase and decrease, respectively, with the decreasing H_2O (pH 6.0)/DMF ratios

Table 2-I. Electrochemical CO_2 Reductions Catalyzed by Ruthenium Bipyridyl Complexes in H_2O/DMF Systems

Entry	Catalyst[a]	H_2O/DMF v/v	(pH)[b]	Coulomb consumed	Product[c] CO	H_2	$HCOO^-$
1	$[Ru(bpy)_2(CO)_2]^{2+}$	1/1	Not fixed[d]	100	262	2	182
2		9/1	(6.0)	100	142	182	——
3		1/0	(6.0)	100	88	282	——
4		1/1	(6.0)	100	217	18	——
5		9/1	(9.5)	100	136	192	199
6	$[Ru(bpy)_2(CO)Cl]^+$	1/1	Not fixed[d]	90	255	21	78
7		9/1	(6.0)	100	107	217	——
8		9/1	(9.5)	75	110	170	101

[a] PF_6^- salt, 5.0×10^{-4} mol dm^{-3}, 20 cm^3. [b] Buffered with H_3PO_4-NaOH. [c] μmol.

[d] LiCl was used as an electrolyte.

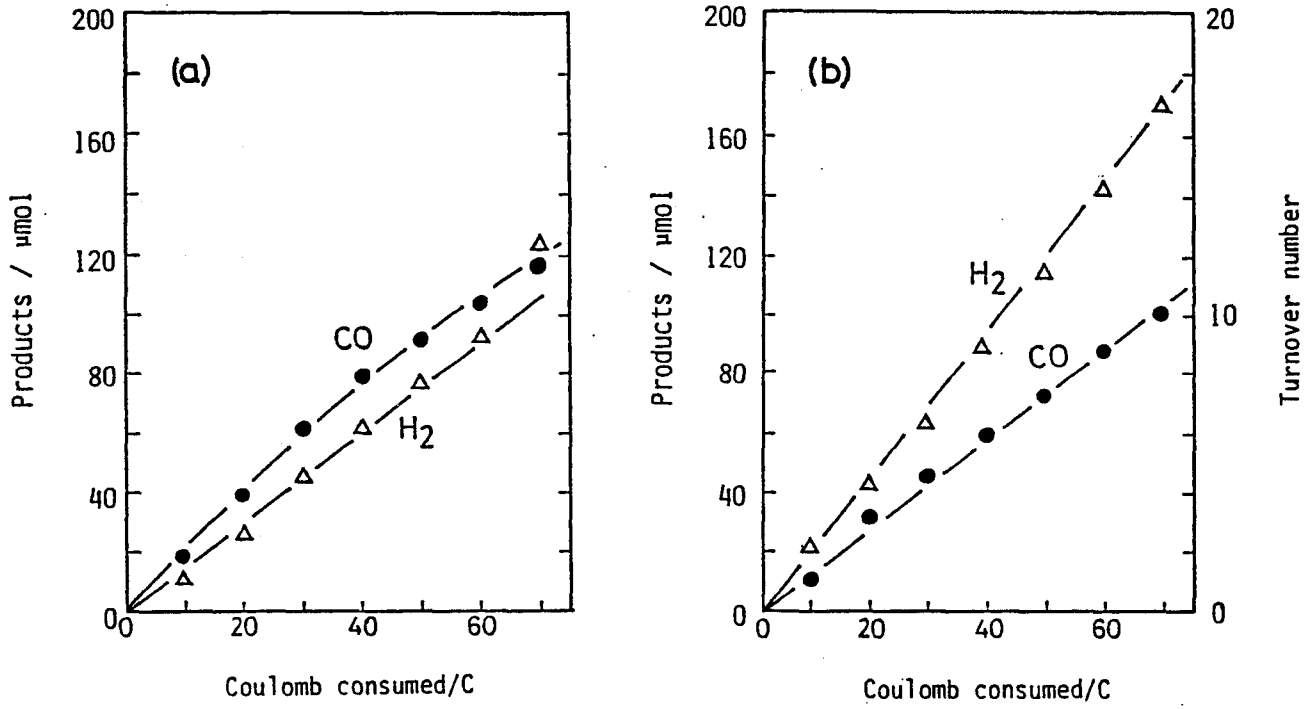

Figure 2-4. Plots of the amounts of products vs. the coulomb number consumed in the electrolysis (-1.50 V vs. SCE) of CO_2-saturated H_2O (pH 6.0)/DMF (9:1 v/v) solutions of (a) $[Ru(bpy)_2(CO)_2](PF_6)_2$ and (b) $[Ru(bpy)_2(CO)Cl](PF_6)$ (5.0×10^{-4} mol dm^{-3}), buffered with H_3PO_4-NaOH.

(entries 2 - 4 in Table 2-I). It is noted that that no $HCOO^-$ has been formed at all irrespective of the proportion of water in H_2O (pH 6.0)/DMF mixtures so long as the pH value of water is kept at 6.0 (entries 2 - 4 and 7 in Table 2-I).

The electrolysis of a CO_2-saturated alkaline solution, H_2O (pH 9.5)/DMF (9:1 v/v), of $[Ru(bpy)_2(CO)_2]^{2+}$ or $[Ru(bpy)_2(CO)Cl]^+$ catalytically produces $HCOO^-$ together with CO and H_2 with no induction period, and the amounts of $HCOO^-$ and CO increase linearly with the progress of the reaction, as shown in Figure 2-5a or 5b. It is well known that CO_2 readily reacts with OH^- in alkaline solutions to afford HCO_3^- and CO_3^{2-}, which exist as equilibrium mixtures with CO_2 in solution.[30] The controlled potential electrolysis of an aqueous solution of Na_2CO_3 or $NaHCO_3$ (0.10 mol dm^{-3}) in place of CO_2 in the presence of $[Ru(bpy)_2(CO)_2]^{2+}$ at -1.50 V vs. SCE, however, has produced only a stoichiometric amount of $HCOO^-$ without evolving CO even after 50 coulombs was consumed in the reduction. Moreover, the electrolysis of an H_2O (pH 9.5)/DMF (9:1 v/v) solution of HCOONa (0.10 mol dm^{-3}) in the presence of $[Ru(bpy)_2(CO)_2]^{2+}$ at -1.50 V has produced only H_2, suggesting that the conversion of $HCOO^-$ to CO does not take place under the present electrolysis conditions (eq. 2-8). Thus, the catalytic formation of CO and $HCOO^-$ in the

$$HCOO^- \longrightarrow CO + OH^- \qquad (2\text{-}8)$$

electrolysis of a CO_2-saturated H_2O (pH 9.5)/DMF (9:1 v/v)

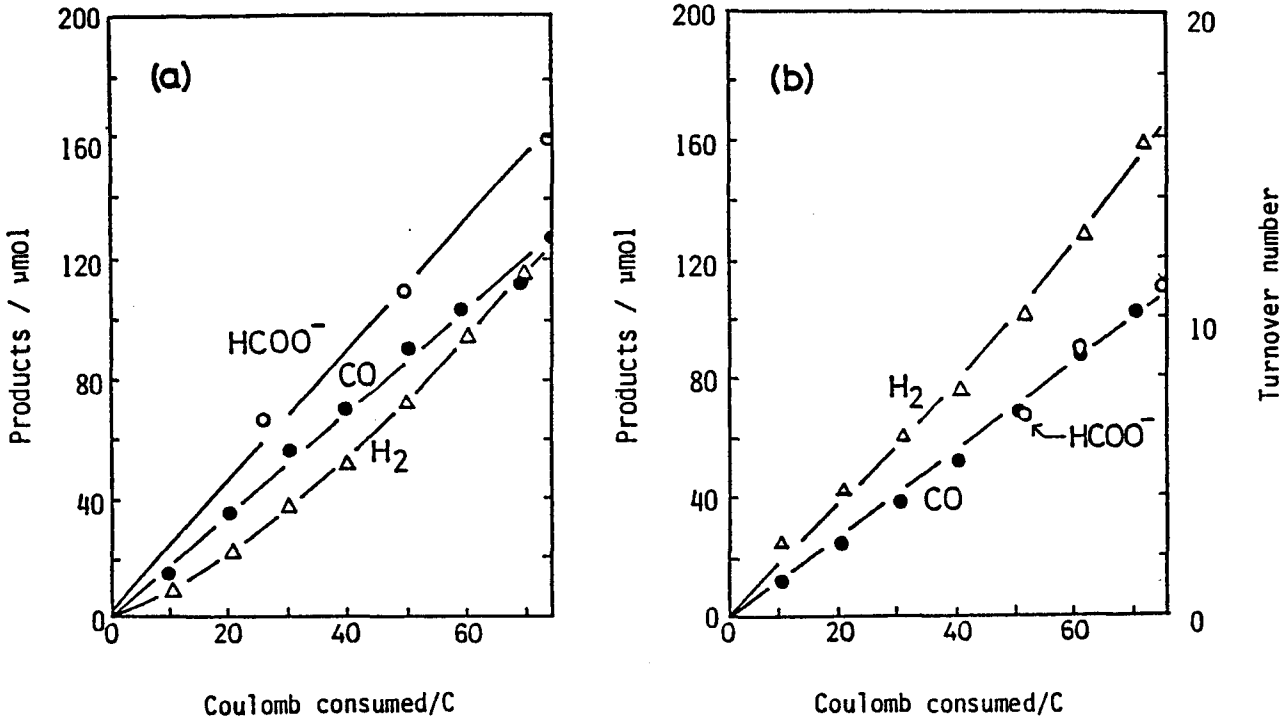

Figure 2-5. Plots of the amounts of products vs. the coulomb number consumed in the electrolysis (-1.50 V vs. SCE) of CO_2-saturated H_2O (pH 9.5)/DMF (9:1 v/v) solutions of (a) $[Ru(bpy)_2(CO)_2](PF_6)_2$ and (b) $[Ru(bpy)_2(CO)Cl](PF_6)$ (5.0×10^{-4} mol dm^{-3}), buffered with H_3PO_4-NaOH.

solution either of $[Ru(bpy)_2(CO)_2]^{2+}$ or of $[Ru(bpy)_2(CO)Cl]^+$ (entries 5 and 8 in Table 2-I) may come from two different precursors.

Active Species in the Electrochemical Reduction of CO_2. In order to obtain information concerning active species in the present reaction, the spectroelectrochemical experiment was carried out with an OTTLE cell. The controlled potential electrolysis of $[Ru(bpy)_2(CO)_2]^{2+}$ in CO_2-saturated DMF at -1.10 V leads to the occurrence of two new bands at 350 (shoulder) and 420 nm in its electronic absorption spectrum, as shown in Figure 2-6. The spectrum obtained upon the electrolysis for 60 min agreed very closely with that of $[Ru(bpy)_2(CO)(COO^-)]^+$ generated in aqueous alkaline solutions, which is consistent also with that of a DMF solution containing $[Ru(bpy)_2(CO)_2]^{2+}$ and 2 molar equiv. of $NBu^n{}_4OH$.[31] These facts strongly suggest that the two-electron reduction product of $[Ru(bpy)_2(CO)_2]^{2+}$ reacts with CO_2 to afford $[Ru(bpy)_2(CO)(COO^-)]^+$, which is supposed to be an important intermediate in the present electrochemical CO_2 reductions.

As described in the previous section, the reduction of CO_2 in H_2O (pH 9.5)/DMF (9:1 v/v) produces $HCOO^-$ as well as CO as main products. Increasing amount of $HCOO^-$ formed upon decreasing the proton concentration may be associated with the shift of an equilibrium among $[Ru(bpy)_2(CO)_2]^{2+}$, $[Ru(bpy)_2(CO)C(O)OH]^+$, and $[Ru(bpy)_2(CO)(COO^-)]^+$ in solutions (eq. 2-9 and 2-10). The equilibrium constants, $K_1 = 1.32 \times 10^5$ mol^{-1} dm^3 and $K_2 = 2.27$ x

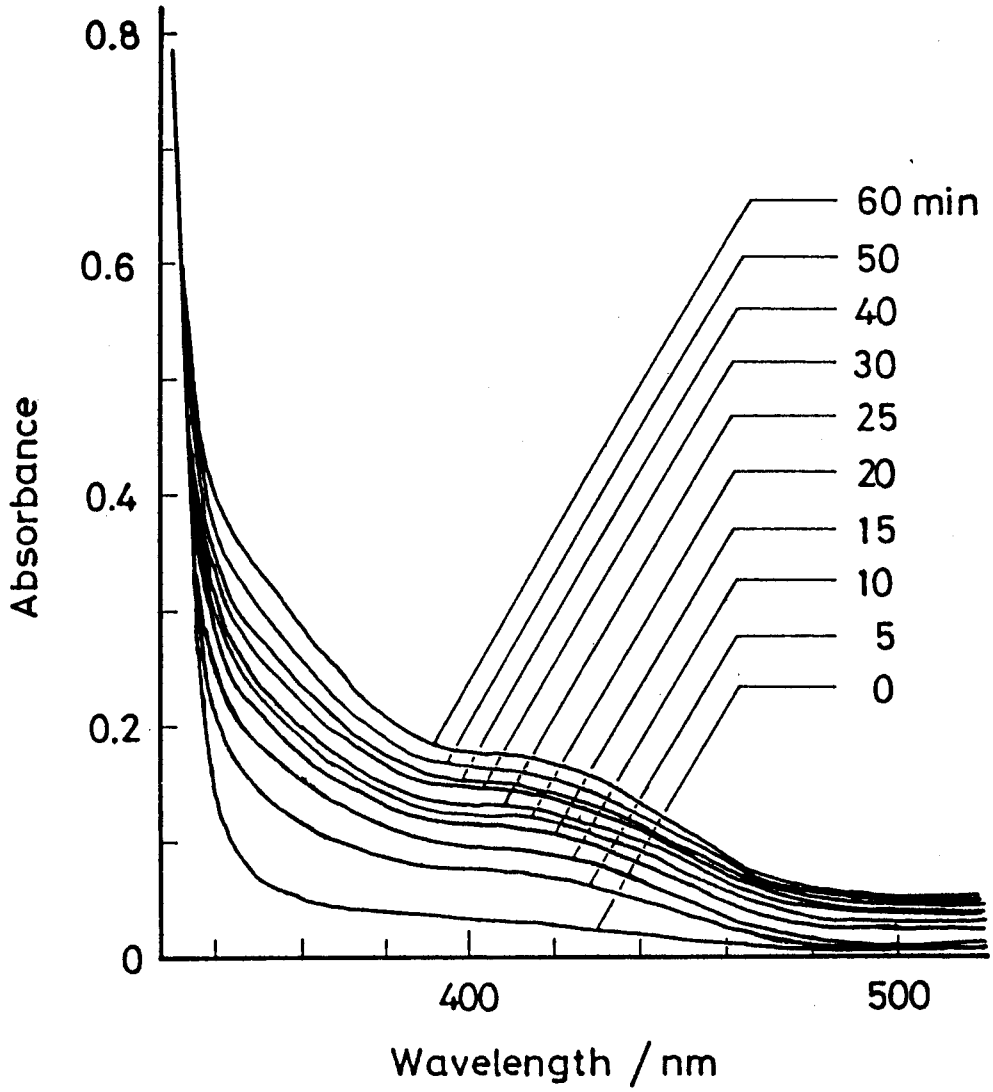

Figure 2-6. Electronic absorption spectra of a CO_2-saturated DMF solution of $[Ru(bpy)_2(CO)_2]^{2+}$ (5.0×10^{-4} mol dm^{-3}) under the controlled potential electrolysis at -1.10 V vs. SCE.

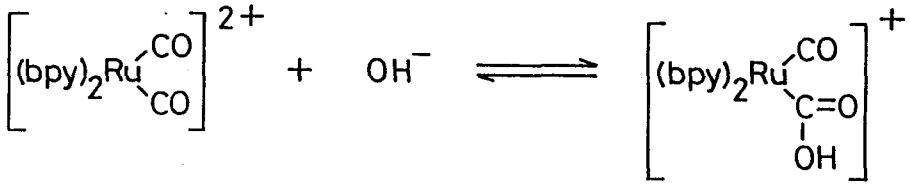

(2-9)

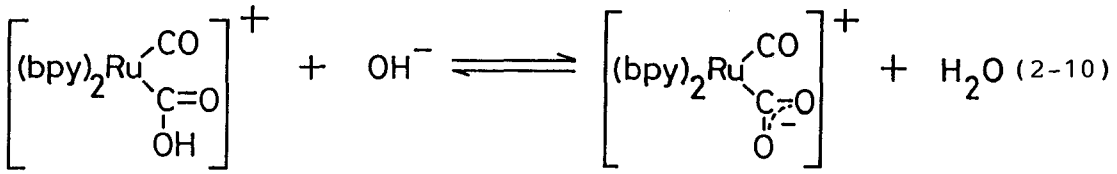

(2-10)

10^4 mol^{-1} dm^3 for eqs. 2-9 and 2-10, respectively, in water at 25°C, have little changed from those in an H_2O (at various pH)/DMF (9:1 v/v) mixture, as confirmed from the comparison of the electronic absorption spectra of $[Ru(bpy)_2(CO)_2]^{2+}$ in both solvents. The distribution curves of $[Ru(bpy)_2(CO)_2]^{2+}$, $[Ru(bpy)_2(CO)C(O)OH]^+$, and $[Ru(bpy)_2(CO)(COO^-)]^+$ calculated from the equilibrium constants K_1 and K_2 in H_2O are depicted in Figure 2-7, which indicates that only $[Ru(bpy)_2(CO)_2]^{2+}$ exists as a stable species under acidic conditions. Therefore, $[Ru(bpy)_2(CO)_2]^{2+}$ may be a precursor for the production of CO in the reduction of CO_2 conducted in H_2O (pH 6.0)/DMF (9:1 v/v).

In weak alkaline solutions, however, $[Ru(bpy)_2(CO)_2]^{2+}$, $[Ru(bpy)_2(CO)C(O)OH]^+$, and $[Ru(bpy)_2(CO)(COO^-)]^+$ coexist as an equilibrium mixture; for instance the proportion of these three ruthenium species in H_2O at pH 9.5 are 12.5 : 51.0 : 36.5. The electrolysis of a weak alkaline solution, such as an H_2O (pH

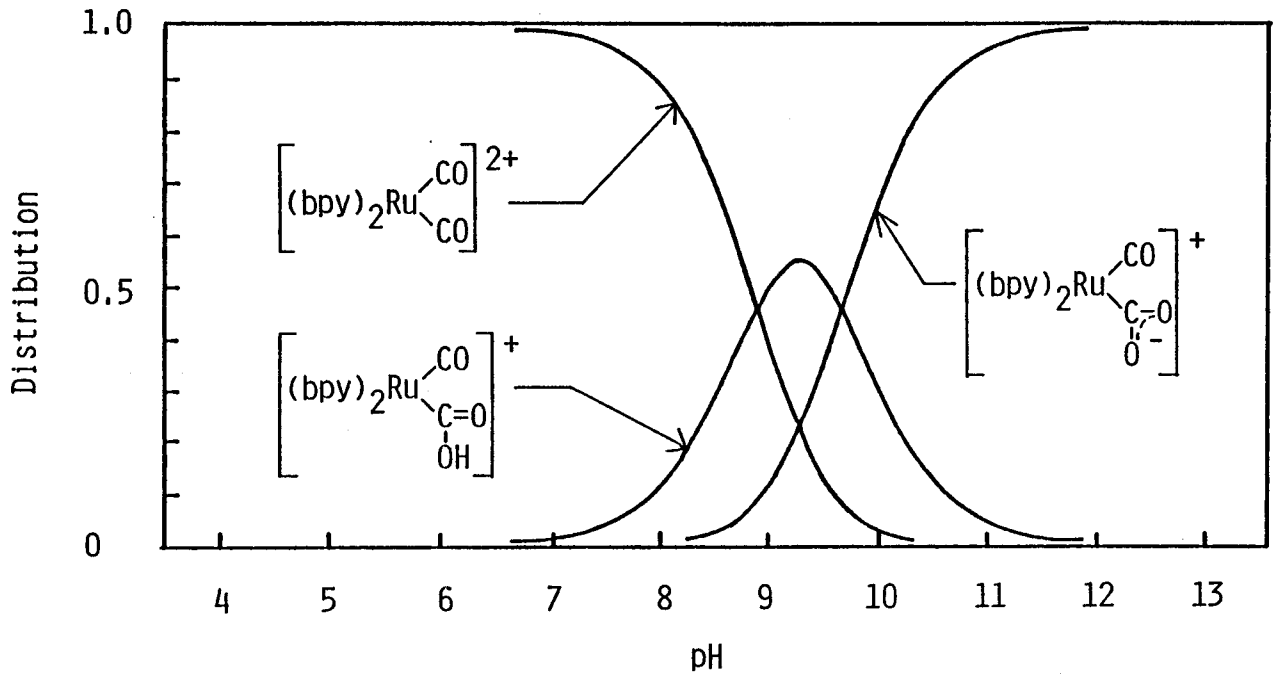

Figure 2-7. Distribution of the ruthenium species in H_2O at various pH at 25°C.

9.5)/DMF (9:1 v/v) mixture, saturated with CO_2 produces an almost equivalent amount of $HCOO^-$ and CO. This is suggestive of $[Ru(bpy)_2(CO)C(O)OH]^+$ or $[Ru(bpy)_2(CO)(COO^-)]^+$ being a precursor for the formation of $HCOO^-$. This is consistent with the result that the electrolysis of an aqueous solution of $[Ru(bpy)_2(CO)_2]^{2+}$ at -1.50 V has produced a stoichiometric amount of $HCOO^-$ at pH 11.0 (buffered with Na_2CO_3), where $[Ru(bpy)_2(CO)(COO^-)]^+$ and a small amount of $[Ru(bpy)_2(CO)C(O)OH]^+$ coexist. For further clarification of the precursor for the formation of $HCOO^-$ in the reduction of CO_2, the reduction potentials of $[Ru(bpy)_2(CO)C(O)OH]^+$ and $[Ru(bpy)_2(CO)(COO^-)]^+$ were examined. The cyclic voltammogram of $[Ru(bpy)_2(CO)_2]^{2+}$ in H_2O at pH 10.5, where $[Ru(bpy)_2(CO)_2]^{2+}$ is almost completely converted to $[Ru(bpy)_2(CO)C(O)OH]^+$ and $[Ru(bpy)_2(CO)(COO^-)]^+$ (Figure 2-7), showed an irreversible cathodic wave at -1.50 V vs. SCE. The peak potential of the cathodic wave was shifted by -30 mV/pH with increasing the pH value, suggesting that the reduction involves two electrons together with one proton; the proton may participate into the diffusion controlled equilibrium reaction between $[Ru(bpy)_2(CO)C(O)OH]^+$ and $[Ru(bpy)_2(CO)(COO^-)]^+$ (eq. 2-10),[22] either of which undergoes a two-electron reduction to produce $HCOO^-$.

Mechanisms of the Reduction of CO_2. A most plausible mechanism of the reduction of CO_2 in this system is presented in Scheme 2-I. $[Ru(bpy)_2(CO)_2]^{2+}$ undergoes an irreversible two-electron reduction at -0.95 V vs. SCE to give $[Ru(bpy)_2(CO)_2]^0$

Scheme 2-I

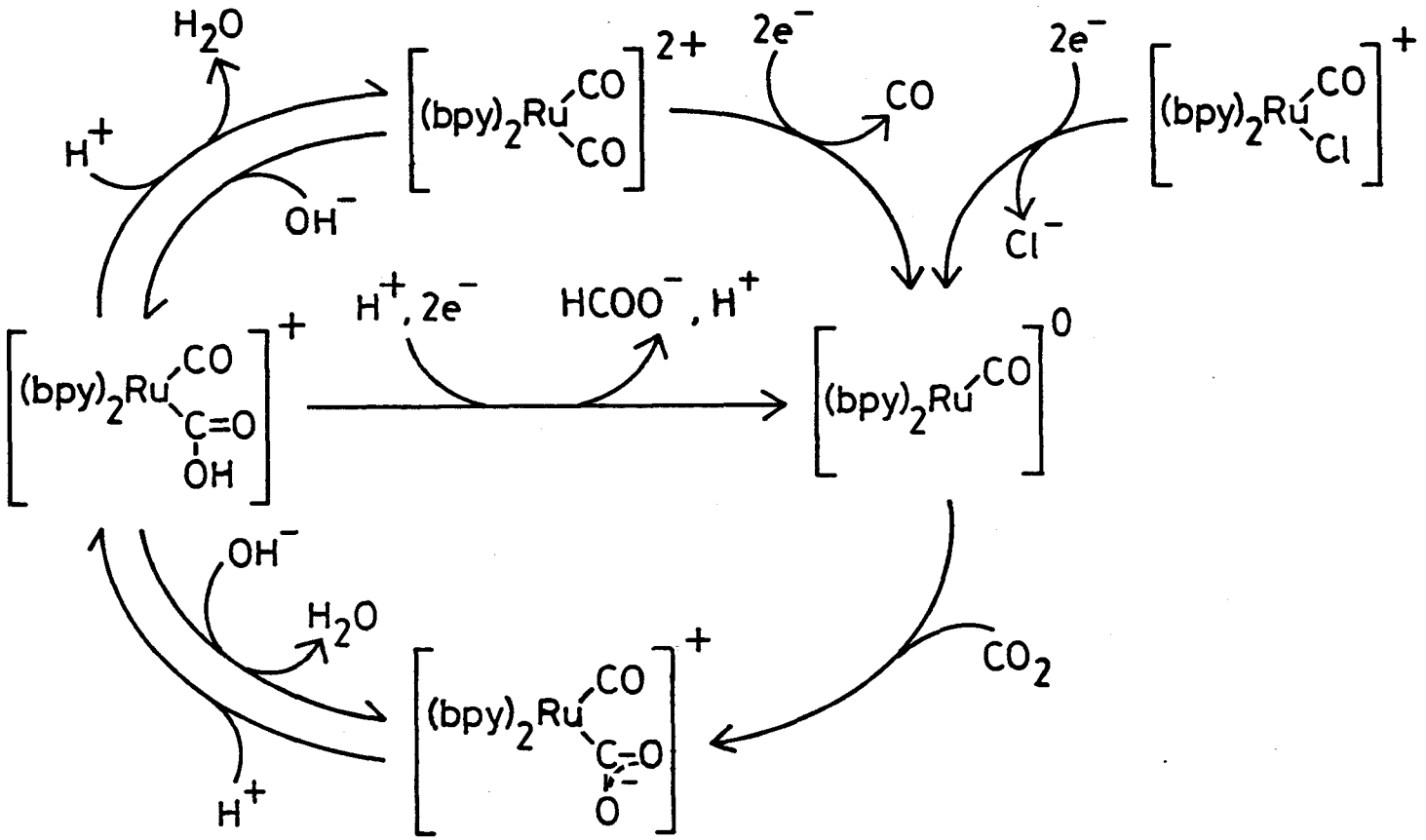
H2O
H+
OH−
[(bpy)2Ru(CO)(CO)]2+
2e−
CO
2e−
[(bpy)2Ru(CO)Cl]+
Cl−
H+, 2e−
HCOO−, H+
[(bpy)2Ru(CO)(C=O)OH]+
[(bpy)2Ru(CO)]0
OH−
H2O
H+
[(bpy)2Ru(CO)(C=O)O−]+
CO2

with 20 electrons, which may liberate CO, generating penta-coordinated $[Ru(bpy)_2(CO)]^0$ with 18 electrons, though unstable. In the absence of CO_2 in solutions, $[Ru(bpy)_2(CO)]^0$ thus formed may be oxidized by a proton to afford $[Ru(bpy)_2(CO)H]^+$,[32] which reacts with another proton to evolve H_2.[33] In the presence of a large excess of CO_2, however, $[Ru(bpy)_2(CO)]^0$ is converted to $[Ru(bpy)_2(CO)(COO^-)]^+$ possibly <u>via</u> $[Ru(bpy)_2(CO)(COO)]^0$. This is consistent with the fact that CO_2 rapidly reacts with a variety of bases B, such as OH^-, RO^-, R^-, and R_nNH_{3-n} (R = alkyl group, n = 0 - 3), to yield the 1:1 adducts, $B\text{-}COO^-$. Of various $\eta^1\text{-}CO_2$ metal complexes reported so far,[34-41] $[W(CO)_5CO_2]^{2-}$ formed in the reaction of $[W(CO)_5]^{2-}$ with CO_2 at -78°C undergoes an oxide transfer reaction with another CO_2 molecule to produce $[W(CO)_6]$ and CO_3^{2-} at room temperature.[34] Although $[Ru(bpy)_2(CO)(COO^-)]^+$ does not undergo such an oxide transfer reaction with another CO_2 molecule, it may easily be converted to $[Ru(bpy)_2(CO)_2]^{2+}$ <u>via</u> $[Ru(bpy)_2(CO)C(O)OH]^+$ in acidic conditions according to the equilibrium reactions shown in eqs. 2-9 and 2-10, and in Scheme 2-I. Thus, the reduction of CO_2 conducted in acidic media produces only CO. On the other hand, in weak alkaline solutions such as pH 9.5, $[Ru(bpy)_2(CO)C(O)OH]^+$ (or $[Ru(bpy)_2(CO)(COO^-)]^+$) exists as a predominant species (Figure 2-7), which may undergo a two-electron reduction involving the participation of one proton to give $HCOO^-$ with regenerating the penta-coordinated ruthenium(0) complex, $[Ru(bpy)_2(CO)]^0$. The evolution of CO at the same time may come from the two-electron reduction of

$[Ru(bpy)_2(CO)_2]^{2+}$ existing as a minor component (Figure 2-7) in the solution.

As described in the previous section, there is a close similarity between $[Ru(bpy)_2(CO)_2]^{2+}$ and $[Ru(bpy)_2(CO)Cl]^{+}$ as catalysts for the reduction of CO_2, suggesting that the two-electron reduction of $[Ru(bpy)_2(CO)_2Cl]^{+}$ results in the dissociation of Cl^- to afford the unstable pentacoordinated intermediate $[Ru(bpy)_2(CO)]^0$, which may react with CO_2 to generate $[Ru(bpy)_2(CO)(COO^-)]^{+}$. Several attempts to identify the formation of $[Ru(bpy)_2(CO)(COO^-)]^{+}$ in electrochemical two-electron reductions of $[Ru(bpy)_2(CO)Cl]^{+}$ at -1.40 to -1.50 V vs. SCE in CO_2-saturated anhydrous DMF, however, have resulted in the formation of only an insoluble black precipitate. This is probably due to instability of $[Ru(bpy)_2(CO)(COO^-)]^{+}$ in anhydrous DMF at such potentials. It is well known that $[Ru(bpy)_2XY]^{n+}$ (X, Y = pyridine derivatives, halides, phosphines, and so on; n = 0 - 2) undergoes two successive one-electron reversible or quasi-reversible reductions,[42] when the added electrons may localize mainly in π^*-orbitals of the bipyridine ligands.[43, 44] A strong π-electron acceptor CO ligand, however, may resist such an electron localization in $[Ru(bpy)_2(CO)_2]^0$ and $[Ru(bpy)_2(CO)Cl]^-$. Thus, two-electron reductions of $[Ru(bpy)_2(CO)_2]^{2+}$ and $[Ru(bpy)_2(CO)Cl]^{+}$ may be followed by chemical reactions possibly to generate $[Ru(bpy)_2(CO)]^0$. The participation of $[Ru(bpy)_2(CO)]^0$ in the catalytic cycle of the present CO_2 reduction reasonably explains the formation of CO and $HCOO^-$ depending on pH of the solutions.

2-4 References

(1) Hawecker, J.; Lehn, J. M.; Ziessel, R. J. Chem. Soc., Chem. Commun. **1984**, 328.

(2) (a) Sullivan, B. P.; Bolinger, C. M.; Conrad, D.; Vining, W. J.; Meyer. T. J. J. Chem. Soc., Chem. Commun. **1985**, 1414. (b) O'Toole, T. R.; Margerum, L. D.; Westmoreland, T. D.; Vining, W. J.; Murray, R. W.; Meyer, T. J. J. Chem. Soc., Chem. Commun. **1985**, 1416.

(3) Ishida, H.; Tanaka, K.; Tanaka, T. Chem. Lett. **1985**, 405.

(4) Bolinger, C. M.; Sullivan, B. P.; Comrad, D.; Gilbert, J. A.; Story, N.; Meyer, T. J. J. Chem. Soc., Chem. Commun. **1985**, 796.

(5) Slater, S.; Wagenknecht, J. H. J. Am. Chem. Soc. **1984**, 106, 5367.

(6) Beley, M.; Collin, J. P.; Ruppert, R.; Sauvage, J. P. J. Chem. Soc., Chem. Commun. **1984**, 1315.

(7) Tezuka, M.; Yajima, T.; Tsuchiya, A.; Matsumoto, Y.; Uchida, Y.; Hidai, M. J. Am. Chem. Soc. **1982**, 104, 6834.

(8) (a) Lieber, C. M.; Lewis, N. S. J. Am. Chem. Soc. **1984**, 106, 5033. (b) Fisher, B.; Eisenberg, R. J. Am. Chem. Soc. **1980**, 102, 7361. (c) Meshitsuka, S; Ichikawa, M.; Tamaru, K. J. Chem. Soc., Chem. Commun. **1974**, 158. (d) Hiratsuka, K.; Takahashi, K.; Sasaki, H.; Toshima, S. Chem. Lett. **1977**, 1137. (e) Takahashi, K.; Hiratsuka, K.; Sasaki, H.; Toshima, S. Chem. Lett. **1979**, 305. (f)

Kapusta, S.; Hackerman, N. J. Electrochem. Soc. **1984**, 131, 1511.

(9) Stalder, C. J.; Chao, S.; Wrighton, M. S. J. Am. Chem. Soc. **1984**, 106, 3673.

(10) Amatore, C.; Saveant, J. M. J. Am. Chem. Soc. **1981**, 103, 5021.

(11) (a) Lehn, J. M.; Ziessel, R. Proc. Natl. Acad. Sci. USA. **1982**, 79, 701. (b) Hawecker, J. M.; Ziessel, R. J. Chem. Soc., Chem. Commun. **1983**, 536. (c) Hawecker, J.; Lehn, J. M.; Ziessel, R. J. Chem. Soc., Chem. Commun. **1985**, 56.

(12) Sullivan, B. P.; Meyer, T. J. J. Chem. Soc., Chem. Commun. **1984**, 1244.

(13) Kitamura, N.; Tazuke, S. Chem. Lett. **1983**, 1109.

(14) Bradley, M. G.; Tysak, T.; Graves, D. J.; Vlachopoulos, N. A. J. Chem. Soc., Chem. Commun. **1983**, 349.

(15) Inoue, T.; Fujishima, A.; Konishi, S.; Honda, K. Nature **1979**, 277, 637.

(16) Parkinson, B. A.; Weaver, P. F. Nature **1984**, 309, 148.

(17) (a) Darensbourg, D. J.; Ovalles, C. J. Am. Chem. Soc. **1984**, 106, 3750. (b) Darenbourg, D. J.; Ovalles, C.; Pala, M. J. Am. Chem. Soc. **1983**, 105, 5937. (c) Darensbourg, D. J.; Rokicki, A.; Darensbourg, M. Y. J. Am. Chem. Soc. **1981**, 103, 3223.

(18) Stalder, C. J.; Chao, S.; Summers, D. P.; Wrighton, M. S. J. Am. Chem. Soc. **1983**, 105, 6318.

(19) (a) Inoue, Y.; Izumida, H.; Sasaki, Y.; Hashimoto, H. Chem. Lett. **1976**, 863. (b) Inoue, Y,; Sasaki, Y.; Hashimoto, H. J. Chem. Soc., Chem. Commun. **1975**, 718.

(20) Tatsumi, T.; Muramatsu, A.; Tominaga, H. Chem. Lett. **1985**, 593.

(21) Haynes, P.; Slaugh, L, H.; Kohnle, J. F. Tetrahedron Lett. **1970**, 365.

(22) (a) Ishida, H.; Tanaka, K.; Morimoto, M.; Tanaka, K. Organometallics. **1986**, 5, 724. (b) Tanaka, K.; Morimoto, M.; Tanaka, T. Chem. Lett. **1983**, 901.

(23) Sullivan, B. P.; Salmon, D. J.; Meyer, T. J. Inorg. Chem. **1978**, 17, 3334.

(24) Lexa, D.; Savent, J. M.; Zickler, J. J. Am. Chem. Soc., **1977**, 99, 2786.

(25) Tanaka, K.; Honjo, M.; Tanaka, T. J. Inorg. Biochem. **1984**, 22, 187.

(26) Bard, A. J.; Faulkner, L. R. "Electrochemical Methods"; Wiley: New York, **1980**, 218.

(27) The diffusion constant of $[Ru(bpy)_3]^{2+}$ in DMF was determined as 3.2×10^{-6} cm^2 s^{-1} by the same procedure, suggesting that the charge of the complexes does not influence the diffusion constant significantly.

(28) Bard, A. J.; Faulkner, L. R. "Electrochemical Methods"; Wiley: New York, 1980, 222.

(29) The amount of CO dissolved in DMF solutions has not been determined.

(30) Kern, D. M. J. Chem. Educ. **1960**, 37, 14.

(31) The absorptivity of $[Ru(bpy)_2(CO)(COO^-)]^+$ formed in the electrolysis of $[Ru(bpy)_2(CO)_2]^{2+}$ at -1.10 V for 60 min in CO_2-saturated DMF was about 60% based on that formed in the reaction of $[Ru(bpy)_2(CO)_2]^{2+}$ with 2 molar equiv. of NBu^n_4OH in DMF, since a prolonged electrolysis of $[Ru(bpy)_2(CO)_2]^{2+}$ under anhydrous conditions results in a partial decomposition even at -1.10 V.

(32) The thermal decarboxylation of $[Ru(bpy)_2(CO)C(O)OH]^+$ affording $[Ru(bpy)_2(CO)H]^+$ does not take place up to 100°C.

(33) (a) Kelly, J. M.; Vos, J. G. Angew. Chem. Int. Ed. Engl. **1982**, 21, 628. (b) Kelly, J. M.; Vos, J. G. J. Chem. Soc. Dalton. Trans. **1986**, 1045.

(34) (a) Maher, J. M.; Lee, G. R.; Cooper, N. J. J. Am. Chem. Soc. **1982**, 104, 6797. (b) Maher, J. M.; Cooper, N. J. J. Am. Chem. Soc. **1980**, 102, 7604.

(35) (a) Gambarotta, S.; Arena, F.; Floriani, C.; Zanazzi, P. F. J. Am. Chem. Soc. **1982**, 104, 5082. (b) Fachinetti, G.; Floriani, C.; Zanazzi, P. F. J. Am. Chem. Soc. **1978**, 100, 7405.

(36) Bianchini, C.; Meli, A. J. Am. Chem. Soc. **1984**, 106, 2698.

(37) (a) Lee, G. R.; Cooper, N. J. Organometallics **1985**, 4, 794. (b) Forshner, T.; Menard, K.; Culter, A. J. Chem. Soc., Chem. Commun. **1984**, 121. (c) Bodnar, T.; Coman, E.; Menard, K.; Culter, A. Inorg. Chem. **1982**, 21, 1275.

(38) (a) Francis, B. R.; Green, M. L. H.; Luong-thi, T.; Moser,

G. A. J. Chem. Soc., Dalton Trans. **1976**, 1339. (b) Green, M. L. H.; Luong-thi, T.; Moser, G. A.; Packer, I.; Pettit, F.; Roe, D. M. J. Chem. Soc., Dalton. **1976**, 1988. (c) Green, M. L. H.; Mackenzie, R. E.; Poland, J. S. J. Chem. Soc., Dalton Trans. **1976**, 1993.

(39) Bianchini, C.; Mealli, C.; Meli, A.; Sabat, M. Inorg. Chem. **1984**, 23, 2731.

(40) Calabrese, J. C.; Herskovitz, T.; Kinney, J. B. J. Am. Chem. Soc. **1983**, 105, 5914.

(41) (a) Yoshida, T.; Ueda, Y.; Otsuka, S. J. Am. Chem. Soc. **1978**, 100, 3941. (b) Grice, N.; Kao, S. C.; Pettit, R. J. Am. Chem. Soc. **1979**, 101, 1627.

(42) Sullivan, B. P.; Conrad, D.; Meyer, T. J. Inorg. Chem. **1985**, 24, 3640.

(43) Pinnick, D. V.; Durham, B. Inorg. Chem. **1984**, 23, 1440.

(44) (a) Morris, D. E.; Hanck, K. W.; DeArmond, M. K. J. Am. Chem. Soc. **1983**, 105, 3032. (b) Morris, D. E.; Hanck, K. W.; DeArmond, M. K. J. Electroanal. Chem. **1983**, 149, 115. (c) Ohsawa, Y.; DeAmond, M. K.; Hanck, K. W.; Morris, D. E.; Whitten, D. G.; Neveux, P. E., Jr. J. Am. Chem. Soc. **1983**, 105, 6522.

Chapter 3

Selective $HCOO^-$ Formation on the Electrochemical CO_2 Reduction

3-1 Introduction

In the electrochemical CO_2 reductions catalyzed by transition metal complexes,[1-4] Ni(cyclam)[1] and $Re(bpy)(CO)_3Cl$[2] are well known to catalyze selective CO formation. As a catalyst for the electrochemical generation of $HCOO^-$ is reported $Rh(diphos)_2Cl$, however the maximum current efficiency is relatively low: 42.5%. Selective $HCOO^-$ formation from HCO_3^- (eq. 3-1) is reported also

$$HCO_3^- + 2H^+ + 2e^- \longrightarrow HCOO^- + H_2O \qquad (3\text{-}1)$$

in the Pd-impregnated Pt or W electrode[3]; the current efficiency is high (85%), while the current density is cosiderably low (0.05 - 0.1 mA cm^{-1}). Thus, selective $HCOO^-$ formation by the electrochemical CO_2 reduction catalyzed by transition metal complexes is hardly reported so far.

In the previous chapter, it has been described that the CO_2 reduction catalyzed by $[Ru(bpy)_2(CO)_2]^{2+}$ (bpy = 2,2'-bipyridine) produced only CO under the controlled potential electrolysis at -1.50 V vs. SCE in a DMF/H_2O (1:9 v/v) solution buffered at pH

6.0, while a mixture of CO and $HCOO^-$ (7:10) was formed at pH 9.5 under otherwise the same electrolysis conditions. Increasing the pH of aqueous solutions, however, resulted in decreasing the reactivity due to the conversion from CO_2 to HCO_3^- and CO_3^{2-} (eqs. 3-2 and 3-3), being inactive species toward the reduction

$$CO_2 + OH^- \rightleftharpoons HCO_3^- \qquad (3\text{-}2)$$

$$HCO_3^- + OH^- \rightleftharpoons CO_3^{2-} + H_2O \qquad (3\text{-}3)$$

with $[Ru(bpy)_2(CO)_2]^{2+}$. Therefore, selective $HCOO^-$ formation has never been attained.

This chapter describes the formation of $HCOO^-$ depending on the acidity of proton sources in the electrochemical CO_2 reductions catalyzed by $[Ru(bpy)_2(CO)_2]^{2+}$ in CH_3OH and CH_3CN, where very efficient formation of $HCOO^-$ has been accomplished.

3-2 Experimental Section

Materials. Methyl amine hydrochlorides are purchased or prepared by the reaction between methyl amines and hydrogen chrolide, and recrystallyzed several times with CH_3CN/diethyl ether. Commercially available guaranteed reagent grades of phenol and $NBu^n_4ClO_4$ were used without further purification. CH_3OH was distilled with Na, and CH_3CN was purified by distillation five times with P_2O_5.

Electrochemical CO_2 Reductions. The electrolysis cell is essentially the same as described in chapter 2, except that anode and cathode compartments are seperated by a nafion membrane. An Hg pool (3.1 cm^2) and a platinum plate (ca. 3 cm^2) were used as working and auxiliary electrodes, respectively. The reaction was conducted in CO_2-saturated CH_3OH or CH_3CN (20 cm^3) containing $NBu^n{}_4ClO_4$ (0.10 mol dm^{-3}) and $[Ru(bpy)_2(CO)_2]^{2+}$ (5.0×10^{-4} mol dm^{-3}). CO and H_2 were analyzed by gas chromatography and the amount of $HCOO^-$ was determined by an isotachophoretic analyzer, in which an aqueous Triton X-100 (0.2 vol%) solution containing β-alanine (0.02 mol dm^{-3}) and HCl (0.01 mol dm^{-3}) is used as a leading electrolyte.

3-3 Results and Discussion

Electrochemical CO_2 Reductions in Alcohols. In order to attain selective $HCOO^-$ formation on electrochemical CO_2 reductions catalyzed by $[Ru(bpy)_2(CO)_2]^{2+}$, the reaction requires proton sources excluding H_2O, which is a comparatively strong acid as well as giving OH^- in the course of the reaction to afford HCO_3^- and CO_3^{2-} as inactive species for the reduction with $[Ru(bpy)_2(CO)_2]^{2+}$. Therefore, the electrochemical CO_2 reductions were performed by using CH_3OH as a proton source. Cyclic voltammograms of $[Ru(bpy)_2(CO)_2]^{2+}$ in CH_3OH under N_2 and CO_2 atmospheres by using a hanging mercury drop electrode (HMDE) with the

surface area 2.22 ± 0.07 mm^2 are shown in Figure 3-1. The cyclic voltammogram in an N_2-saturated CH_3OH solution shows a reduction peak at -1.05 V vs. SCE and a shoulder peak at -1.45 V in the irreversible cathodic wave, the latter of which may correspond to the H_2 evolution. On the other hand, the cyclic voltammogram under CO_2 atmosphere shows strong cathodic currents begin to flow around -1.0 V vs. SCE with a shoulder peak at -1.10 V vs. SCE. Removal of CO_2 from CO_2-saturated CH_3OH containing $[Ru(bpy)_2(CO)_2]^{2+}$ by bubbling N_2 through the solution for 30 min resulted in complete disappearance of the strong cathodic current to give the cyclic voltammogram in N_2-saturated CH_3OH. Therefore, the cyclic voltammograms exhibit that CH_3OH functions efficiently as a proton source (pK_a = ca. 16,[5] eq. 3-4) for the electrochemical

$$CH_3OH \rightleftharpoons CH_3O^- + H^+ \qquad (pK_a = \text{ca. } 16) \qquad (3\text{-}4)$$

CO_2 reduction catalyzed by $[Ru(bpy)_2(CO)_2]^{2+}$.

The result of the controlled potential electrolysis of a CO_2-saturated CH_3OH solution containing $NBu^n_4ClO_4$ (0.10 mol dm^{-3}) as a supporting electrolyte and $[Ru(bpy)_2(CO)_2]^{2+}$ (5.0×10^{-4} mol dm^{-3}) as a catalyst at -1.50 V vs. SCE is depicted in Figure 3-2a, which shows $HCOO^-$, CO and H_2 being produced catalytically and the amounts increasing almost linearly against coulombs consumed. The main product is $HCOO^-$ whose amount of 254 μmol at 100 coulombs, and the current efficiency was 49%. CO and H_2 also were formed with current efficiencies of 32 and 5%, respectively.

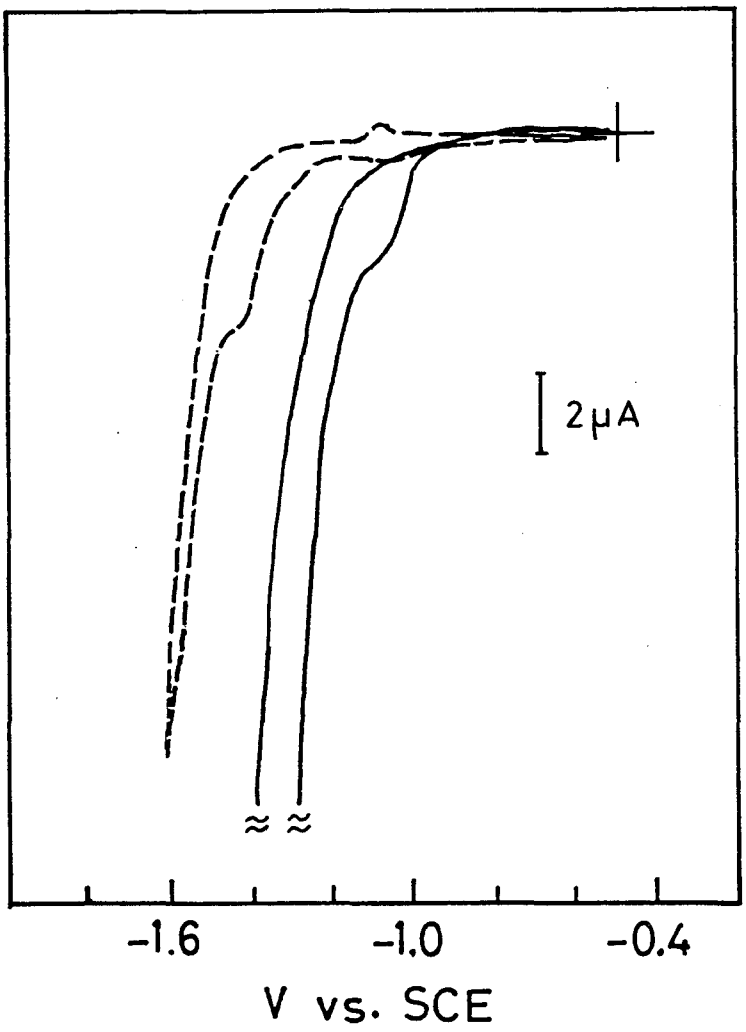

Figure 3-1. Cyclic voltammograms of $[Ru(bpy)_2(CO)_2]^{2+}$ (5.0×10^{-4} mol dm^{-3}) in CH_3OH containing $NBu^n_4ClO_4$ (0.10 mol dm^{-3}) as a supporting electrolyte under N_2 (– – –) and CO_2 (———) atmospheres, using an Hg electrode (sweep rate = 0.10 V s^{-1}).

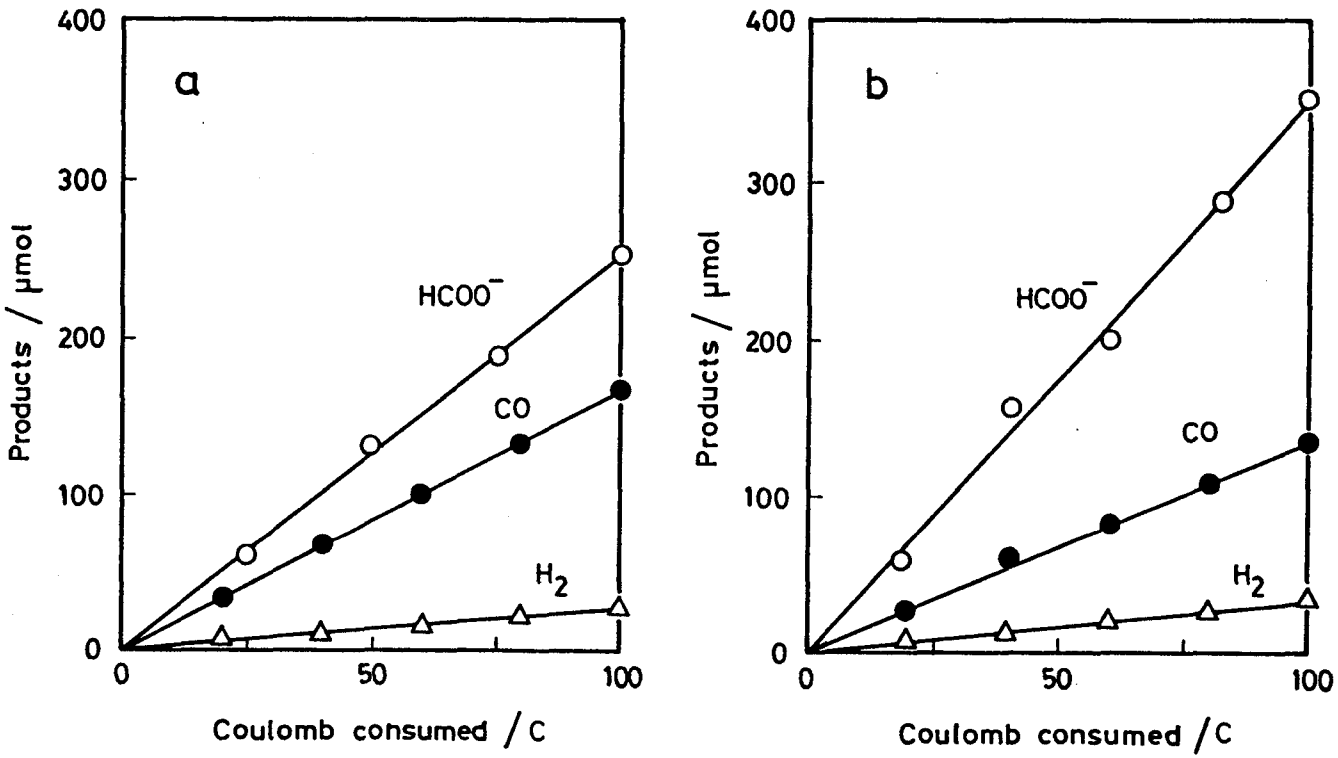

Figure 3-2. Electrochemical CO_2 reduction catalyzed by $[Ru(bpy)_2(CO)_2]^{2+}$ in CH_3OH (a) and in CH_3OH containing CH_3ONa (0.10 mol dm^{-3}) (b); -1.50 V vs. SCE, $NBu^n{}_4ClO_4$ (0.10 mol dm^{-3}).

Therefore, it is proved that CH_3OH can act as a proton donor. In order to perform more selective $HCOO^-$ formation for the present CO_2 reduction, the electrolysis was conducted in CO_2-saturated CH_3OH containing sodium methoxide, $CH_3O^-Na^+$ (0.1 mol dm^{-3}) as an electrolyte at -1.50 V vs. SCE. The result is shown in Figure 3-2b, which reveals that $HCOO^-$, CO, and H_2 are produced almost linearly against coulombs consumed with current efficiencies of 68, 26, and 6%, respectively. The reaction in CH_3OH under alkaline conditions also increased the amount of $HCOO^-$, and decreased that of CO, however highly selective $HCOO^-$ formation has never been achieved. The reaction has not been conducted under further alkaline conditions since the reaction of $CH_3O^-Na^+$ with CO_2 occurred to produce $CH_3OCO_2^-Na^+$ (eq. 3-5), which

$$CH_3O^-Na^+ + CO_2 \longrightarrow CH_3OCO_2^-Na^+ \qquad (3\text{-}5)$$

is inactive species for the present CO_2 reduction.

Ethanol as a less donative proton source was examined for the reduction of CO_2 under the controlled potential electrolysis conditions. However, the reaction has scarcely proceeded; the amounts of $HCOO^-$ and CO produced were very small. Thus, the pK_a of ethanol (ca. 18[5]; eq. 3-6) may be too large to function as the

$$C_2H_5OH \rightleftharpoons C_2H_5O^- + H^+ \quad (pK_a = \text{ca. } 18) \qquad (3\text{-}6)$$

proton source in the present electrochemical CO_2 reduction.

Therefore, no highly selective $HCOO^-$ formation has been achieved in alcohol though the selectivity of $HCOO^-$ generation was largely improved as compared with that in DMF/water.

Electrochemical CO_2 Reductions in CH_3CN in the presence of organic acids. The controlled potential electrolysis was conducted in a CO_2-saturated CH_3CN solution containing organic acids as proton sources. The results are summarized in Table 3-I, which confirms that the relative amounts of reduction products, $HCOO^-$, CO, and H_2 are largely dependent on the pK_a value of proton sources; the amount of $HCOO^-$ increases with increasing the pK_a value, and the current efficiency (η) for its formation reaches 84.3% in the presence of $(CH_3)_2NH\cdot HCl$ as a proton source. This is because no conversion from the intermediate, $[Ru(bpy)_2(CO)(COO^-)]^+$ to $[Ru(bpy)_2(CO)_2]^{2+}$ may occur for low acidity of $(CH_3)_2NH\cdot HCl$. On the other hand, the amounts of H_2 evolution increases with decreasing the pK_a value. In the case of benzoic acid used as a proton source, the current efficiency for H_2 evolution attains 50.7%, suggesting that the attack of CO_2 and H_2 to the active site of the catalyst occurs competitively.

The present electrochemical CO_2 reduction reveals not only high selectivity of the $HCOO^-$ formation but also high current density in the reduction of CO_2, the latter of which corresponds to large reaction velocity. The largest $\eta(HCOO^-)$ value reported so far in the reduction of HCO_3^- is ca. 85% upon using a viologen

Table 3-I. The electrochemical CO_2 reduction catalyzed by $[Ru(bpy)_2(CO)_2]^{2+}$ in the presence of several proton sources in CH_3CN[a)]

Proton source[b)]	pK_a[c)] in CH_3CN	Product[d)] / μ mol			Current density[e)]
		$HCOO^-$	CO	H_2	mA cm^{-2}
$(CH_3)NH_2 \cdot HCl$	15.6	332 (64.1)	103 (19.9)	17 (3.3)	1.6
$(CH_3)_2NH \cdot HCl$	15.8	437 (84.3)	13 (2.4)	35 (6.8)	3.3
$(CH_3)_3N \cdot HCl$	14.8	288 (55.5)	32 (6.1)	158 (30.5)	3.3
C_6H_5COOH	12.0	117 (22.5)	51 (9.9)	263 (50.7)	2.2
C_6H_5OH	f)	420 (81.0)	84 (16.3)	2 (0.3)	2.3

a) -1.30 V vs. SCE. b) 0.20 mol dm^{-3}. c) Charlot, G.; Tretmillon, B. "Chemical Reactions in Solvents and Melts"; Pergamon Press, New York, 1969. d) The current efficiency (%) for the formation of the product after the consumption of 100 C in parenthesis. e) Average value for 100 C. f) No available datum in literatures.

polymer coated Pd electrode, however the current density in the reaction was very low (0.05 - 0.1 mA cm^{-2}).[3] In view of large current densities of the present reactions (1.6 - 3.3 mA cm^{-2}, Table 3-I), the electrochemical CO_2 reduction described here is not only most selective for the $HCOO^-$ formation but also fastest in the rate of reduction.

3-4 References

(1) (a) Beley, M.; Collin, J. P.; Ruppert, R.; Sauvage, J.-P. J. Chem. Soc., Chem. Commun. **1984**, 1315. (b) Beley, M.; Collin, J.-P.; Ruppert, R.; Sauvage, J. P. J. Am. Chem. Soc., **1986**, 108, 7461.

(2) (a) Hawecker, J.; Lehn, J. M.; Ziessel, R. J. Chem. Soc., Chem. Commun. **1984**, 328. (b) Sullivan, B. P.; Bolinger, C. M.; Conrad, D.; Vining, W. J.; Meyer. T. J. J. Chem. Soc., Chem. Commun. **1985**, 1414. (c) O'Toole, T. R.; Margerum, L. D.; Westmoreland, T. D.; Vining, W. J.; Murray, R. W.; Meyer, T. J. J. Chem. Soc., Chem. Commun. **1985**, 1416.

(3) Stalder, C. J.; Chao, S.; Wrighton, M. S. J. Am. Chem. Soc. **1984**, 106, 3673.

(4) (a) Bolinger, C. M.; Sullivan, B. P.; Comrad, D.; Gilbert, J. A.; Story, N.; Meyer, T. J. J. Chem. Soc., Chem. Commun. **1985**, 796. (b) Slater, S.; Wagenknecht, J. H. J. Am. Chem. Soc. **1984**, 106, 5367. (c) Tezuka, M.; Yajima, T.; Tsuchiya, A.; Matsumoto, Y.; Uchida, Y.; Hidai, M. J. Am.

Chem. Soc. **1982**, 104, 6834. (d) Lieber, C. M.; Lewis, N. S. J. Am. Chem. Soc. **1984**, 106, 5033. (e) Fisher, B.; Eisenberg, R. J. Am. Chem. Soc. **1980**, 102, 7361. (f) Meshitsuka, S; Ichikawa, M.; Tamaru, K. J. Chem. Soc., Chem. Commun. **1974**, 158. (g) Hiratsuka, K.; Takahashi, K.; Sasaki, H.; Toshima, S. Chem. Lett. **1977**, 1137. (h) Takahashi, K.; Hiratsuka, K.; Sasaki, H.; Toshima, S. Chem. Lett. **1979**, 305. (i) Kapusta, S.; Hackerman, N. J. Electrochem. Soc. **1984**, 131, 1511.

Chapter 4

Ligand Effect of the Ruthenium Complexes on Electrochemical CO_2 Reduction

4-1 Introduction

Products obtained in the electrochemical CO_2 reductions may depend on the nature not only of central metal ions but also of ligands of transition metal catalysts. For instance, Ni and Co complexes with macrocycles,[1] Pd-phophine complexes,[2] and pyridine complexes of Re,[3] Ru[4] and Rh[5] are known as catalysts to generate CO in the electrochemical CO_2 reductions. On the other hand, as the catalysts for $HCOO^-$ formation are reported Rh-phosphine complexes,[6] phtalocyanine complexes and macrocycles of Co and Ni,[7] Pd-based electrode,[8] Ru-bipyridine complexes,[9] and iron-sulfur clusters.[10] As other products in the CO_2 reduction are reported HCHO,[11] CH_3OH,[12] and CH_4,[13] all of which are those produced by solid metal catalysts except for the reduction of CO_2 with $K_2Fe[Fe(CN)_6]$ to afford CH_3OH.[12a] Thus, the electrochemical reduction of CO_2 can be controlled by changing the metal ion and/or the ligand of transition metal catalysts. While a variety of metal ions have been examined as transition metal complex catalysts for the electrochemical CO_2 reduction, there are only a few reports concerning on the effect of ligands on the catalytic

activity of transition metal complexes.[14]

This chapter describes the electrochemical CO_2 reductions catalyzed by ruthenium complexes of bipyridine derivatives, 2,2'-bipyridine (bpy), 4,4'-dimethyl-2,2'-bipyridine (dmbpy), and 1,10-phenanthroline (phen). Electrochemical properties of those ruthenium complexes and the equilibrium reaction between the ruthenium complexes and OH^- also are discussed.

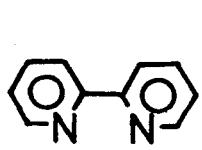

bpy

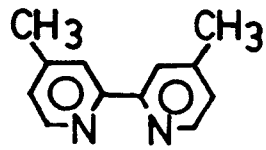

dmbpy

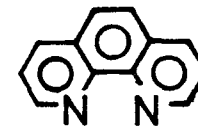

phen

4-2 Experimental Section

Material. NBu^n_4OH was purchased as a 10% methanol solution, and used without further purification.

Preparation of $[Ru(CO)_2Cl_2]_n$. A 90%-HCOOH solution (50 cm^3) containing $RuCl_3 \cdot nH_2O$ (1.0 g, 3.8 mmol), which is commercially available, was refluxed under N_2 in the dark for 3 h, during which time color of the solution turned to orange from dark blue. Then, the solution was allowed to stand at room temperature, followed by evaporation to dryness in vacuo. Thus a polymeric ruthenium complex $[Ru(CO)_2Cl_2]_n$ was obtained as an orange solid. Anal. Calcd for $RuC_2O_2Cl_2$: C, 10.5, H, 0.0%.

Found: C, 11.7, H, 0.6%.

Preparation of $Ru(bpy)(CO)_2Cl_2$. An ethanol/water (1:1 v/v; 38 cm^3) solution containing $[Ru(CO)_2Cl_2]_n$ (0.5 g, 2.2 mmol) and 2,2'-bipyridine (0.3 g, 1.9 mmol) was refluxed at 70 - 80°C for one hour under N_2. After refluxed, a yellow crystal precipitated was collected by filtration and recrystallized from acetonitrile; 68% yield, mp > 300°C. Anal. Calcd for $RuC_{12}H_8N_2O_2Cl_2$: C, 37.60, H, 2.09, N, 7.31%. Found: C, 37.42, H, 2.27, N, 7.26%.

Preparation of $Ru(dmbpy)(CO)_2Cl_2$. $Ru(dmbpy)(CO)_2Cl_2$ was prepared by the method similar to $Ru(bpy)(CO)_2Cl_2$ by using 4,4'-dimethyl-2,2'-bipyridine in place of 2,2'-bipyridine; 23% yield. Anal. Calcd for $RuC_{14}H_{12}N_2O_2Cl_2$: C, 40.79, H, 2.93, N, 6.80%. Found: C, 41.19, H, 3.10, N, 7.06%.

Preparation of $[Ru(bpy)_2(CO)_2](PF_6)_2$. Being different from the method described in Chapter 1, where the yield was very low; $[Ru(bpy)_2(CO)_2](PF_6)_2$ was prepared as follow; an ethanol/water (5:4 v/v; 180 cm^3) solution containing $[Ru(CO)_2Cl_2]_n$ (2.0 g, 8.8 mmol) and 2,2'-bipyridine (5.0 g, 32 mmol) was refluxed under N_2 for 4 h. The solution was cooled, followed by the addition of NH_4PF_6 dissolved in a small amount of water to afford a white precipitate, which was recrystallized twice with acetone/ether; 10% yield. Anal. Calcd for $RuC_{22}H_{16}N_4O_2P_2F_{16}$: C, 34.80, H, 2.12, N, 7.38%. Found: C, 35.01, H, 2.15, N, 7.40%.

Preparation of $[Ru(bpy)(dmbpy)(CO)_2](PF_6)_2 \cdot 0.5(CH_3)_2CO$. An ethanol/water (10:7 v/v; 170 cm^3) solution containing $Ru(dmbpy)(CO)_2Cl_2$ (0.41 g, 1.0 mmol) and 2,2'-bipyridine (0.18 g, 1.2 mmol) was refluxed under N_2 for 24 h. After cooled to room temperature, ethanol in the solution was evaporated to a half volume in vacuo, and the resulting precipitates of unreacted $Ru(dmbpy)(CO)_2Cl_2$ and 2,2'-bipyridine were filtered. To the filtrate was added an aqueous NH_4PF_6 solution to give a precipitate, which was recrystallized twice with acetone/ether, giving yellow crystals; 53% yield; $\nu(C\equiv O)$ 2024, 2076 cm^{-1}. Anal. Calcd for $RuC_{25.5}H_{23}N_4O_{2.5}P_2F_{12}$: C, 37.60, H, 2.76, N, 6.95%. Found: C, 37.52, H, 2.84, N, 6.86%.

Preparation of $[Ru(dmbpy)_2(CO)_2](PF_6)_2$. $[Ru(dmbpy)_2(CO)_2](PF_6)_2$ was prepared by the method similar to $[Ru(bpy)_2(CO)_2](PF_6)_2$, using 4,4'-dimethyl-2,2'-bipyridine in place of 2,2'-bipyridine; 12% yield; $\nu(C\equiv O)$ 2024, 2080 cm^{-1}. Anal. Calcd for $RuC_{26}H_{24}N_4O_2P_2F_{12}$: C, 38.28, H, 2.94, N, 6.87%. Found: C, 38.21, H, 3.04, N, 6.77%.

Preparation of $[Ru(phen)_2(CO)_2](PF_6)_2$. An aqueous 90% formic acid solution (50 cm^3) of $RuCl_3 \cdot nH_2O$ (1.0 g) was refluxed under N_2 for 5 h. The resulting clear orange solution was allowed to stand at room temperature, and evaporated to dryness under reduced pressure to afford an orange solid, which was

dissolved in H_2O/ethanol (1:4 v/v) containing 1,10-phenanthroline (1.0 g, 5.5 mmol). Then, the solution was refluxed under N_2 for 2 h, followed by cooling to 0°C to give an orange precipitate of $Ru(phen)(CO)_2Cl_2$. The crude product thus obtained and 1,10-phenanthroline (1.0 g, 5.5 mmol) was dissolved in H_2O/ethanol (2:1 v/v, 100 cm^3), and heated under refluxing conditions for 24 h. To the solution was added a concentrated aqueous solution of NH_4PF_6 at room temperature to yield an off-white precipitate, which was purified by recrystallization from acetone/ether; 78% yield. Anal. Calcd for $C_{26}H_{16}F_{12}N_4O_2P_2Ru$: C, 38.65; H, 2.00; N, 6.93%. Found: C, 38.73; H, 2.13; N, 7.08%.

Preparation of $[Ru(phen)_2(CO)Cl](PF_6)$. A DMF solution (20 cm^3) containing $RuCl_3 \cdot nH_2O$ (1.0 g, 3.8 mmol), 1,10-phenanthroline (1.4 g, 7.7 mmol), and LiCl (1.5 g, 0.35 mmol) was refluxed under N_2 for 8 h. After cooled to room temperature, the solution was mixed with acetone (100 cm^3) and the mixture was allowed to stand overnight at 0°C to give a precipitate of $Ru(phen)_2Cl_2$, which was collected by filtration, washed with ether and then water, and dried in vacuo. $Ru(phen)_2Cl_2 \cdot 2H_2O$ (1.0 g, 1.8 mmol) thus obtained was dissolved in 90%-HCOOH (30 cm^3) and the solution was refluxed under N_2 for 6 h. After cooled to room temperature, the solution was evaporated to dryness. The resulting residue was dissolved in H_2O, followed by the addition of an aqueous NH_4PF_6 solution to afford a solid, which was collected by filtration and recrystallized from acetone/ether.

Anal. Calcd for $RuC_{25}H_{16}N_4OClPF_6$: C, 44.82, H, 2.41, N, 8.36%. Found: C, 44.38, H, 2.75, N, 8.02%.

4-3 Results and Discussion

Equilibrium reactions among $[RuL_1L_2(CO)_2]^{2+}$, $[RuL_1L_2(CO)C(O)OH]^+$, and $[RuL_1L_2(CO)(COO^-)]^+$. The electronic absorption spectra of $[Ru(bpy)(dmbpy)(CO)_2]^{2+}$ in an aqueous solution (pH 5.31) and upon the addition of an aqueous KOH solution to the original weak acidic solution are shown in Figure 4-1, which reveals that the bands at 251, 301 and 311 nm observed in the acidic medium are weakened with increasing the pH value, and new bands at 277, 343 and 422 nm are strengthened with isosbestic points at 259, 296 and 322 nm. Similar spectra are observed for an aqueous $[Ru(dmbpy)_2(CO)_2]^{2+}$ solution; upon increasing the pH value, the absorption bands at 248, 301 and 313 nm disappeared and the bands at 268, 342 and 428 nm newly appeared with isosbestic points at 256, 296 and 322 nm, as shown in Figure 4-2. Spectral changes of the both complexes are essentially consistent with that of the corresponding bis(2,2'-bipyridine) complex, $[Ru(bpy)_2(CO)_2]^{2+}$; in alkaline media one of the carbonyl groups of $[Ru(bpy)_2(CO)_2]^{2+}$ may be attacked by OH^- to give $[Ru(bpy)_2(CO)C(O)OH]^+$, which undergoes the deprotonation reaction to afford $[Ru(bpy)_2(CO)(COO^-)]^+$. The equilibrium constants between $[RuL_1L_2(CO)_2]^{2+}$ and $[RuL_1L_2(CO)C(O)OH]^+$ (K_1), and between the latter and $[RuL_1L_2(CO)(COO^-)]^+$ (K_2) evaluated

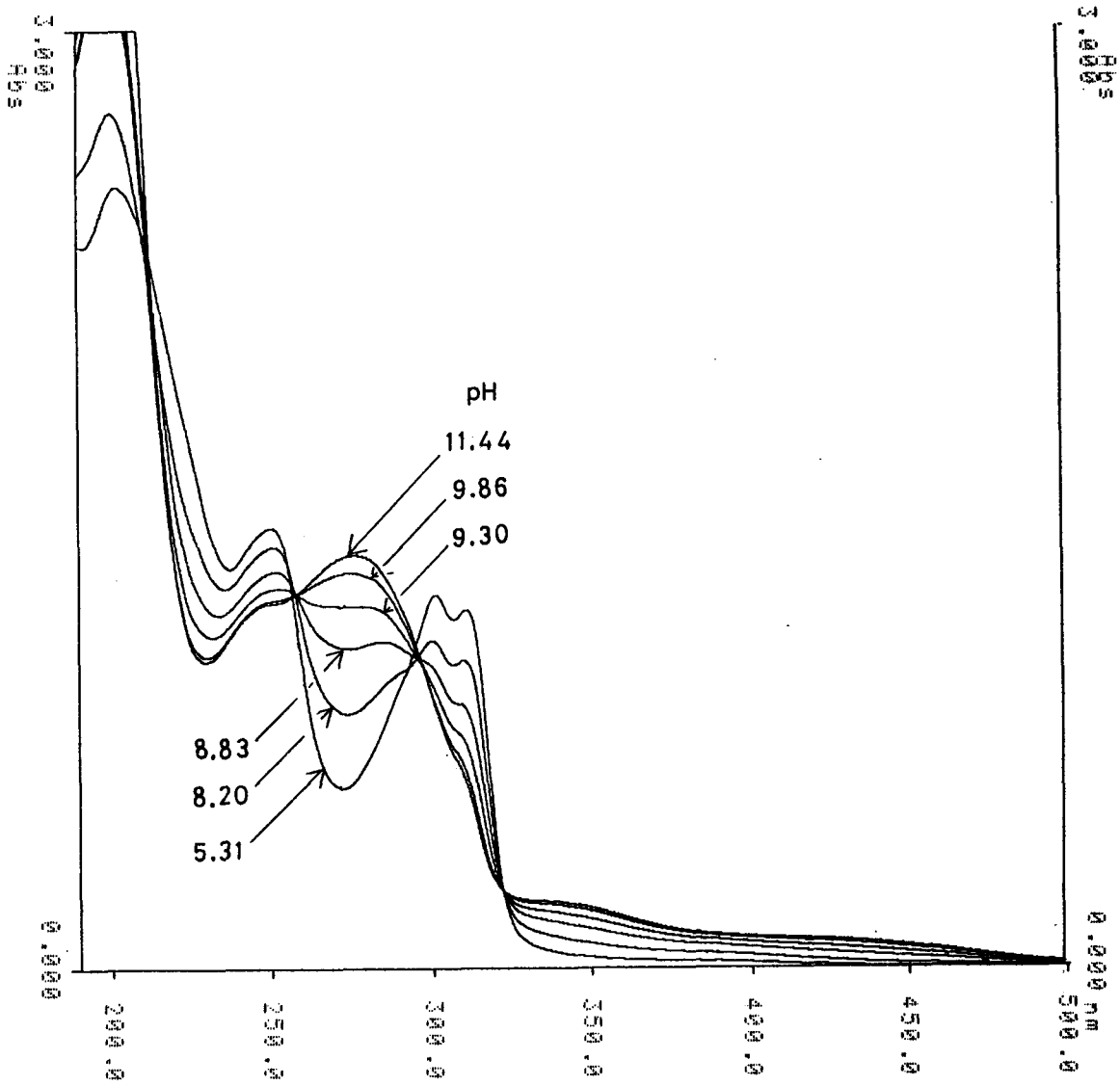

Figure 4-1. Electronic absorption spectra of [Ru(bpy)(dmbpy)-$(CO)_2]^{2+}$ (5.0 x 10^{-5} mol dm^{-3}) in H_2O at various pH (25°C).

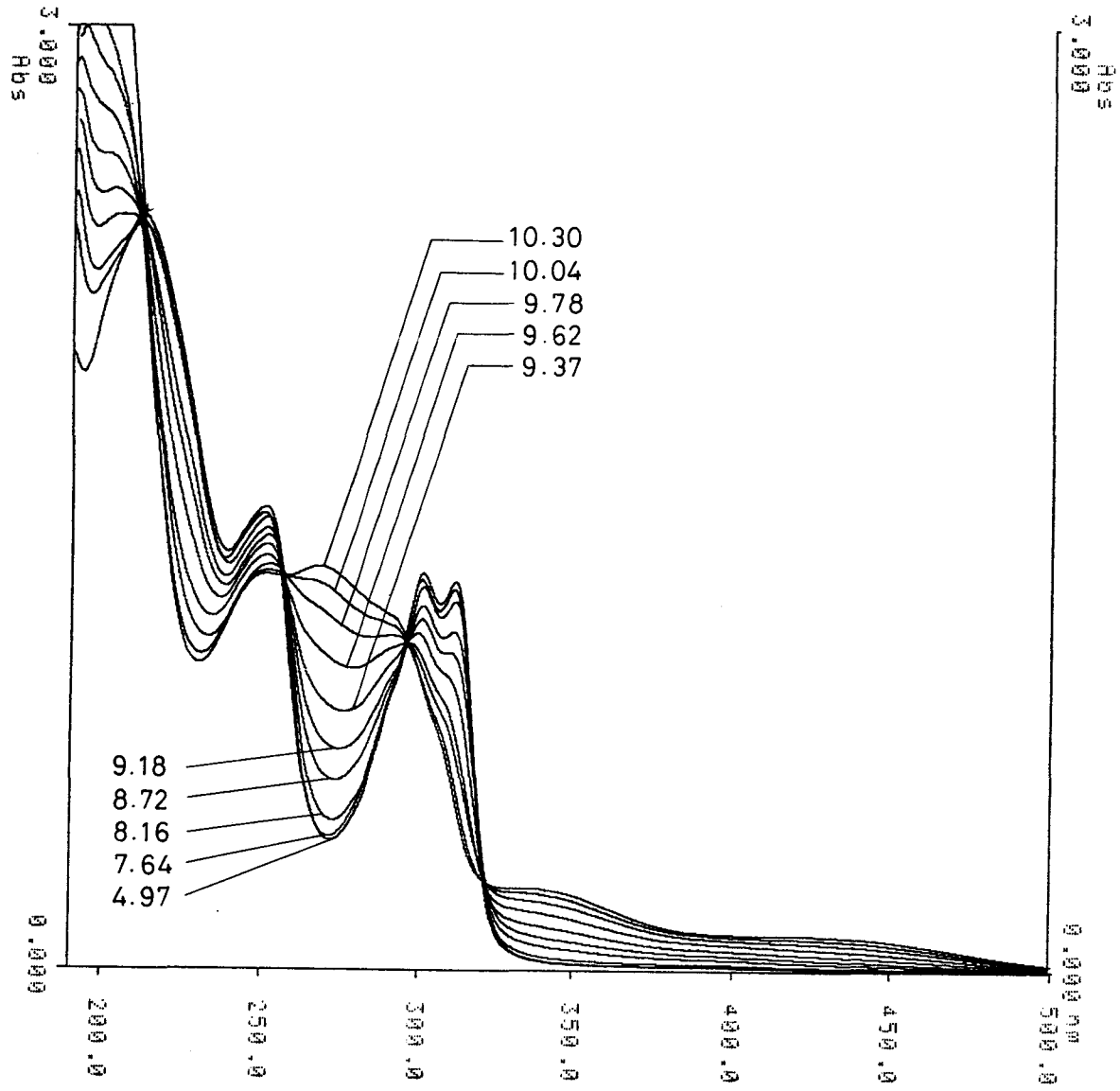

Figure 4-2. Electronic absorption spectra of $[Ru(dmbpy)_2(CO)_2]^{2+}$ (5.0×10^{-5} mol dm^{-3}) in H_2O at various pH (25°C).

from titration curves are listed in Table 4-I. Both the equilibrium constants become small with introducing 4,4'-dimethyl-2,2'-bipyridine with an electron donating CH_3 group as a ligand in place of 2,2'-bipyridine.

Electrochemical properties of ruthenium species. The cyclic voltammograms of $[Ru(bpy)_2(CO)_2]^{2+}$ in CH_3CN under N_2 and CO_2 atmospheres are shown in Figure 4-3a; there are observed an irreversible cathode peak around -1.03 V vs. SCE and some anode peaks in the range -1.0 to +1.5 V vs. SCE under N_2 atmosphere, of which the peak around -0.5 V vs. SCE is strong. Those anodic currents may correspond to oxidation of the reduction products of $[Ru(bpy)_2(CO)_2]^{2+}$, because no anode peak is observed when the scanning was conducted in the range 0 V to +1.5 V vs. SCE (a dotted line in Figure 4-3a). The cathode peak of $[Ru(bpy)_2(CO)_2]^{2+}$ at -1.03 V vs. SCE is shifted to negative potentials upon introduction of a dmbpy ligand in place of bpy and the potentials exhibited by $[RuL_1L_2(CO)_2]^{2+}$ (L_1L_2 = $(bpy)_2$, (bpy)(dmbpy), $(dmbpy)_2$, $(phen)_2$) in CH_3CN are more negative than those in DMF, as listed in Table 4-II. The cyclic voltammogram in the presence of low concentrations of CO_2 gives a large cathode current around -1.7 V vs. SCE as well as two shoulders at ca. 1.4 and -1.6 V vs. SCE. The anode peak at -0.5 V vs. SCE disappeared and the new oxidation peaks around -1.5 V, -1.3 V and -1.0 V vs. SCE generated.

On the other hand, the addition of NBu^n_4OH to a CH_3CN

Table 4-I. The equilibrium constants (mol^{-1} dm^3) between $[RuL_1L_2(CO)_2]^{2+}$ and $[RuL_1L_2(CO)C(O)OH]^+$ (K_1), and between the latter and $[RuL_1L_2(CO)(COO^-)]^+$ (K_2)

L_1	L_2	K_1	K_2
bpy	bpy	1.32×10^5	2.27×10^4
bpy	dmbpy	3.96×10^4	9.08×10^3
dmbpy	dmbpy	4.41×10^4	4.64×10^3

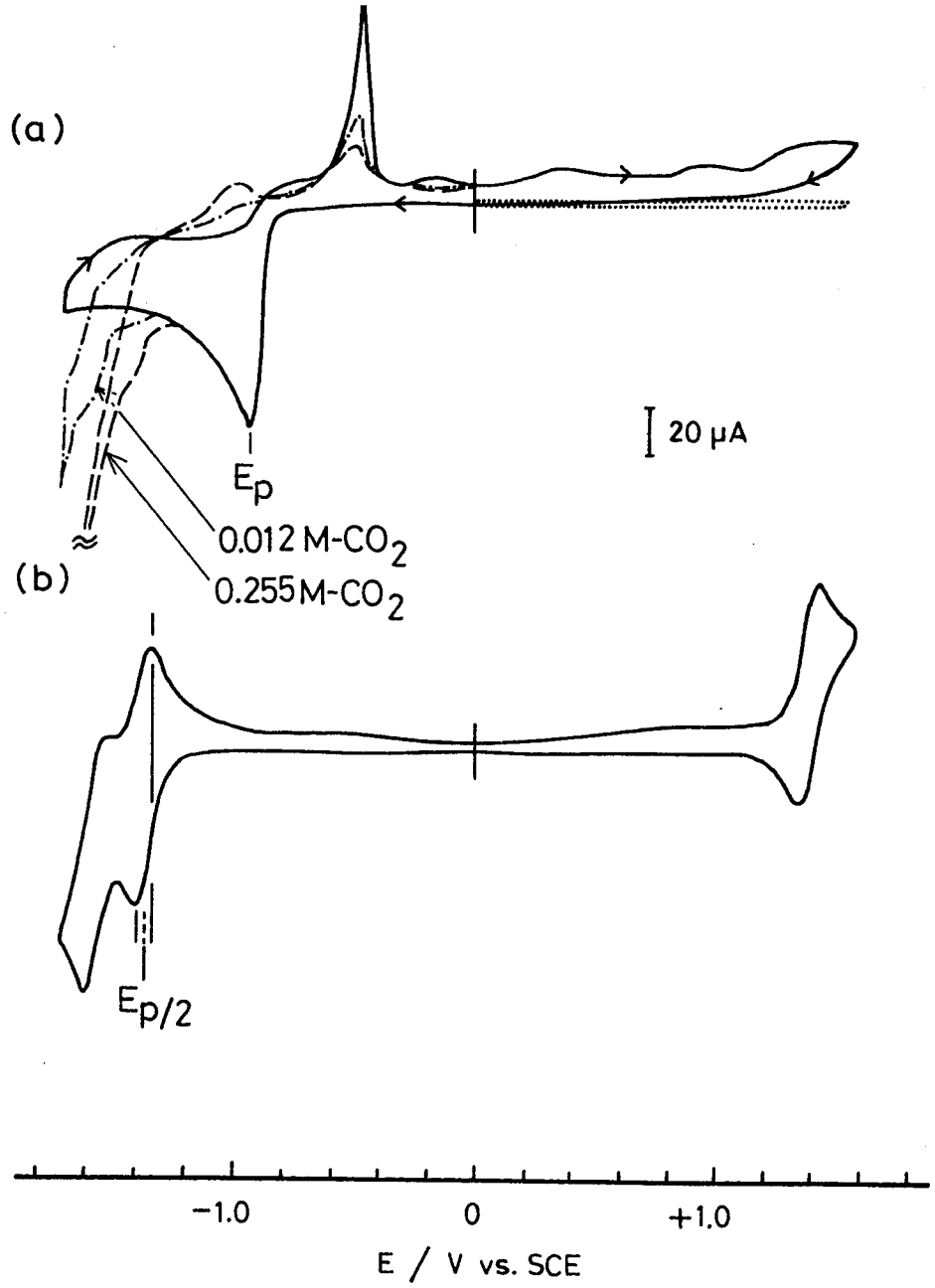

Figure 4-3. Cyclic voltammograms of $[Ru(bpy)_2(CO)_2]^{2+}$ (a) and $[Ru(bpy)_2(CO)(COO^-)]^+$ (b) in CH_3CN under N_2 (—— and ·····) and CO_2 (—·— and – – –) atmospheres.

Table 4-II. Peak potentials of the irreversible reduction in the cyclic voltammograms of $[RuL_1L_2(CO)_2]^{2+}$ [a]

L_1	L_2	E_p / V vs. SCE	Solvent
bpy	bpy	-0.95	DMF
		-1.03	CH_3CN
bpy	dmbpy	-1.05	DMF
		-1.13	CH_3CN
dmbpy	dmbpy	-1.05	DMF
		-1.13	CH_3CN
phen	phen	-1.07	CH_3CN

[a] $[RuL_1L_2(CO)_2]^{2+}$ 1.0×10^{-3} mol dm^{-3}; $NBu^n_4ClO_4$ 0.10 mol dm^{-3}; sweep rate 0.10 V s^{-1}.

solution of $[Ru(bpy)_2(CO)_2]^{2+}$ under N_2 atmospheres results in disappearance of the cathode peak at -1.0 V vs. SCE, instead there occurs new peaks at ca. -1.4 and -1.6 V vs. SCE. The equimolar and twice molar addition of NBu^n_4OH to $[Ru(bpy)_2(CO)_2]^{2+}$ produces $[Ru(bpy)_2(CO)C(O)OH]^+$ and $[Ru(bpy)_2(CO)(COO^-)]^+$, respectively, as confirmed from the fact that the former exhibits the same cyclic voltammogram as the latter. However, the further addition of NBu^n_4OH resulted in decomposition of the ruthenium complex; color of the solution turned to green from orange. The cyclic voltammogram of $[Ru(bpy)_2(CO)(COO^-)]^+$ which is generated by twice molar addition of NBu^n_4OH to $[Ru(bpy)_2(CO)_2]^{2+}$ is shown in Figure 4-3b, which reveals three redox couples. Of those two redox couples around -1.4 V and +1.4 V vs. SCE are pseudo-reversible, whereas the remaining couple around -1.6 V vs. SCE is irreversible. The reduction potentials around -1.4 and -1.6 V vs. SCE agree closely with those in the cyclic voltammograms of $[Ru(bpy)_2(CO)_2]^{2+}$ under a low concentration of CO_2, as shown in Figure 4-3a. This result also supports the formation of $[Ru(bpy)_2(CO)(COO^-)]^+$ as an intermediate of the present CO_2 fixation. The first one-electron reduction potentials of $[RuL_1L_2(CO)(COO^-)]^+$ (L_1L_2 = $(bpy)_2$, (bpy)(dmbpy), $(dmbpy)_2$, $(phen)_2$) also are shifted to negative values with introducing dmbpy ligands, as listed in Table 4-III.

Cyclic Voltammograms of $Ru(bpy)(CO)_2Cl_2$. Mono-bipyridine

Table 4-III. Reduction potentials of $[RuL_1L_2(CO)(COO^-)]^+$ [a]

L_1	L_2	$E_{P/2}$ V vs. SCE	Solvent
bpy	bpy	-1.26	DMF
		-1.37	CH_3CN
bpy	dmbpy	-1.38	DMF
		-1.45	CH_3CN
dmbpy	dmbpy	-1.40	DMF
		-1.48	CH_3CN
phen	phen	-1.38	CH_3CN

[a] $[RuL_1L_2(CO)_2]^{2+}$ 1.0 x 10^{-3} mol dm^{-3}; NBu^n_4OH 2.0 x 10^{-3} mol dm^{-3}; $NBu^n_4ClO_4$ 0.10 mol dm^{-3}; sweep rate 0.10 V s^{-1}.

complexes of rhenium, $Re(bpy)(CO)_3X$ (X = Br, Cl), are known to catalyze electrochemical CO_2 reduction,[3] while no catalytic activity has been reported for the corresponding ruthenium complexes. The cyclic voltammogram of $Ru(bpy)(CO)_2Cl_2$ in CH_3CN exhibits an irreversible cathode peak at -1.2 V vs. SCE and an anode peak weaker than the cathode one at -0.4 V vs. SCE under N_2 atmospheres, as shown in Figure 4-4. On the other hand, the same complex in CH_3CN under CO_2 atmospheres displays a strong cathode peak around -1.85 V vs. SCE, which is more negative potential than that of $[Ru(bpy)_2(CO)_2]^{2+}$, and rather close to the reduction potential (-2.0 V vs. SCE) of CO_2 without any catalysts. In view of this result, the CO_2 activation by $Ru(bpy)(CO)_2Cl_2$ may be effective less than that by $[Ru(bpy)_2(CO)_2]^{2+}$. The cyclic voltammogram in CH_3CN/H_2O (9:1 v/v) under CO_2 atmospheres, however, shows a large cathodic current around -1.2 V vs. SCE, which may correspond to CO_2 reduction. Thus, $Ru(bpy)(CO)_2Cl_2$ may function as a catalyst for the electrochemical CO_2 reduction, in particular being efficient in CH_3CN/H_2O (9:1 v/v).

Electrochemical CO_2 Reductions Catalyzed by Several Ruthenium Complexes. The CO_2 reductions were performed in CH_3CN/H_2O (4:1 v/v) solutions containing several ruthenium complexes shown in Table 4-IV by the controlled potential electrolysis at -1.30 V vs. SCE. The current densities in the electrolysis are almost the same (2 - 3 mA cm^{-2}) between the ruthenium complexes with 2,2'-bipyridine and 4,4'-dimethyl-2,2'-

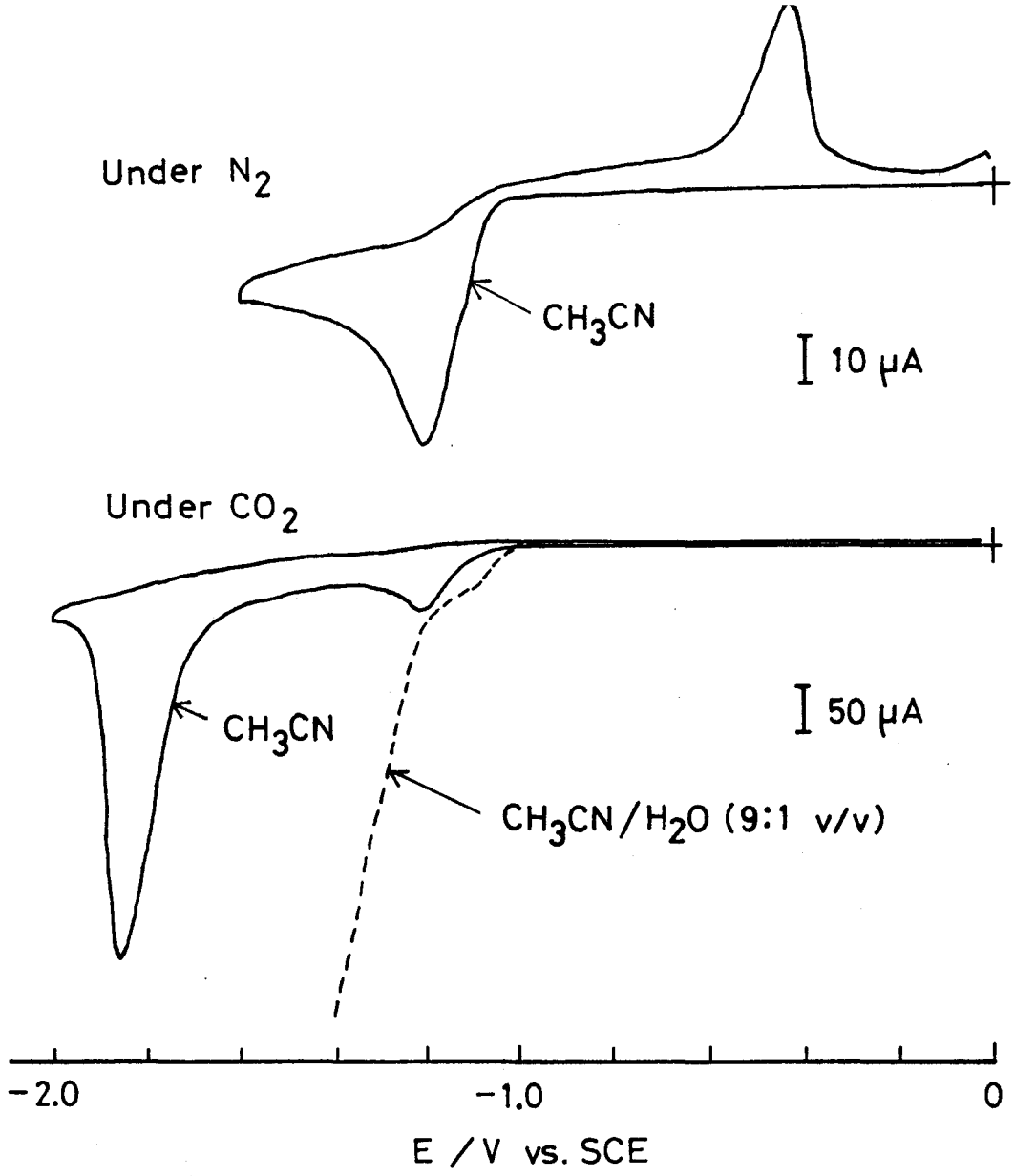

Figure 4-4. Cyclic Voltammograms of $Ru(bpy)(CO)_2Cl_2$ in CH_3CN (——) and CH_3CN/H_2O (9:1 v/v) (— — —) under N_2 and CO_2 atmospheres.

Table 4-IV. The electrochemical CO_2 reductions catalyzed by several ruthenium complexes in MeCN/H_2O (4:1 v/v)[a]

Catalyst	Product[b] / μ mol CO
$[Ru(bpy)_2(CO)_2]^{2+}$	209 (67.2%)
$[Ru(bpy)(dmbpy)(CO)_2]^{2+}$	223 (71.8%)
$[Ru(dmbpy)_2(CO)_2]^{2+}$	203 (65.3%)
$[Ru(phen)_2(CO)_2]^{2+}$	191 (61.5%)
$[Ru(phen)_2(CO)Cl]^{+}$	207 (66.6%)
$Ru(bpy)(CO)_2Cl_2$	273 (87.8%)
$Ru(dmbpy)(CO)_2Cl_2$	205 (66.0%)

[a] -1.30 V vs. SCE; an Hg electrode (3.3 cm^2); 60 coulombs consumed. [b] The current efficiency (%) in parentheses.

bipyridine as catalysts, while they are influenced by stirring speed. The electrochemical CO_2 reduction proceeds catalytically in the presence of either ruthenium complex, while the rate of reductions is somewhat slow when the ruthenium complexes with 1,10-phenanthroline are used as catalysts. The reduction product is only carbon monoxide even in either case, and the amount is independent of the catalyst (Table 4-IV).

The electrochemical CO_2 reduction also proceeds in CH_3OH, while the current densities are relatively low (ca. 0.5 - 1.0 mA cm^{-2}). In the reduction upon using $[Ru(phen)_2(CO)_2]^{2+}$ or $[Ru(phen)(CO)Cl]^+$, CH_3CN/CH_3OH (4:1 v/v) is used as a solvent due to poor solubility of these ruthenium complexes to CH_3OH. The reduction products in CH_3OH, however, are not only carbon monoxide but also formic acid, as shown in Table 4-V. The amounts of these products are dependent on the catalyst; carbon monoxide increases and formic acid decreases in the amount with increasing the donor property of the ligand. For instance, the amount of carbon monoxide generated increases in the order $[Ru(bpy)_2(CO)_2]^{2+}$ < $[Ru(bpy)(dmbpy)(CO)_2]^{2+}$ < $[Ru(dmbpy)_2(CO)_2]^{2+}$, whereas the amount of formic acid produced is opposite. Similar increasing amount of carbon monoxide was observed as follows; $Ru(bpy)(CO)_2Cl_2$ < $Ru(dmbpy)(CO)_2Cl_2$.

Mechanisms of CO_2 Reduction. The mechanisms for the electrochemical CO_2 reductions using $[Ru(bpy)(dmbpy)(CO)_2]^{2+}$ and $[Ru(dmbpy)_2(CO)_2]^{2+}$ as catalysts may be the same as that by using

Table 4-V. The electrochemical CO_2 reductions catalyzed by the ruthenium complexes in MeOH[a]

Catalyst	Products[b] / μmol	
	CO	$HCOO^-$
$[Ru(bpy)_2(CO)_2]^{2+}$	81 (26.1%)	154 (49.5%)
$[Ru(bpy)(dmbpy)(CO)_2]^{2+}$	106 (34.2%)	123 (39.8%)
$[Ru(dmbpy)_2(CO)_2]^{2+}$	139 (44.7%)	101 (32.5%)
$[Ru(phen)_2(CO)_2]^{2+}$ [c]	108 (34.7%)	76 (24.5%)
$[Ru(phen)_2(CO)Cl]^{+}$ [c]	123 (39.6%)	40 (12.9%)
$Ru(bpy)(CO)_2Cl_2$	85 (27.3%)	117 (37.7%)
$Ru(dmbpy)(CO)_2Cl_2$	122 (39.2%)	83 (26.8%)

[a] -1.30 V vs. SCE; an Hg electrode (3.3 cm^2); 60 coulombs consumed. [b] The current efficiency (%) in parentheses. [c] In MeCN/MeOH (4:1 v/v).

$[Ru(bpy)_2(CO)_2]^{2+}$ as a catalyst, as described in chapter 2. The change of products distribution may be associated with the equilibrium reactions among $[RuL_1L_2(CO)_2]^{2+}$, $[RuL_1L_2(CO)C(O)OH]^{+}$, and $[RuL_1L_2(CO)(COO^{-})]^{+}$ (L_1, L_2 = bpy, dmbpy, phen); the equilibrium concentration of $[RuL_1L_2(CO)_2]^{2+}$ becomes small with replacing the dmbpy ligand for L_1 and L_2 as bpy, because of the donor property of the CH_3 group. Thus, the amount of carbon monoxide generated becomes large with introducing the dmbpy ligand when the electrochemical reduction of CO_2 was conducted in CH_3OH.

The electrochemical CO_2 reduction catalyzed by $Ru(bpy)(CO)_2Cl_2$ or $Ru(dmbpy)(CO)_2Cl_2$ gives a result similar to that catalyzed by the ruthenium bis(bipyridine) complexes. In order to obtain the information on active species in the catalytic system, electrochemical spectra of $Ru(bpy)(CO)_2Cl_2$ and $Ru(dmbpy)(CO)_2Cl_2$ were measured in CH_3CN to result in the decomposition of the ruthenium complexes. On the other hand, the measurement of electronic absorption spectra of $Ru(bpy)(CO)_2Cl_2$ and $Ru(dmbpy)(CO)_2Cl_2$ in H_2O has indicated that these complexes irreversibly react with OH^{-} to lead the dissociation of the chloride or CO ligand. Thus, further study may required for elucidating active species in the present CO_2 reduction by monobipyridine catalysts.

In conclusion, the amounts of carbon monoxide become large with introducing the dmbpy ligand in the electrochemical CO_2 reductions catalytically by $[RuL_1L_2(CO)_2]^{2+}$ (L_1L_2 = $(bpy)_2$, (bpy)(dmbpy), $(dmbpy)_2$) in CH_3OH. It is attributed to that the equilibrium constants among $[RuL_1L_2(CO)_2]^{2+}$, $[RuL_1L_2(CO)C(O)OH]^{+}$,

and $[RuL_1L_2(CO)(COO^-)]^+$ become small with replacing the dmbpy ligand for L_1 and L_2 as bpy, because of the donor property of the CH_3 group. This finding is first example which observes the ligand effects toward the products selectivity for electrochemical CO_2 reductions catalyzed by transition metal complexes.

4-4 References

(1) (a) Beley, M.; Collin, J.-P.; Ruppert, R.; Sauvage, J.-P. J. Am. Chem. Soc. **1986**, 108, 7461. (b) Beley, M.; Collin, J.-P.; Ruppert, R.; Sauvage, J.-P. J. Chem. Soc., Chem. Commun. **1984**, 1315. (c) Pearce, D. J.; Plether, D. J. Electroanal. Chem. **1986**, 197, 317. (d) Lieber, C. M.; Lewis, N. S. J. Am. Chem. Soc. **1984**, 106, 5033. (e) Fisher, B.; Eisenberg, R. J. Am. Chem. Soc. **1980**, 102, 7361.

(2) DuBois, D. L.; Miedaner, A. J. Am. Chem. Soc. **1987**, 109, 113.

(3) (a) Hawecker, J.; Lehn, J.-M.; Ziessel, R. J. Chem. Soc., Chem. Commun. **1984**, 328. (b) Sullivan, B. P.; Bolinger, C. M.; Conrad, D.; Vining, W. J.; Meyer, T. J. J. Chem. Soc., Chem. Commun. **1985**, 1414.

(4) (a) Ishida, H.; Tanaka, K.; Tanaka, T. Organometallics **1987**, 6, 181. (b) Ishida, H.; Tanaka, K.; Tanaka, T. Chem. Lett. **1985**, 405.

(5) Bolinger, C. M.; Sullivan, B. P.; Conrad, D.; Gilbert, J. A.; Story, N.; Meyer, T. J. J. Chem. Soc., Chem. Commun.

1985, 796.

(6) Slater, S.; Wagenknecht, J. H. J. Am. Chem. Soc. **1984**, 106, 5367.

(7) (a) Kapusta, S.; Hackerman, N. J. Electrochem. Soc. **1984**, 131, 1511. (b) Takahashi, K.; Hiratsuka, K.; Sasaki, H.; Toshima, S. Chem. Lett. **1979**, 305.

(8) Stalder, C. J.; Chao, S.; Wrighton, M. S. J. Am. Chem. Soc. **1984**, 106, 3673.

(9) Ishida, H.; Tanaka, H.; Tanaka, K.; Tanaka, T. J. Chem. Soc., Chem. Commun. **1987**, 131.

(10) Nakazawa, M.; Mizobe, Y.; Matsumoto, Y.; Uchida, Y.; Tezuka, M.; Hidai, M. Bull. Chem. Soc. Jpn. **1986**, 59, 809.

(11) (a) Sears, W. M.; Morrison, S. R. J. Phys. Chem. **1985**, 89, 3295. (b) Ito, K.; Ikeda, S.; Yoshida, M.; Ohta, S.; Iida, T. Bull. Chem. Soc. Jpn. **1984**, 57, 583. (c) Taniguchi, Y.; Yoneyama, H.; Tamura, H. Bull. Chem. Soc. Jpn. **1982**, 55, 2034. (d) Inoue, T; Fujishima, A.; Konishi, S.; Honda, K. Nature **1979**, 277, 637.

(12) (a) Ogura, K.; Takamagari, K. J. Chem. Soc., Dalton Trans. **1986**, 1519. (b) Frese, K. W., Jr.; Canfield, D. J. Electrochem. Soc. **1984**, 131, 2518. (c) Canfield, D.; Frese, K. W., Jr. J. Electrochem. Soc. **1983**, 130, 1772.

(13) (a) Hori, Y.; Kikuchi, K.; Murata, A.; Suzuki, S. Chem. Lett. **1986**, 897. (b) Frese, K. W., Jr.; Leach, S. J. Electrochem. Soc. **1985**, 132, 259.

(14) Sulivan, B. P.; Meyer, T. J. Organometallics, **1986**, 5, 1500.

Chapter 5

Generation of N,N-Dimethylformamide by the Electrochemical CO_2 Reduction with $(CH_3)_2NH$, Catalyzed by a Ruthenium Complex

5-1 Introduction

Although electrochemical CO_2 reductions catalyzed by transition metal complexes have extensively been studied in recent years, the reduction products in most cases are limited to CO and/or $HCOO^-$. The conversion of CO_2 to organic molecules other than $HCOO^-$, therefore, is highly desired in the viewpoint of utilization of CO_2.[1]

Transition metal complexes are known to catalyze the thermal reaction of carbon monoxide with dialkyl amine to give formamide (eq. 5-1).[2] As described in previous chapters, some ruthe-

$$HNR_2 + CO \longrightarrow HC(=O)NR_2 \qquad (5\text{-}1)$$

nium(II) complexes have successfully used as catalysts in the electrochemical conversion of CO_2 to CO and/or $HCOO^-$. This chapter described the generation of N,N-dimethylformamide by the electrochemical CO_2 reduction with $(CH_3)_2NH$, catalyzed by $[Ru(bpy)_2(CO)_2]^{2+}$, including the identification of reaction interme-

diates.

5-2 Experimental Sections

Materials. An anhydrous CH_3CN solution of dimethylamine was prepared as follow; commercially available dimethylamine was heated in the presence of NaOH under N_2 atmospheres to give dry dimethylamine vapor, which was bubbled into anhydrous CH_3CN through $CaCl_2$ tube. The concentration of dimethylamine in CH_3CN was determined by titration. Na_2SO_4 was heated at 150°C for one day before use.

Electrochemical CO_2 Reductions in the Presence of Dimethylamine. The electrochemical reduction was performed with the same electrolysis cell as that described in Chapter 3. An CH_3CN solution containing ruthenium complexes, $(CH_3)_2NH \cdot HCl$, and Na_2SO_4 was bubbled with CO_2 for 30 min, followed by the addition of an CH_3CN solution of dimethylamine. The resulting solution was further bubbled with CO_2 for ca. 5 min. The diterminations of CO, H_2 and $HCOO^-$ produced in the electrochemical reaction were performed by the methods described in Chapter 3. DMF was analyzed with a Shimadzu GC-7A gaschromatograph equipped with FID using a 2 m column filled with Chromosorb 103 under N_2 carrier gas.

5-3 Results and discussion

Formation of the carbamoyl complex, $[Ru(bpy)_2(CO)C(O)N(CH_3)_2]^+$, as a Reaction Intermediate. In the amide synthesis by the reaction of amine with carbon monoxide, catalyzed by transition metal complexes under high pressures and temperatures, carbamoyl metal complexes have been considered as important precursors.[3] Thus, the reaction of $[Ru(bpy)_2(CO)_2]^{2+}$ with $(CH_3)_2NH$ was monitored by IR spectra of the acetonitrile solutions to examine the possibility of the formation of such complexes. The IR spectrum of $[Ru(bpy)_2(CO)_2](PF_6)_2$ (13.0 mmol dm^{-3}) exhibits two $\nu(C\equiv O)$ bands at 2050 and 2101 cm^{-1} (a broken line in Figure 5-1), both of which completely disappear upon the addition of $(CH_3)_2NH$ (26.0 mmol dm^{-3}), instead two new bands appear at 1947 and 1624 cm^{-1} (a solid line in Figure 5-1). The removal of $(CH_3)_2NH$ from the solution by bubbling N_2 or by evaporation under reduced pressures followed by dissolution in accetonitrile resulted in regeneration of the IR spectrum of $[Ru(bpy)_2(CO)_2]^{2+}$, suggesting that $(CH_3)_2NH$ reversibly reacts with $[Ru(bpy)_2(CO)_2]^{2+}$. The 1947 and 1624 cm^{-1} bands appeared in the presence of $(CH_3)_2NH$ may be assigned to the $\nu(C\equiv O)$ and $\nu(C=O)$, respectively, of $[Ru(bpy)_2(CO)C(O)N(CH_3)_2]^+$, since carbamoyl metal complexes was reported to exhibit the $\nu(C=O)$ bands in the 1500 - 1700 cm^{-1} range.[4]

The elctronic spectra of $[Ru(bpy)_2(CO)_2]^{2+}$ are drastically changed by the addition of $(CH_3)_2NH$ as shown in Figure 5-2; two

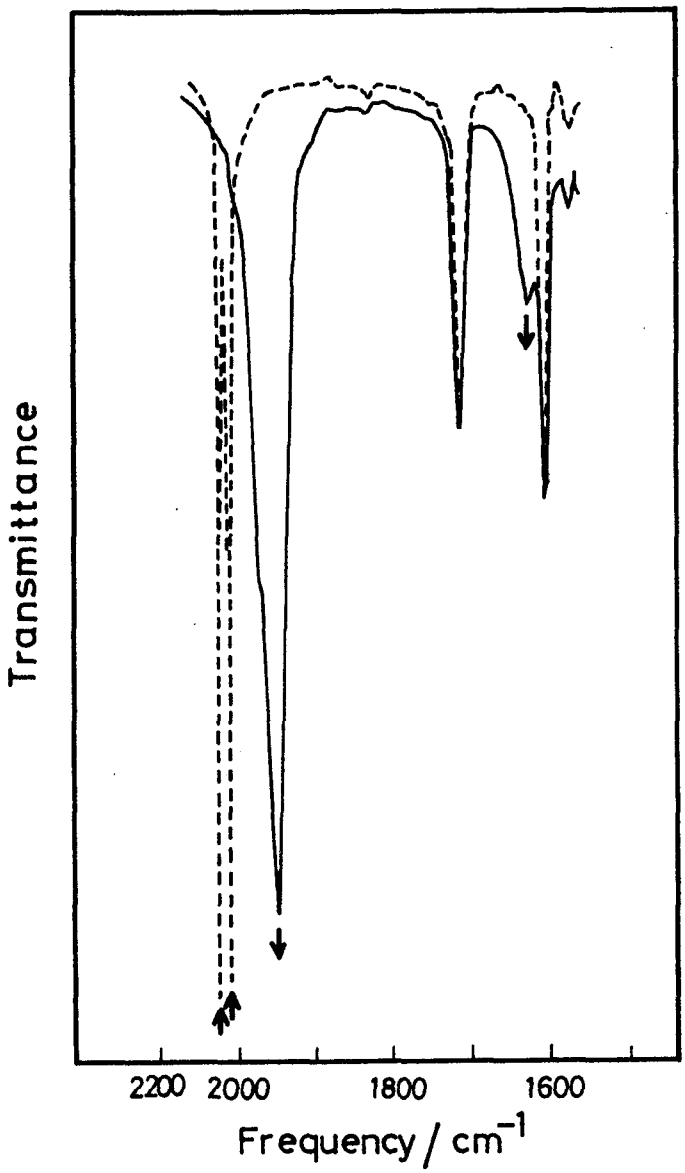

Figure 5-1. FT-IR spectra of $[Ru(bpy)_2(CO)_2]^{2+}$ in acetonitrile in the presence (———) and absence (----) of $(CH_3)_2NH$.

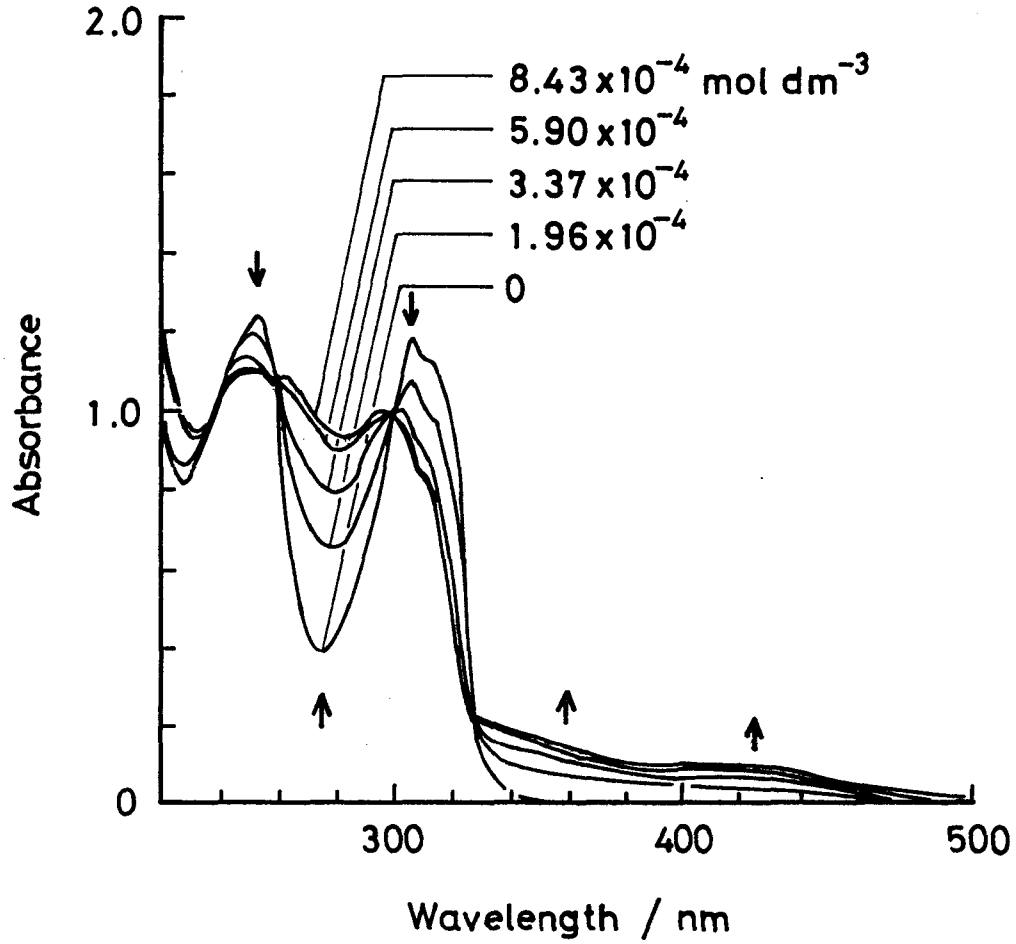

Figure 5-2. Electronic absorption spectra of $[Ru(bpy)_2(CO)_2]^{2+}$ (4.32×10^{-5} mol dm^{-3}) in CH_3CN in the presence of $(CH_3)_2NH$ (0, 1.96×10^{-4}, 3.37×10^{-4}, 5.90×10^{-4}, 8.43×10^{-4} mol dm^{-3}) at 25°C.

absorption bands of the dicarbonyl complex at 253 and 307 nm disappear, and four bands newly appear at 263, 295, 357 and 425 nm. The changes in the electronic spectra and the IR spectra are essentially the same as the spectral changes of $[Ru(bpy)_2(CO)_2]^{2+}$ under alkaline conditions, where the carbonyl group of $[Ru(bpy)_2(CO)_2]^{2+}$ undergoes nucleophilic attack with OH^- to afford a hydroxy carbonyl complex $[Ru(bpy)_2(CO)C(O)OH]^+$. Therefore, $[Ru(bpy)_2(CO)C(O)N(CH_3)_2]^+$ may be formed by nucleophilic attack of $(CH_3)_2NH$ to a carbonyl group of $[Ru(bpy)_2(CO)_2]^{2+}$.

The formation of $[Ru(bpy)_2(CO)C(O)N(CH_3)_2]^+$ is supported also from the ^1H NMR spectrum of a mixture of $[Ru(bpy)_2(CO)_2]^{2+}$ (66 mmol dm^{-3}) with $(CH_3)_2NH$ (132 mmol dm^{-3}) in acetonitrile-d_3, which shows a singlet signal at δ 2.85 (Figure 5-3) as well as the methyl proton signals of $(CH_3)_2NH_2^+$ (δ 3.80) and $(CH_3)_2NH$ (δ 2.43) at room temperature. The δ 2.85 signal may be assigned to the N-CH_3 proton of $[Ru(bpy)_2(CO)C(O)N(CH_3)_2]^+$, since it becomes broaden with lowering the temperature and splits into two signals with the same intensity below -30°C (Figure 5-3) owing to the restriction of free rotation around the N-C bond. Several attempts to isolate $[Ru(bpy)_2(CO)C(O)N(CH_3)_2]^+$ have been unsuccessful to recover the starting complex $[Ru(bpy)_2(CO)_2](PF_6)_2$. This may be due to the fact that $[Ru(bpy)_2(CO)C(O)N(CH_3)_2]^+$ exists as an equilibrium mixture with $[Ru(bpy)_2(CO)_2]^{2+}$ in acetonitrile in the presence of $(CH_3)_2NH$, as expressed by eq. 5-2. The equilibrium constant for eq. 5-2 was

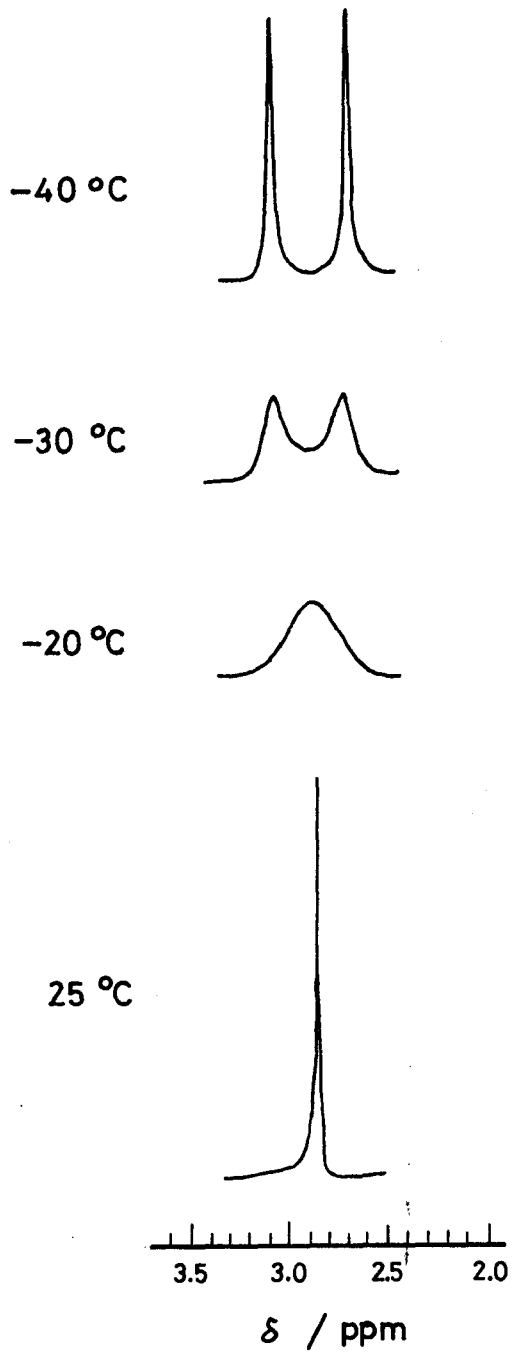

Figure 5-3. Temperature dependence of the methyl proton signals of $[Ru(bpy)_2(CO)C(O)N(CH_3)_2]^+$ in CD_3CN.

$$[Ru(bpy)_2(CO)_2]^{2+} + 2(CH_3)_2NH \rightleftharpoons [Ru(bpy)_2(CO)C(O)N(CH_3)_2]^{+} + (CH_3)_2NH_2^{+} \quad (5\text{-}2)$$

determined as 1.67×10^7 mol^{-2} dm^6 at 25°C from the change of electronic absorption spectra of $[Ru(bpy)_2(CO)_2]^{2+}$ in the presence of various amounts of $(CH_3)_2NH$ in acetonitrile.

Generation of DMF and mechanisms of the electrochemical CO_2 Reduction. The controlled potential electrolysis was performed on an Hg working electrode at -1.30 V vs. SCE for a CO_2-saturated acetonitrile solution containing $[Ru(bpy)_2(CO)_2]^{2+}$, $Bu^n{}_4NClO_4$, $(CH_3)_2NH$, $(CH_3)_2NH \cdot HCl$ and Na_2SO_4 as a catalyst, an electrolyte, a substrate, a proton source, and dehydration chemicals, respectively. As the result, two-electron reductions of CO_2 take place to produce not only $HCOO^-$, CO, and H_2 but also DMF (eqs. 5-3 - 5-6). The amounts of these products increase

$$CO_2 + H^+ + 2e^- \longrightarrow HCOO^- \quad (5\text{-}3)$$

$$CO_2 + 2H^+ + 2e^- \longrightarrow CO + H_2O \quad (5\text{-}4)$$

$$2H^+ + 2e^- \longrightarrow H_2 \quad (5\text{-}5)$$

$$CO_2 + (CH_3)_2NH + 2H^+ + 2e^- \longrightarrow HC(=O)N(CH_3)_2 + H_2O \quad (5\text{-}6)$$

linearly with increasing the electricity consumed in the reduction, and the turnover number for the formation of DMF is more than 10 (based on the amount of $[Ru(bpy)_2(CO)_2]^{2+}$) at the consumption of 75 coulombs, as depicted in Figure 5-4. The current efficiency for the formation of $HCOO^-$, CO, H_2, and DMF were 75.7, 1.0, 0.7, and 21.4%, respectively, suggesting that any reactions other than eqs. 5-3 - 5-6 hardly take place. In the absence of Na_2SO_4, the current efficiency for the formation of DMF gradually decreased with the progress of the reduction, since the adduct formation between $(CH_3)_2NH$ and $[Ru(bpy)_2(CO)_2]^{2+}$ may strongly be hindered by H_2O formed in the reaction of eqs. 5-4 and 5-6.

Scheme 5-I shows a possible catalytic cycle for the present reaction. As described in the previous chapters, $[Ru(bpy)_2(CO)_2]^{2+}$ undergoes a simultaneous two electron reduction to give $[Ru(bpy)_2(CO)]^0$ with liberating a single CO molecule in the absence of $(CH_3)_2NH$. The penta-coordinated Ru(0) complex thus formed reacts with CO_2 to yield $[Ru(bpy)_2(CO)(COO^-)]^+$, which exists as an equilibrium mixture with $[Ru(bpy)_2(CO)C(O)OH]^+$ and $[Ru(bpy)_2(CO)_2]^{2+}$; the amount of each species depends on the proton concentration in the reaction mixture, and the latter two are reduced with two electrons to produce $HCOO^-$ and CO, respectively. The acidity of $(CH_3)_2NH\cdot HCl$ used as a proton source in the present study is so low that the conversion from $[Ru(bpy)_2(CO)C(O)N(CH_3)_2]^+$ to $[Ru(bpy)_2(CO)_2]^{2+}$ hardly occurrs. Thus, the formation of $HCOO^-$ may be predominant. In the presence

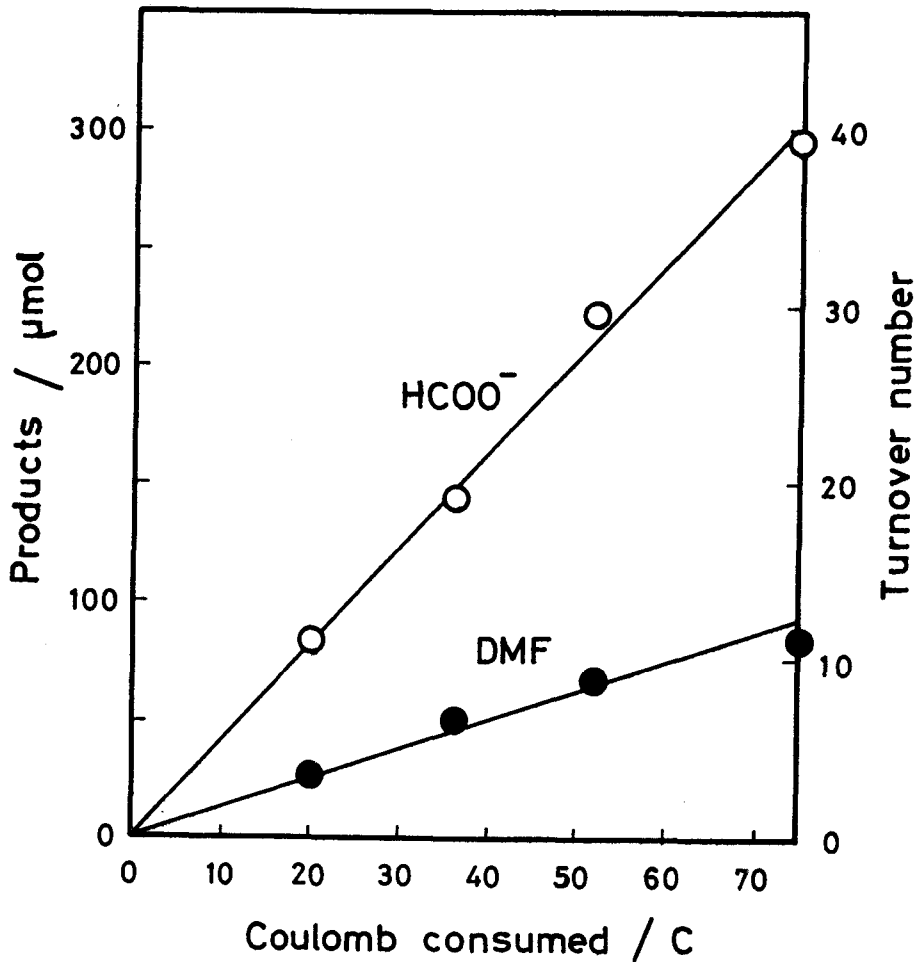

Figure 5-4. Amounts of the products in the electrolysis (-1.30 V vs. SCE) of a CO_2-saturated acetonitrile solution containing $[Ru(bpy)_2(CO)_2](PF_6)_2$, $NBu^n_4ClO_4$, $(CH_3)_2NH$, $(CH_3)_2NH \cdot HCl$ and Na_2SO_4 at 30°C.

Scheme 5-I

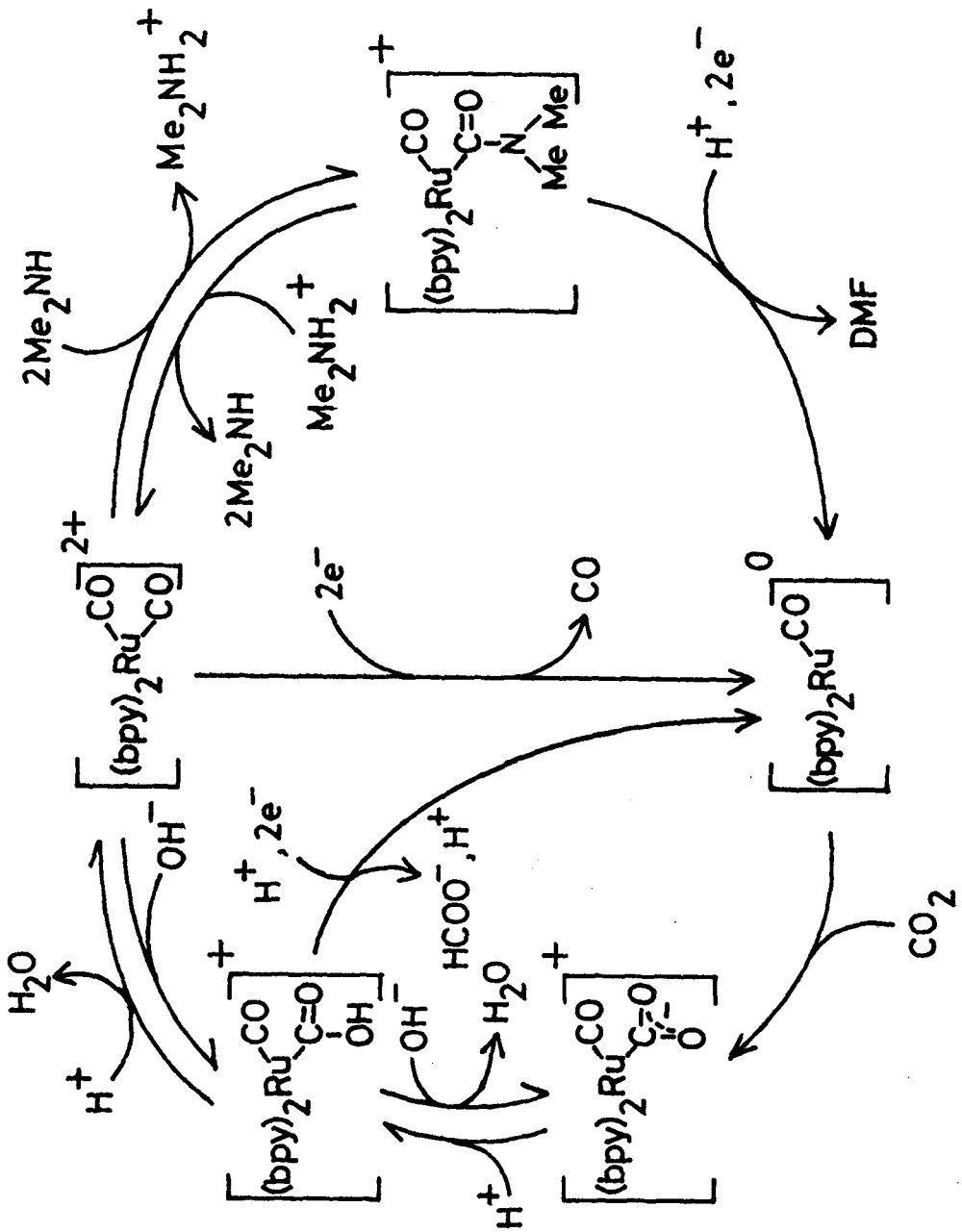
2Me2NH
Me2NH2+
2Me2NH
Me2NH2+
(bpy)2Ru(CO)(CO)2+
(bpy)2Ru(CO)(C=O)(N(Me)Me)+
H+, 2e−
DMF
2e−
CO
(bpy)2Ru(CO)0
OH−
H+, 2e−
HCOO−, H+
CO2
H2O
H+
(bpy)2Ru(CO)(C=O)(OH)+
OH−
H2O
H+
(bpy)2Ru(CO)(C=O)(O−)+

of $(CH_3)_2NH$, $[Ru(bpy)_2(CO)_2]^{2+}$ may effectively react with the amine to produce $[Ru(bpy)_2(CO)C(O)N(CH_3)_2]^+$, which undergoes two-electron reduction to afford DMF with regenerating the penta-coordinated Ru(0) species $[Ru(bpy)_2(CO)]^0$. Possibility of the DMF formation in the thermal reaction between $HCOO^-$ (or CO) and $(CH_3)_2NH$ may be excluded by the fact that no DMF has been formed in the reaction of $(CH_3)_2NH$ with either HCOOH or CO in the presence of $[Ru(bpy)_2(CO)_2]^{2+}$ at 30°C.

5-4 References

1) (a) Torii, S.; Tanaka, H.; Hamatani, T.; Morisaki, K.; Jutand, A.; Peluger, F.; Fauvarque, J. F. Chem. Lett., **1986**, 169. (b) Becker, J. Y.; Vainas, B.; Eger, R.; Kaufman, L. J. Chem. Soc., Chem. Commun. **1985**, 1471. (c) Tezuka, M.; Yajima, T.; Tsuchiya, A.; Matsumoto, Y.; Uchida, Y.; Hidai, M. J. Am. Chem. Soc. **1982**, 104, 6834. (d) Willner, I.; Mandler, D.; Riklin, A. J. Chem. Soc., Chem. Commun. **1986**, 1022. (e) Sugimura, K.; Kuwabata, S.; Yoneyama, H. J. Am. Chem. Soc., **1989**, 111, 2361. (f) Ikeda, Y.; Manda, E. Bull. Chem. Soc., JPN., **1985**, 58, 1723. (g) Ikeda, Y.; Manda, E. Chem. Lett., **1984**, 453. (h) Silnestri, G.; Gambino, S. Filarda, G. Tetrahedron Lett. **1986**, 27, 3429. (i) Silnestri, G.; Gambino, S.; Filardo, G.; Greco, G.; Gulotta, A. Tetrahedron Lett. **1984**, 25, 4307. (j) Sock, O.; Trompel, M.; Perichon, J. Tetrahedron Lett., **1985**, 26, 1509. (k)

Bestmann, H. J.; Denzel, T.; Salbaum, H. Tetrahedron Lett., **1974**, 1275.

2) Sternberg, H. W.; Wender, I.; Friedel, R. A.; Orchin, M. J. Am. Chem. Soc., **1953**, 75, 3148.

3) (a) Angelici, R. J. Acc. Chem. Res., **1972**, 5, 335. (b) Angelici, R. J.; Blacik, L. J. Inorg. Chem., **1972**, 11, 1754.

4) Jetz, W.; Angelici, R. J. J. Am. Chem. Soc., **1972**, 94, 3799.

Chapter 6

Photochemical and Catalytic Reduction of CO_2 in the $[Ru(bpy)_2(CO)_2]^{2+}$ / $[Ru(bpy)_3]^{2+}$ / Triethanolamine / N,N-Dimethylformamide System

6-1 Introduction

Photochemical CO_2 fixation is especially of interest in connection with biological photosynthetic systems,[1] and is desired also in terms of construction of economically efficient and clean systems such as utilization of solar energy.[2-13] The photochemical CO_2 reductions reported so far are almost carried out in the system composed of photsensitizer/catalyst/electron donor, where $[Ru(bpy)_3]^{2+}$ is widely used as a photosensitizer.[2-7]

There have been three conflicting reports in those systems containing $[Ru(bpy)_3]^{2+}$; (i) the irradiation of light (λ > 320 nm) to a CO_2-saturated TEOA/DMF solution containing $[Ru(bpy)_3]^{2+}$ (6.0×10^{-5} mol dm^{-3}) and MV^{2+} has been reported to produce $HCOO^-$.[2] (ii) $HCOO^-$ has, however, been suggested to come from the decomposition of TEOA based on ^{13}C nmr investigations.[14] On the other hand, (iii) Lehn et al. has demonstrated the selective formation of $H^{13}COO^-$ in similar photochemical (λ > 400 nm) $^{13}CO_2$ reductions using a very high concentration of $[Ru(bpy)_3]^{2+}$ (1.1×10^{-2} mol dm^{-3}) in TEOA/DMF even in the absence of MV^{2+}.[3] Such a

conflict may be solved by consideration that the actual catalyst in the CO_2 reduction may be neither $[Ru(bpy)_3]^{2+}$ nor MV^{2+} but a ruthenium bis(bipyridine) complex resulting from dissociation of a bpy ligand of $[Ru(bpy)_3]^{2+}$. However, the photochemical CO_2 reductions catalyzed by ruthenium bis(bipyridine) complexes have never been investigated.

This chapter describes the details of the photochemical CO_2 reduction catalyzed by $[Ru(bpy)_2(CO)_2]^{2+}$ in the presence of $[Ru(bpy)_3]^{2+}$ as a photosensitizer and TEOA as an electron donor.

6-2 Experimental Section

Material. $[Ru(phen)_3](PF_6)_2$ was prepared according to the literature.[15] The preparation of $[Ru(bpy)_2(CO)_2](PF_6)_2$, $[Ru(bpy)_3]Cl_2 \cdot 6H_2O$, and $Ru(bpy)_2Cl_2 \cdot 2H_2O$ were described in the previous chapters. N,N-dimethylformamide (DMF) was purified by azeotropic distillation with benzene, followed by distillation under reduced pressures, and stored under an N_2 atmosphere. Triethanolamine (TEOA), d^7-DMF, and $Na_2{}^{13}CO_3$ were purchased from Wako Pure Chemicals and used without further purification. Potassium ferrioxalate[16] used as an actinometer was purified by recrystallization from hot water.

Photochemical CO_2 Reduction. A TEOA/DMF (1:4 v/v; 5 cm^3) mixture containing fixed amounts of $[Ru(bpy)_3]Cl_2 \cdot 6H_2O$ and [Ru-

$(bpy)_2(CO)_2](PF_6)_2$ was bubbled with CO_2 through a septum cap attached to the top of a pyrex tube (32 cm^3) with teflon tube for 30 min. The photochemical reduction of CO_2 thus saturated in the solution was initiated by irradiating light with a 300 W Hg lamp through a cut-off chemical filter (1 cm) prepared 0.50 mol dm^{-3} of $CuSO_4$ ($\lambda > 320$ nm). After the lapse of a fixed time, 0.1 cm^3 portions of gas and the solution were sampled from the gaseous and liquid phases, respectively, in the flask through the septum cap with syringe techniques. Quantitative analysis of the gas was performed on a Shimazu gas chromatograph GC-3BT with a 2 m column filled with Molecular Sieve 13X at 343 K using He (40 cm^3 min^{-1}) as a carrier gas. $HCOO^-$ formed in the solution was determined with a Shimazu Isotachophoretic Analyzer IP-2A using a mixture of β-alanine (0.02 mol dm^{-3}) and HCl (0.01 mol dm^{-3}) in an aqueous Triton X-100 (0.2 vol%) solution, and caproic acid (0.01 mol dm^{-3}) in H_2O as leading and terminal electrolytes, respectively.

^{13}C nmr experiments were perfomed in a ^{7}d-DMF/DMF/TEOA (5:3:2 v/v, 1.0 cm^3) solution containing an equal amount (5.0×10^{-4} mol dm^{-3}) of $[Ru(bpy)_3]Cl_2 \cdot 6H_2O$ and $[Ru(bpy)_2(CO)_2](PF_6)_2$ in an nmr tube (i.d. = 1.0 cm). The tube was throughly flushed with He with teflon tube to remove air, and then $^{13}CO_2$ prepared by addition of H_2SO_4 (0.10 N) to an aqueous solution of 99%-$Na_2{}^{13}CO_3$ (1.0 g) was bubbled into the solution through a glass tube packed with $CaCl_2$. After photoirradiation for 20 h, the ^{13}C nmr spectra of the solution were measured at 15.3 MHz using the pulse fourier

technique with a JEOL EX-60 spectrometer against TMS as the internal standard.

Quantum Yield Determination. Quantum yields of the photochemical CO_2 reduction were determined in a square quartz cuvette (1.0 cm). After CO_2 was bubbled into the quartz cuvette containing the test solution (2.0 cm^3) with Teflon tube for 30 min, the solution was photoirradiated with a 300 W Xenon lamp (Ushio Model U1-501) through a Toshiba glass filter Y-43 transmitting light of $\lambda > 400$ nm for 5, 10, and 15 min. The rate of the photochemical CO_2 reduction was determined by the analysis of the reduction products in the gaseous (CO) and liquid phases ($HCOO^-$). Potassium ferrioxalate was used as a standard actinometer for the quantum yield determinations on the photochemical CO_2 reductions. Calculations of the quantum yield were performed according to the literature.[17]

6-3 Results and Discussion

Photochemical CO_2 reduction catalyzed by $[Ru(bpy)_2(CO)_2]^{2+}$ in the presence of $[Ru(bpy)_3]^{2+}$ in TEOA/DMF. An irradiation of light ($\lambda > 400$ nm) to a CO_2-saturated TEOA/DMF (1:4 v/v) solution containing $[Ru(bpy)_3]^{2+}$ (1.1×10^{-2} mol dm^{-3}) has produced 997 μmol of $HCOO^-$ for 20 h, while the photochemical CO_2 reduction using a low concentration of $[Ru(bpy)_3]^{2+}$ (5.0×10^{-4} mol dm^{-3})

afforded only 7 μmol of $HCOO^-$ in the same solvent (entry 1 in Table 6-I). The addition of $[Ru(bpy)_2(CO)_2]^{2+}$ to the low concentration solution of $[Ru(bpy)_3]^{2+}$ brings about a drastic change of the formation of $HCOO^-$; the amount of $HCOO^-$ increases with increasing the concentration of $[Ru(bpy)_2(CO)_2]^{2+}$ (entry 2 - 6 in Table 6-I), and attains the maximum value 394 μmol when the concentration of $[Ru(bpy)_2(CO)_2]^{2+}$ is the same as that of $[Ru(bpy)_3]^{2+}$ (5.0×10^{-4} mol dm^{-3}) (entry 5 in Table 6-I). A further increase of the $[Ru(bpy)_2(CO)_2]^{2+}$ concentration in the solution, however, results in a gradual decrease of the amount of $HCOO^-$ (entry 7 and 8 in Table 6-I). In addition, no photochemical CO_2 reduction with $[Ru(bpy)_2(CO)_2]^{2+}$ takes place in the absence of $[Ru(bpy)_3]^{2+}$ (entry 9 in Table 6-I). These results reveal that both $[Ru(bpy)_3]^{2+}$ and $[Ru(bpy)_2(CO)_2]^{2+}$ are essential components to proceed an effective photochemical CO_2 reduction. Similar photochemical CO_2 reductions take place also in a TEOA/CH_3CN (1:4 v/v) solution, though the amount of $HCOO^-$ formed is low compared with that in TEOA/DMF (entry 10 - 12 in Table 6-I).

The photochemical $^{13}CO_2$ reduction was carried out also in a $^{13}CO_2$-saturated d^7-DMF/DMF/TEOA (5:3:2 v/v) solution containing an equal amount of $[Ru(bpy)_2(CO)_2]^{2+}$ and $[Ru(bpy)_3]^{2+}$ (5.0×10^{-4} mol dm^{-3}). The ^{13}C nmr specrum of the reaction mixture obtained after irradiation of light ($\lambda > 320$ nm) for 20 h clearly indicats the formation of $H^{13}COO^-$ (δ 168.1 ppm) together with hydroxyacetaldehyde (δ 93.0 ppm)[3] and diethanolamine[18] as

Table 6-I. Photochemical CO_2 reductions in CO_2-saturated TEOA/DMF (1:4 v/v, 5 cm^3) containing $[Ru(bpy)_3]^{2+}$ and $[Ru(bpy)_2(CO)_2]^{2+}$ under irradiation of light ($\lambda > 320$ nm)[a] for 20 h

Entry	Concentration / mol dm^{-3}		$HCOO^-$ / μmol
	$[Ru(bpy)_3]^{2+}$	$[Ru(bpy)_2(CO)_2]^{2+}$	
1	5.0×10^{-4}	0	7
2	5.0×10^{-4}	1.0×10^{-5}	186
3	5.0×10^{-4}	5.0×10^{-5}	258
4	5.0×10^{-4}	1.0×10^{-4}	315
5	5.0×10^{-4}	5.0×10^{-4}	394
6	5.0×10^{-4}	1.0×10^{-3}	324
7	5.0×10^{-4}	1.5×10^{-3}	265
8	5.0×10^{-4}	2.0×10^{-3}	265
9	0	5.0×10^{-4}	0
10[b]	5.0×10^{-4}	0	1
11[b]	5.0×10^{-4}	5.0×10^{-4}	93
12[b]	0	5.0×10^{-4}	0

[a] 300 W-Hg lamp. [b] In TEOA/CH_3CN (1:4 v/v).

decomposition products of TEOA, as shown in Figure 6-1. The amount of $H^{13}COO^-$ determined by the signal intensity at δ 168.1 was consistent with that determined by an isotachophoretic analyzer. Thus, the $[Ru(bpy)_2(CO)_2]^{2+}/[Ru(bpy)_3]^{2+}$/TEOA system effectively reduces CO_2 to produce selectively $HCOO^-$ under irradiation of light in DMF. Plots of the amount of $HCOO^-$ formed against time under the optimum conditions in the present study (entry 5 in Table 6-I) displays a gradual deviation from a linear relation, as shown in Figure 6-2, which suggests that the system slowly loses the catalytic activity for the photochemical CO_2 reduction. This is compatible with the formation of a black precipitate during the photochemical CO_2 reduction. The formation of such a black precipitate was observed also when the photochemical CO_2 reduction was conducted with the mole ratio of $[Ru(bpy)_2(CO)_2]^{2+}/[Ru(bpy)_3]^{2+}$ being larger than 1. Thus, the decrease in the rate of the $HCOO^-$ formation with the lapse of time (Figure 6-2) may be caused not only by the gradual decomposition of the catalyst but also by the inner filter effect due to dispersion of the black solid in solutions.

The quantum yield for the photochemical CO_2 reduction under the concentration of $[Ru(bpy)_3]^{2+}$ (5.0×10^{-4} mol dm^{-3}) increases with increasing the concentration of $[Ru(bpy)_2(CO)_2]^{2+}$ up to 5.0×10^{-5} mol dm^{-3}, and reaches to the constant value 14%, as shown in Figure 6-3, which indicates that 10 mole % of $[Ru(bpy)_2(CO)_2]^{2+}$ per $[Ru(bpy)_3]^{2+}$ suffices in the amount for the catalytic CO_2 reduction. On the other hand, an equimolar mixture

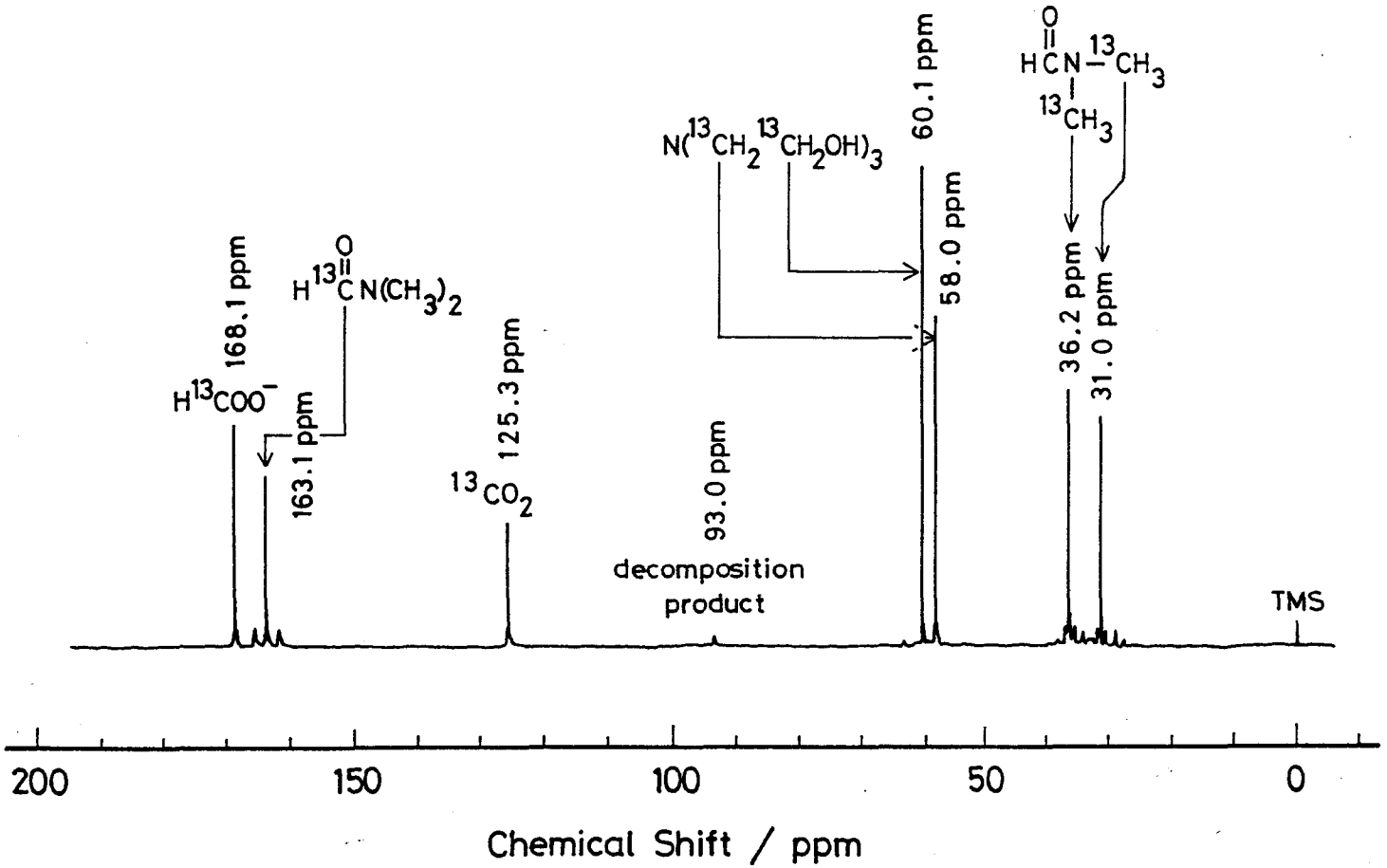

Figure 6-1. ^{13}C nmr spectrum of a $^{13}CO_2$ saturated d^7-DMF/DMF/TEOA (5:3:2 v/v) solution containing an equimolar mixture of $[Ru(bpy)_3]^{2+}$ and $[Ru(bpy)_2(CO)_2]^{2+}$ (5.0×10^{-4} mol dm^{-3}) after irradiation of light ($\lambda > 320$ nm) for 20 h.

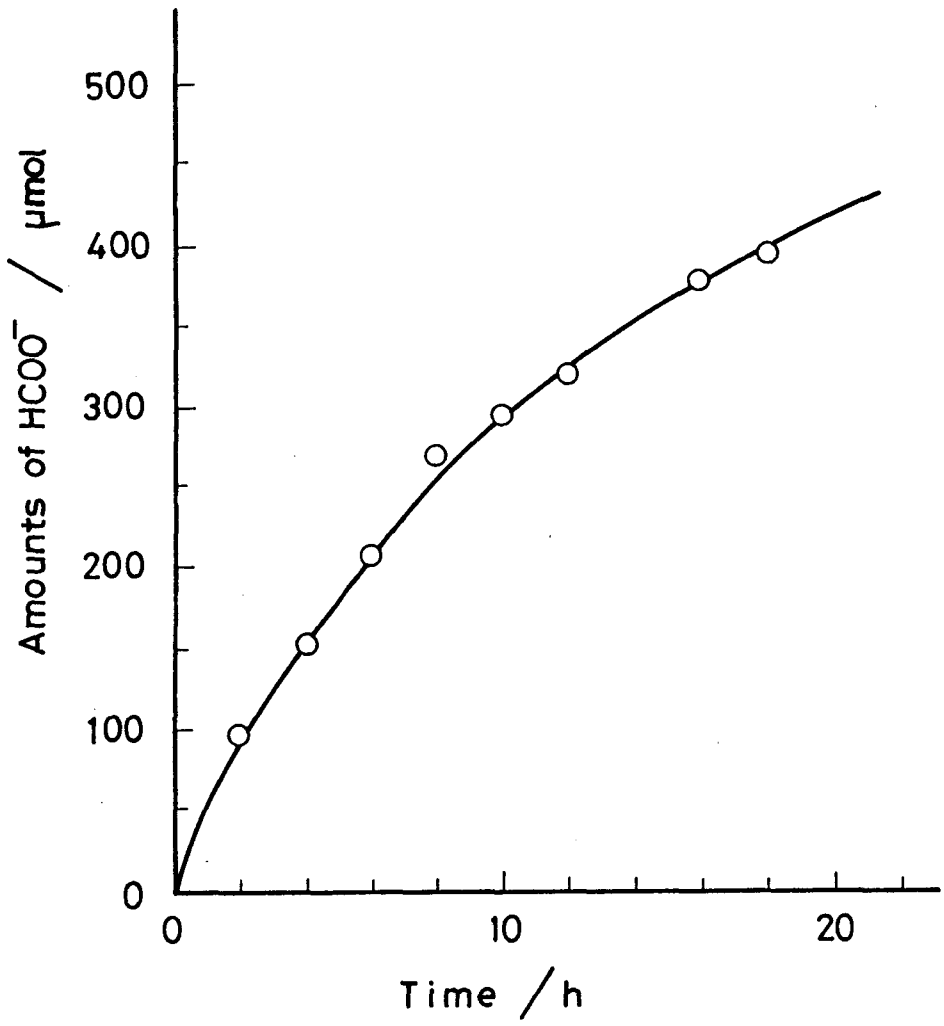

Figure 6-2. Plots of the amount of $HCOO^-$ formed vs. irradiation time in the photochemical CO_2 reduction in TEOA/DMF (1:4 v/v) containing an equmolar amount of $[Ru(bpy)_3]^{2+}$ and $[Ru(bpy)_2(CO)_2]^{2+}$ (5.0×10^{-4} mol dm^{-3}); $\lambda > 320$ nm.

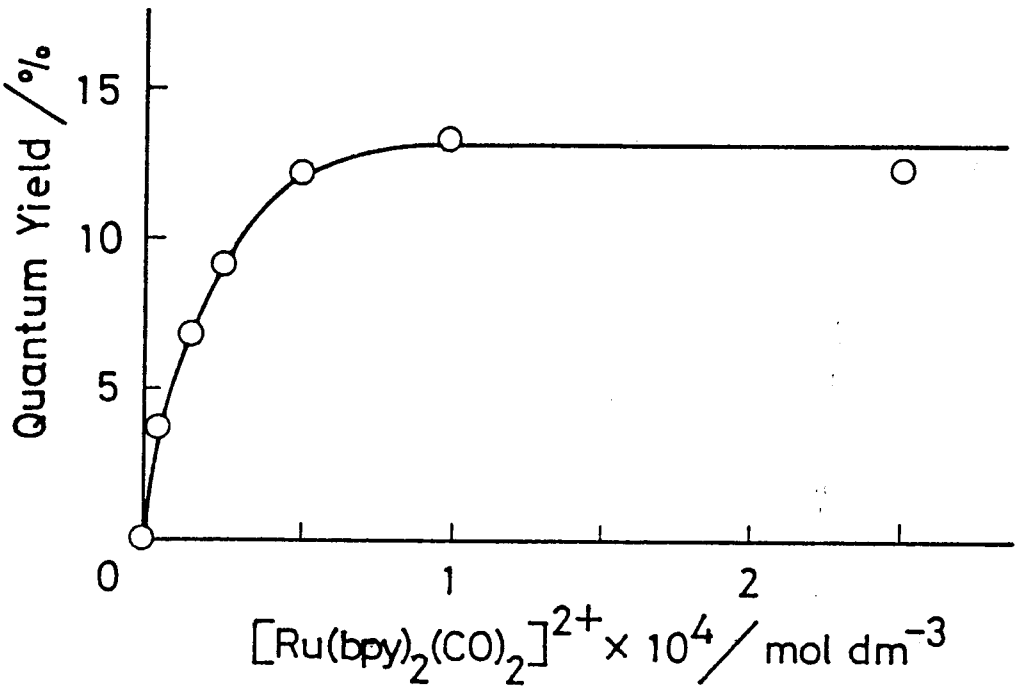

Figure 6-3. Quantum yields of the $HCOO^-$ formation at various concentrations of $[Ru(bpy)_2(CO)_2]^{2+}$; the concentration of $[Ru(bpy)_3]^{2+}$ 5.0×10^{-4} mol dm^{-3}.

of $[Ru(bpy)_2(CO)_2]^{2+}$ and $[Ru(bpy)_3]^{2+}$ gave the maximum yield for the formation of $HCOO^-$ (entry 5 in Table 6-I). This discrepancy may be associated with a gradual decrease of catalytic activities of the $[Ru(bpy)_2(CO)_2]^{2+}/[Ru(bpy)_3]^{2+}$/TEOA system with time (Figure 6-2). Such a slow degradation of the catalytic activity may be caused by the decomposition of $[Ru(bpy)_2(CO)_2]^{2+}$ rather than $[Ru(bpy)_3]^{2+}$ under prolonged irradiation of light, since the electrochemical reduction of $[Ru(bpy)_2(CO)_2]^{2+}$ at more negative potentials than -1.0 V vs. SCE in CO_2-saturated dry DMF also leads to the formation of a black precipitate, which is inactive toward both photochemical and electrochemical CO_2 reductions. The concentration of TEOA also largely influences on the quantum yield for the formation of $HCOO^-$; the value under constant concentrations of $[Ru(bpy)_2(CO)_2]^{2+}$ (1.0×10^{-4} mol dm^{-3}) and $[Ru(bpy)_3]^{2+}$ (5.0×10^{-4} mol dm^{-3}) increases with increasing the concentration of TEOA up to 2.0 mol dm^{-3} to attain 16%, as shown in Figure 6-4. The maximum quantum yield thus obtained under irradiation of light ($\lambda > 400$ nm) is almost same as that in the photochemical CO_2 reduction catalyzed by fac-Re(bpy)$(CO)_3X$ in TEOA/DMF,[9] where CO_2 is selectively reduced to CO in contrast to the present study.

Function of $[Ru(bpy)_2(CO)_2]^{2+}$ and $[Ru(bpy)_3]^{2+}$. As described in the previous sections, $[Ru(bpy)_2(CO)_2]^{2+}$ is an efficient catalyst for the electrochemical CO_2 reduction under the controlled potential electrolysis conditions at -1.30 V vs.

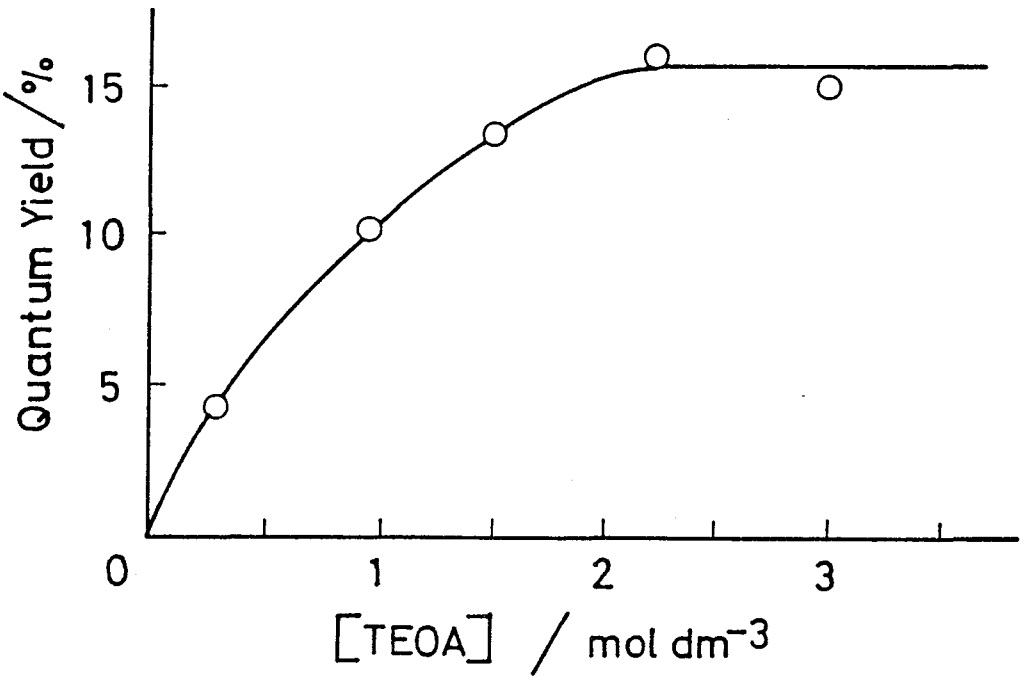

Figure 6-4. Quantum yields for the formation of $HCOO^-$ in the photoreduction of CO_2 in CO_2 saturated DMF containing $[Ru(bpy)_3]^{2+}$ (5.0×10^{-4} mol dm^{-3}) and $[Ru(bpy)_2(CO)_2]^{2+}$ (1.0×10^{-4} mol dm^{-3}) at various concentrations of TEOA.

SCE. In contrast to $Re(bpy)(CO)_3X$, however, $[Ru(bpy)_2(CO)_2]^{2+}$ has no ability of catalyzing the photochemical CO_2 reduction unless the presence of $[Ru(bpy)_3]^{2+}$ (entry 9 in Table 6-I). This may be due to the absence of any appreciable electronic absorption band in $[Ru(bpy)_2(CO)_2]^{2+}$ in the visible region (λ > 320 nm). In addition, $[Ru(bpy)_2(CO)_2]^{2+}$ may not be reduced by the luminescent state of $[Ru(bpy)_3]^{2+*}$, since the luminescence from $[Ru(bpy)_3]^{2+*}$ (λ_{max} 608 nm) has not been quenched at all by the present experimental concentrations of $[Ru(bpy)_2(CO)_2]^{2+}$ (the order of 10^{-4} mol dm^{-3}). This may be ascribed to the more negative reduction potentials of $[Ru(bpy)_2(CO)_2]^{2+}$ (-0.95 V vs. SCE) than the excited oxidation potential of $[Ru(bpy)_3]^{2+*}$ (-0.81 V vs. SCE).[19] On the other hand, the luminescent state of $[Ru(bpy)_3]^{2+*}$ is reductively quenched by TEOA to produce $[Ru(bpy)_3]^{+}$ and the $TEOA^{\dagger}$ radical cation with the quenching rate constant k_q = 1.7 x 10^5 mol^{-1} dm^3 s^{-1} in DMF (eq. 6-1).[4a] The oxidation

$$[Ru(bpy)_3]^{2+*} + TEOA \longrightarrow [Ru(bpy)_3]^{+} + TEOA^{\dagger} \quad (6\text{-}1)$$

potential of $[Ru(bpy)_3]^{+}$ is -1.33 V vs. SCE,[19] which is negative enough to reduce $[Ru(bpy)_2(CO)_2]^{2+}$ and close to the potential applied in the electrochemical CO_2 reduction catalyzed by $[Ru(bpy)_2(CO)_2]^{2+}$.

There has been a disagreement concerning the role of MV^{2+} as an electron relay in photochemical CO_2 reductions. The irradiation of light to CO_2-saturated TEOA/DMF (1:4 v/v)

containing a high concentration of $[Ru(bpy)_3]^{2+}$ (1.1×10^{-2} mol dm^{-3}) produced 997 μmol of $HCOO^-$ even in the absence of MV^{2+}, suggesting that MV^{2+} is not an essential component in the photochemical CO_2 reduction in DMF. On the other hand, similar photochemical CO_2 reductions using a low concentration of $[Ru(bpy)_3]^{2+}$ (5.0×10^{-4} mol dm^{-3}) yielded as low as 7 μmol of $HCOO^-$. Such a marked difference between the amounts of $HCOO^-$ formed in those reactions may be explained in terms of photo-assisted bipyridine (bpy) ligand dissociation from the coordinatively saturated complex $[Ru(bpy)_3]^{2+}$ affording a bis(bpy)ruthenium complex, which catalyzes the reduction of CO_2. In accordance with this, the photoirradiation ($\lambda > 400$ nm) to a CO_2-saturated TEOA/DMF (1:4 v/v) solution containing equimolar amounts of $[Ru(bpy)_3]^{2+}$ and $Ru(bpy)_2Cl_2$ (5.0×10^{-4} mol dm^{-3}) produced 193 μmol of $HCOO^-$ for 20 h. The minor activity of $Ru(bpy)_2Cl_2$ compared with $[Ru(bpy)_2(CO)_2]^{2+}$ as a catalyst for the reduction of CO_2 (entry 5 in Table 6-I) was observed also in the electrochemical CO_2 reduction catalyzed by those complexes in H_2O/DMF. This may be associated with the reduction potential of $Ru(bpy)_2Cl_2$ ($E_{1/2}$ = -1.61 V vs. SCE)[20] being fairly negative compared with that of $[Ru(bpy)_2(CO)_2]^{2+}$ (E_{red} = -0.95 V vs. SCE).

The preceding discussion suggests that the actual species for the reduction of CO_2 is generated by the photo-assisted ligand dissociation from $[Ru(bpy)_3]^{2+}$. In connection with this, $[Ru(phen)_3]^{2+}$ may be more suitable than $[Ru(bpy)_3]^{2+}$ as a photosensitizer. Thus, the photochemical CO_2 reduction in CO_2-

saturated TEOA/DMF (1:4 v/v) containing $[Ru(phen)_3]^{2+}$, in place of $[Ru(bpy)_3]^{2+}$, and $[Ru(bpy)_2(CO)_2]^{2+}$. The result is summarized in Table 6-II, which reveals the formation of a small amount of $HCOO^-$ (5 μmol) in the absence of $[Ru(bpy)_2(CO)_2]^{2+}$ (entry 1 in Table 6-II). Coexistence of $[Ru(phen)_3]^{2+}$ and $[Ru(bpy)_2(CO)_2]^{2+}$, however, results in a remarkable increase of the amount of $HCOO^-$ produced (entry 2 - 7 in Table 6-II). The dependence of the amount of $HCOO^-$ formed on the concentration of $[Ru(bpy)_2(CO)_2]^{2+}$ in the presence of a fixed concentration of $[Ru(phen)_3]^{2+}$ (5.0×10^{-4} mol dm^{-3}) is similar to that in the $[Ru(bpy)_2(CO)_2]^{2+}$/$[Ru(bpy)_3]^{2+}$ system (compare entry 2 - 8 in Table 6-I with entry 2 - 7 in Table 6-II). The weak catalytic activity of $[Ru(phen)_3]^{2+}$ used as a photosensitizer compared with $[Ru(bpy)_3]^{2+}$ may be due to no efficient formation of $[Ru(phen)_2(CO)_2]^{2+}$ by photo-assisted decomposition of $[Ru(phen)_3]^{2+}$. This is compatible with the catalytic activity of $[Ru(phen)_2(CO)_2]^{2+}$ toward the reduction of CO_2, as confirmed from the experiment that the irradiation of light to a CO_2-saturated TEOA/CH_3CN (1:4 v/v) solution containing $[Ru(phen)_2(CO)_2]^{2+}$ (1.0×10^{-4} mol dm^{-3}) and $[Ru(bpy)_3]^{2+}$ (5.0×10^{-4} mol dm^{-3}) produced 73 μmol of $HCOO^-$ for 20 h. Thus, $[Ru(bpy)_2(CO)_2]^{2+}$ functions as an actual catalyst and $[Ru(bpy)_3]^{2+}$ plays only a role of photosensitizer in the photochemical CO_2 reduction. The catalytic ability of the present system, therefore, can be evaluated in terms of a turnover number for the formation of $HCOO^-$, based on the amount of $[Ru(bpy)_2(CO)_2]^{2+}$.[21] The maximum value has attained 3580

Table 6-II. Photochemical CO_2 reductions in CO_2-saturated TEOA/DMF (1:4 v/v, 5 cm^3) containing $[Ru(phen)_3]^{2+}$ and $[Ru(bpy)_2(CO)_2]^{2+}$ under the irradiation of light (λ > 320 nm)[a] for 20 h

Entry	Concentration / mol dm^{-3}		$HCOO^-$ / μ mol
	$[Ru(phen)_3]^{2+}$	$[Ru(bpy)_2(CO)_2]^{2+}$	
1	5.0×10^{-4}	0	5
2	5.0×10^{-4}	2.5×10^{-4}	117
3	5.0×10^{-4}	5.0×10^{-4}	139
4	5.0×10^{-4}	7.5×10^{-4}	150
5	5.0×10^{-4}	1.0×10^{-3}	118
6	5.0×10^{-4}	1.5×10^{-3}	114
7	5.0×10^{-4}	2.0×10^{-3}	89

[a] 300 W-Hg lamp.

(entry 2 in Table 6-I). Even when the turnover number was calculated based on the total mole of $[Ru(bpy)_2(CO)_2]^{2+}$ and $[Ru(bpy)_3]^{2+}$, the value is 105 (entry 4 in Table 6-I), which is still fairly larger than the value (27) in the photochemical CO_2 reduction conducted in the presence of a high concentration of $[Ru(bpy)_3]^{2+}$, reported by Lehn et al.[3] The detail of mechanisms of the present photochemical CO_2 reductions will be described in the next chapter.

6-4 References

(1) Inoue, S.; Yamazaki, N. (Eds), "The organic and Bioorganic Chemistry of Carbon Dioxide"; Halstead Press: New York, **1982**; Friedli, H.; Lötscher, H.; Siegenthaler, U.;Stauffer, B. Nature **1986**, 324, 237.

(2) Kitamura, N.; Tazuke, S. Chem. Lett. **1983**, 1109.

(3) Hawecker, J.; Lehn, J.-M.; Ziessel, R. J. Chem. Soc., Chem. Commun. **1985**, 56.

(4) (a) Ziessel, R.; Hawecker, J.; Lehn, J.-M. Helv. Chim. Acta **1986**, 69, 1065. (b) Lehn, J. M.; Ziessel, R. Proc. Natl. Acad. Sci. USA **1982**, 79, 701.

(5) Grant, J. L.; Goswami, K.; Spreer, L. O.; Otvos, J. W.; Calvin, M. J. Chem. Soc., Dalton Trans. **1987**, 2105.

(6) Willner, I.; Mandler, D.; Riklin, A. J. Chem. Soc., Chem. Commun. **1986**, 1022.

(7) (a) Maidan, R.; Willner, I. J. Am. Chem. Soc. **1986**, 108,

8100. (b) Willner, I.; Maidam, R.; Mandler, D.; Dürr, H.; Dörr, G.; Zengerle, K. J. Am. Chem. Soc., **1987**, 109, 6080.

(8) (a) Mandler, D.; Willner, I. J. Am. Chem. Soc. **1987**, 109, 7884. (b) Willner, I.; Mandler, D. J. Am. Chem. Soc. **1989**, 111, 1330.

(9) (a) Kutal, C.; Corbin, A. J.; Ferraudi, G. Organometallics, **1987**, 6, 553. (b) Hawecher, J.; Lehn, J.-M.; Ziessel, R. Helv. Chim. Acta **1986**, 69, 1990. (c) Kutal, C.; Weber, M. A.; Ferraudi, G.; Geiger, D. Organometallics **1985**, 4, 2161. (d) Hawecker, J.; Lehn, J.-M.; Ziessel, R. J. Chem. Soc., Chem. Commun. **1983**, 536.

(10) Bradley, M. G.; Tysak, T.; Graves, D. J.; Valchopoulos, N. A. J. Chem. Soc., Chem. Commun. **1983**, 349.

(11) Parkinson, B.; Weaver, P. Nature **1984**, 309, 148.

(12) Ikeda, S.; Yoshida, M.; Ito, K. Bull. Chem. Soc. Jpn. **1985**, 58, 1353.

(13) (a) Sears, W. M.; Morrison, S. R. J. Phys. Chem. **1985**, 89, 3295. (b) Ito, K.; Ikeda, S.; Yoshida, M.; Ohta, S.; Iida, T. Bull. Chem. Soc. Jpn. **1984**, 57, 583. (c) Taniguchi, Y.; Yoneyama, H.; Tamura, H. Bull. Chem. Soc. Jpn. **1982**, 55, 2034. (d) Inoue, T; Fujishima, A.; Konishi, S.; Honda, K. Natura **1979**, 277, 637.

(14) Kase, H.; Iida, T.; Yamane, K.; Mitamura, T. Denki Kagaku **1986**, 54, 437.

(15) (a) Lin, C-T.; Böttcher, W.; Chou, M.; Creutz, C.; Sutin, N. J. Am. Chem. Soc. **1976**, 98, 6536. (b) Mercer, E. E.;

Buckley, R. R. Inorg. Chem. **1965**, 4, 1692.

(16) (a) Hatchard, C. G.; Parker, C. A. Proc. R. Soc. London, Ser. A **1956**, 235, 518. (b) Calvert, J. G.; Parker, J. N. "Photochemistry"; Wiley: New York, 1966; p 783.

(17) Fukuzumi, S.; Hironaka, K.; Tanaka, T. J. Am. Chem. Soc. **1983**, 105, 4722.

(18) The signals appears at the foot of the ^{13}C nmr signals of TEOA (δ 58.0 and 60.1 ppm).

(19) Kalyanasundaram, K. Coord. Chem. Rev. **1982**, 46, 159.

(20) Sullivan, B. P.; Conrad, D.; Meyer, T. J. Inorg. Chem. **1985**, 24, 3640.

(21) The turnover number for the formation of $HCOO^-$ based on $[Ru(bpy)_2(CO)_2]^{2+}$ was corrected by subtracting 7 μmol from the actual amount of $HCOO^-$ generated, since 7 μmol of $HCOO^-$ was formed even in the absence of $[Ru(bpy)_2(CO)_2]^{2+}$.

Chapter 7

Photochemical CO_2 Reduction with an NADH Model Compound, Catalyzed by Ruthenium Complexes

7-1 Introduction

All living things on earth depend for their existence on the photosynthesis and the CO_2 fixation using solar energy.[1] In the natural photosynthesis, nicotinamide adenine dinucleotide phosphate ($NADP^+$) is reduced by H_2O to afford NADPH and O_2, the former of which functions as an electron donor in the CO_2 fixation.[2] NAD(P)H is a coenzyme which acts as reductants in biological redox systems, and many investigations on the model reactions of NAD(P)H have been reported.[3] However, there is no report on the CO_2 fixation with NAD(P)H model compounds.

On the other hand, there have been several papers reporting that the photochemical CO_2 reduction catalyzed by ruthenium complexes yields carbon monoxide as a main product.[4] This chapter describes the photochemical CO_2 reduction with an NAD(P)H model, 1-benzyl-1,4-dihydronicotinamide (BNAH) as an electron donor, catalyzed by $[Ru(bpy)_2(CO)_2]^{2+}$.

7-2 Experimental Section

Material. BNAH prepared according to the literature[5] was purified by recrystallization from ethanol, and stored under N_2 in a refrigerator.

Photochemical CO_2 Reduction with BNAH. The manipulation for the CO_2 reduction was essentially the same as that described in Chapter 6; DMF or H_2O/DMF was used as a reaction solvent, and an aqueous $NaNO_2$ solution (0.50 mol dm^{-3}) was used as a cut-off chemical filter (1 cm; $\lambda > 400$ nm). A DMF or H_2O/DMF solution of ruthenium complexes was bubbled with CO_2 for 30 min, followed by the addition of BNAH. The resulting solution was bubbled with CO_2 for further 5 min. Quantum yields were determined by the method as described in Chapter 6.

Oxidation products of BNAH were determined by HPLC, ^1H nmr, and electronic spectra. HPLC was carried out with JASCO 880-PU equipped with a 20 cm column filled with JASCO Finepack SIL C18 using CH_3OH/H_2O (3:2 v/v) as an eluent, and monitored at 355 nm by JASCO 875-UV spectrophotometer. ^1H nmr spectra were recorded on a JEOL-PS-100 spectrometer. Electronic absorption spectra were measured with a Union SM-401 spectrophotometer.

Quenching experiment of the luminescence state of $[Ru(bpy)_3]^{2+*}$. The relative emission intensities at 610 nm of $[Ru(bpy)_3]^{2+*}$ were determined under irradiation of light at 550 nm to an N_2-saturated DMF solution of $[Ru(bpy)_3]Cl_2$ (2.5×10^{-4} mol dm^{-3}) in the presence of various amounts of BNAH as a

quencher with a Hitachi 650-10S Fluorescence Spectrophotometer. The Stern-Volmer relationship (eq. 7-1) was obtained between the

$$I_0/I = 1 + k_q\tau[Q] \qquad (7\text{-}1)$$

concentration of the quencher (Q) and the relative emission intensity (I_0/I), where I_0 and I represent the intensity at 610 nm in the absence (I_0) and the presence of a quencher (I), respectively. The quenching rate constant k_q ($= K_q\tau^{-1}$) was determined from the Stern-Volmer constant K_q and the emission lifetime τ ($[Ru(bpy)_3]^{2+*}$ 930 ns in DMF).[6]

7-3 Results and Discussion

Photochemical CO_2 Reduction by using BNAH as an Electron Donor. As mentioned in the preceeding chapter, triethanolamine is an efficient electron donor in the photochemical CO_2 reduction catalyzed by $[Ru(bpy)_2(CO)_2]^{2+}$. On the other hand, H_2O may largely influence on the photochemical CO_2 reduction; the catalytic system composed of $[Ru(bpy)_2(CO)_2]^{2+}$ (1.0×10^{-4} mol dm^{-3}) and $[Ru(bpy)_3]^{2+}$ (5.0×10^{-4} mol dm^{-3}) afforded $HCOO^-$ (315 μmol) in CO_2-saturated TEOA/DMF (1:4 v/v) for 20 h as described in Chapter 6, whereas the amount of $HCOO^-$ decreased (209 μmol) and no carbon monoxide generated in the CO_2 reduction conducted in H_2O/TEOA/DMF (1:2:7 v/v) otherwise the same conditions. The decrease in the amount of $HCOO^-$ produced in the

latter may arise from the decreasing electron donor ability of TEOA due to the protonation to TEOA (pK_a = 7.9) in protic conditions (eq. 7-2).[7] The electrochemical CO_2 reduction catalyzed by

$$(HOCH_2CH_2)_3N + H^+ \rightleftharpoons (HOCH_2CH_2)_3NH^+ \qquad (7\text{-}2)$$

$[Ru(bpy)_2(CO)_2]^{2+}$ produced CO and $HCOO^-$, whose relative amounts depend on the proton concentration in the medium used. For examining such an effect of the proton concentration on the photochemical CO_2 reduction, however, a strong basic electron donor such as TEOA may be improper. Photochemical CO_2 reduction using BNAH as an electron donor under protic conditions is, therefore, of much interest in the viewpoint that BNAH is a model compound of NAD(P)H, which functions as an electron donor in biological photosyntheses.

Irradiation of visible light ($\lambda > 400$ nm) to a CO_2-saturated dry DMF solution[8] containing $[Ru(bpy)_2(CO)_2]^{2+}$ (1.0×10^{-4} mol dm^{-3}), $[Ru(bpy)_3]^{2+}$ (5.0×10^{-4} mol dm^{-3}), and BNAH (0.10 mol dm^{-3}) produces trace amounts of $HCOO^-$ and CO, as shown by a broken line in Figure 7-1, where a black precipitate occurred. On the other hand, the amounts of those reaction products are largely increased when the redution is conducted in CO_2-saturated H_2O/DMF (1:9 v/v) (a solid line in Figure 7-1), and no appreciable black precipitate was formed in the reaction mixture. These results suggest that H_2O functions as a proton donor to depress the decomposition of $[Ru(bpy)_2(CO)_2]^{2+}$ in the photochemical CO_2

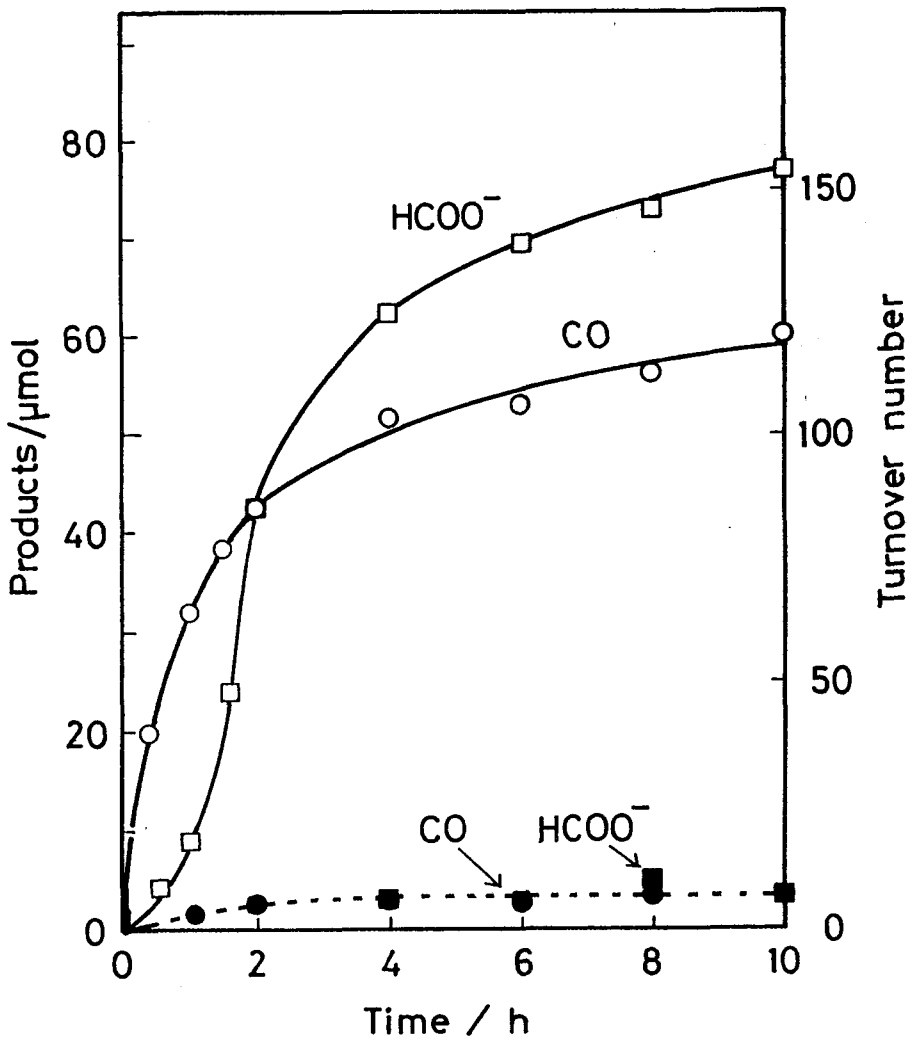

Figure 7-1. The photochemical CO_2 reduction with the $[Ru(bpy)_3]^{2+}$ (5.0×10^{-4} mol dm^{-3})/$[Ru(bpy)_2(CO)_2]^{2+}$ (1.0×10^{-4} mol dm^{-3})/BNAH (0.10 mol dm^{-3}) system in CO_2-saturated H_2O/DMF (1:9 v/v) (——) and in DMF (----); $\lambda > 400$ nm.

reduction.[9] It should be noted that $HCOO^-$ is selectively formed in the photochemical CO_2 reduction by using TEOA as an electron donor, as described in Chapter 6, while not only $HCOO^-$ but also CO are formed in the similar CO_2 reduction when BNAH is used as an electron donor in H_2O/DMF (1:9 v/v), where the quantum yields for the formation of CO and $HCOO^-$ in the initial stage were 14.8 and 2.7%, respectively. In the initial 2 h, CO is produced as the main product, whereas the rate of formation of CO is rapidly lowered after 2 h, and then $HCOO^-$ becomes the main product (Figure 7-1). Such alternation of the main product in the photochemical CO_2 reduction with the $[Ru(bpy)_2(CO)_2]^{2+}$/$[Ru(bpy)_3]^{2+}$ /BNAH system may not be due to decomposition of the catalytic system during the irradiation of light, since the catalytic system does not lose the ability of the photochemical CO_2 reduction in H_2O/DMF (3:7 v/v) even after 10 h, as depicted in Figure 7-2, which shows CO as the main product throughout the reaction. The initial rates of the formation of both CO and $HCOO^-$ in H_2O/DMF (3:7 v/v) are, however, slower than that in H_2O/DMF (1:9 v/v), and the quantum yields for the formation of CO and $HCOO^-$ were decreased down to 8.6 and 1.9%, respectively, in H_2O/DMF (3:7 v/v).

The function of BNAH in the photochemical CO_2 reduction is essentially the same as that of TEOA, since the former is not excited by irradiation of light ($\lambda > 400$ nm). The quenching constant (k_q) of the luminescence state of $[Ru(bpy)_3]^{2+}$ by BNAH (eq. 7-3) is 2.0×10^8 mol^{-1} dm^3 s^{-1} (in DMF), which is fairly

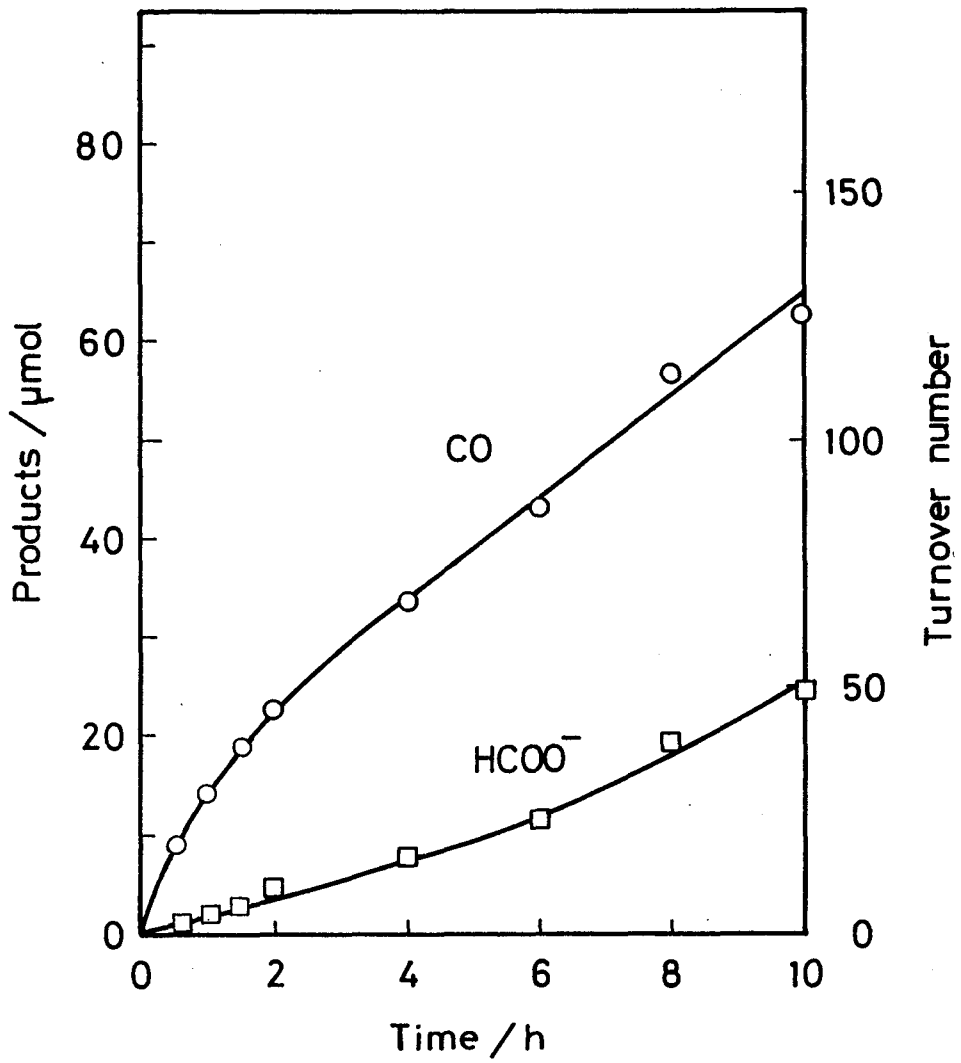

Figure 7-2. The photochemical CO_2 reduction with the $[Ru(bpy)_3]^{2+}$ (5.0×10^{-4} mol dm^{-3})/$[Ru(bpy)_2(CO)_2]^{2+}$ (1.0×10^{-4} mol dm^{-3})/BNAH (0.10 mol dm^{-3}) system in CO_2-saturated H_2O/DMF (3:7 v/v); $\lambda > 400$ nm.

$$[Ru(bpy)_3]^{2+*} + BNAH \longrightarrow [Ru(bpy)_3]^{+} + BNAH^{\ddagger} \quad (7\text{-}3)$$

larger than that by TEOA owing to the difference of the oxidation potential of BNAH (+0.57 V vs. SCE)[6] and TEOA (+0.82 V vs. SCE).[10] Thus, BNAH is superior to TEOA as an electron donor. In accordance with this, the quantum yields for the formation of $HCOO^-$ with the $[Ru(bpy)_2(CO)_2]^{2+}$ (1.0×10^{-4} mol dm^{-3})/$[Ru(bpy)_3]^{2+}$ (5.0×10^{-4} mol dm^{-3})/TEOA (0.10 mol dm^{-3}) system under irradiation of light ($\lambda > 400$ nm) were as low as 1 and 2% in CO_2-saturated DMF and H_2O/DMF (1:9 v/v), respectively. On the other hand, 4,4'- and 4,6'-linked dimer of BNAH are generated as oxidation products of BNAH in the course of the present photoreduction, suggesting that the dimerization reaction of $BNAH^{\ddagger}$ generated in the photoreaction is faster than the deprotonation reaction of $BNAH^{\ddagger}$, though $BNAH^{\ddagger}$ is a relatively strong acid ($pK_a = 3.5$). This is consistent with the fact that the present reduction requires any proton donors such as water. Thus, it may be concluded that BNAH functions as an electron donor but not a proton donor.

Mechanism of the photochemical CO_2 Reduction Catalyzed by $[Ru(bpy)_2(CO)_2]^{2+}$ in the Presence of Photosensitizer. It has been proposed that the photochemical CO_2 reduction in the presence of a high concentration of $[Ru(bpy)_3]^{2+}$ (1.1×10^{-2} mol dm^{-3}) in TEOA/DMF is initiated by ligand photodissociation of

$[Ru(bpy)_3]^+$, followed by protonation, affording a bis(bipyridine)ruthenium hydride species, which undergoes an insertion reaction by CO_2 to produce a formato complex, followed by the reduction to give $HCOO^-$. This mechanism may, however, be argued against the following points; i) no insertion reaction of CO_2 to the ruthenium hydride species has been observed, ii) $[Ru(bpy)_2(CO)H]^+$ is known to react with water to evolve H_2, though no appreciable H_2 evolution was detected in the present CO_2 reduction in H_2O/DMF, and iii) a formato complex such as $[Ru(bpy)_2(CO)OC(O)H]^+$ may be unreasonable as a precursor for the formation of CO. On the other hand, the variation of the main product in the photochemical CO_2 reduction upon changing not only the electron donor but also the content of H_2O in DMF strongly suggests that the mechanism of the photochemical CO_2 redution may be essentially the same as that of the electrochemical CO_2 reduction, in which CO and $HCOO^-$ are selectively produced by choosing the acidity of the proton source.

As described in Chapter 2, $[Ru(bpy)_2(CO)_2]^{2+}$ undergoes simultaneous irreversible two-electron reduction at -0.95 V vs. SCE to liberate a single CO molecule (eq. 7-4). On the other hand, the electrochemical reduction of $[Ru(bpy)_2(CO)_2]^{2+}$ at -1.10 V vs. SCE in CO_2-saturated dry DMF gives $[Ru(bpy)_2(CO)(COO^-)]^+$ (eq. 7-5), which exists as an equilibrium mixture with $[Ru(bpy)_2(CO)C(O)OH]^+$ (eq. 7-6) and $[Ru(bpy)_2(CO)_2]^{2+}$ (eq. 7-7) in aqueous

$$[Ru(bpy)_2(CO)_2]^{2+} + 2e^- \longrightarrow [Ru(bpy)_2(CO)]^0 + CO \quad (7\text{-}4)$$

$$[Ru(bpy)_2(CO)_2]^{2+} + CO_2 + 2e^- \longrightarrow [Ru(bpy)_2(CO)(COO^-)]^+ + CO \quad (7\text{-}5)$$

$$[Ru(bpy)_2(CO)(COO^-)]^+ + H^+ \rightleftharpoons [Ru(bpy)_2(CO)C(O)OH]^+ \quad (7\text{-}6)$$

$$[Ru(bpy)_2(CO)C(O)OH]^+ + H^+ \rightleftharpoons [Ru(bpy)_2(CO)_2]^{2+} + H_2O \quad (7\text{-}7)$$

solutions. In view of these facts, the most plausible mechanism of the present photochemical CO_2 reduction may be as follows; the luminescent state of $[Ru(bpy)_3]^{2+*}$ is reductively quenched by TEOA and BNAH to afford $[Ru(bpy)_3]^+$ together with $TEOA^{\ddagger}$ and $BNAH^{\ddagger}$, respectively, the former of which is decomposed to hydroxyacetaldehyde and diethylamine, and the latter dimerizes to give 4,4'- and 4,6'-linked dimers.[11] On the other hand, $[Ru(bpy)_2(CO)_2]^{2+}$ (E_{red} = -0.95 V vs. SCE) may be reduced by two moles of $[Ru(bpy)_3]^+$ ($E_{1/2}$ = -1.35 V vs. SCE) with regenerating two moles of $[Ru(bpy)_3]^{2+}$; the one-electron reduced species of $[Ru(bpy)_2(CO)_2]^{2+}$ may be unstable to liberate a single CO ligand, and $[Ru(bpy)_2(CO)]^+$ thus formed is further reduced by $[Ru(bpy)_3]^+$ to afford a penta-coordinate complex $[Ru(bpy)_2(CO)]^0$ (eq. 7-4), which reacts with CO_2 to afford a hexa-coordinate CO_2 adduct $[Ru(bpy)_2(CO)(COO^-)]^+$ (eq. 7-5). The equilibrium constants of eqs. 7-6 and 7-7, therefore, may explain the reaction products in the present study. Thus, the formation of CO in H_2O/DMF (1:9 and 3:7 v/v) may be due to the two electron reduction of $[Ru(bpy)_2$-

$(CO)_2]^{2+}$ (eq. 7-4) generated by the protonation to $[Ru(bpy)_2(CO)$-$C(O)OH]^+$ (eq. 7-7) in H_2O/DMF, and the selective formation of $HCOO^-$ in CO_2-saturated TEOA/DMF may be resulted from the irreversible two-electron reduction of either $[Ru(bpy)_2(CO)$-$(COO^-)]^+$ or $[Ru(bpy)_2(CO)C(O)OH]^+$ [12] with two moles of $[Ru$-$(bpy)_3]^+$. Such alternation of the main product from CO to $HCOO^-$ in the photochemical CO_2 reduction in H_2O/DMF (1:9 v/v) may be associated with the shift of the equilibrium of eq. 7-7 to the left owing to the consumption of protons accompanied with the reduction. In accordance with this, the electrochemical CO_2 reduction catalyzed by $[Ru(bpy)_2(CO)_2]^{2+}$ in H_2O/DMF (1:9 v/v) affords CO at pH 6.0, and a mixture of CO and $HCOO^-$ at pH 9.0 (Chapter 2). Furthermore, the selective formation of $HCOO^-$ has been achieved not only in the photochemical CO_2 reduction in TEOA/DMF but also in the electrochemical CO_2 reduction in dry-CH_3CN containing $(CH_3)_2NH_2^+$ or C_6H_5OH as a proton source, as described in Chapter 3.

7-4 References

(1) Inoue, S.; Yamazaki, N. (Eds), "The organic and Bioorganic Chemistry of Carbon Dioxide"; Halstead Press: New York, **1982**; Friedli, H.; Lötscher, H.; Siegenthaler, U.; Stauffer, B. Nature **1986**, 324, 237.

(2) Arnon, D. I. in "Bioorganic Chemistry IV" (van Tamelen, E. E., eds.); p. 4. Academic Press: New York, **1978**.

(3) Fukuzumi, S.; Hironaka, K.; Tanaka, T. J. Am. Chem. Soc. **1983**, 105, 4722, and the references cited therein.

(4) (a) Kitamura, N.; Tazuke, S. Chem. Lett. **1983**, 1109. (b) Hawecker, J.; Lehn, J.-M.; Ziessel, R. J. Chem. Soc., Chem. Commun. **1985**, 56. (c) Ziessel, R.; Hawecker, J.; Lehn, J.-M. Helv. Chim. Acta **1986**, 69, 1065. (d) Lehn, J. M.; Ziessel, R. Proc. Natl. Acad. Sci. USA **1982**, 79, 701. (e) Grant, J. L.; Goswami, K.; Spreer, L. O.; Otvos, J. W.; Calvin, M. J. Chem. Soc., Dalton Trans. **1987**, 2105. (f) Maidan, R.; Willner, I. J. Am. Chem. Soc. **1986**, 108, 8100. (g) Willner, I.; Mandler, D.; Riklin, A. J. Chem. Soc., Chem. Commun. **1986**, 1022.

(5) Anderson, A. G., Jr.; Berkelhammer, G. J. Am. Chem. Soc. **1958**, 80, 992.

(6) Pac, C.; Miyauchi, Y.; Ishitani, O.; Ihama, M.; Yasuda, M.; Sakurai, H. J. Org. Chem. **1984**, 49, 26.

(7) Charlot, G.; TrėMillon, B. "Chemical Reactions in Solvents and Melts" Pergamon Press: New York, 1969.

(8) The DMF solution of $[Ru(bpy)_3]^{2+}$ contains a small amount of H_2O arising from $[Ru(bpy)_3]Cl_2 \cdot 6H_2O$.

(9) The black precipitate has no catalytic activity for the reduction of CO_2, since the addition of water to the reaction mixture obtained after irradiation of visible light to the CO_2-saturated dry DMF containing $[Ru(bpy)_2(CO)_2]^{2+}$ (1.0×10^{-4} mol dm^{-3}), $[Ru(bpy)_3]^{2+}$ (5.0×10^{-4} mol dm^{-3}), and BNAH (0.10 mol dm^{-3}) for 5 h resulted

in no appreciable increase of either $HCOO^-$ or CO compared with the result shown by a dotted line in Figure 7-1.

(10) Kalyanasundaram, K.; Kiwi, J.; Grätzel, M. Helv. Chim. Acta. **1978**, 61, 2720.

(11) Ohnishi, Y.; Kitami, M. Bull. Chem. Soc. Jpn. **1979**, 52, 2674.

(12) The interconversion between $[Ru(bpy)_2(CO)C(O)OH]^+$ and $[Ru(bpy)_2(CO)(COO^-)]^+$ may be a diffusion controlled reaction in water.

Conclusion

The results obtained from the present investigation are summarized as follow.

Chapter 1: The water gas shift reaction (WGSR) catalyzed by bis(2,2'-bipyridine) carbonyl ruthenium(II) complexes under mild conditions (70 - 150°C; 3 - 20 kg cm^{-2} of CO) has been investigated. Turnover numbers for the H_2 formation of about 500 in 20 h have been obtained in an aqueous KOH solution containing $[Ru(bpy)_2(CO)Cl](PF_6)$ (bpy = 2,2'-bipyridine) as a catalyst precursor. The solvolysis of $[Ru(bpy)_2(CO)Cl]^+$ in an aqueous solution affords $[Ru(bpy)_2(CO)(H_2O)]^{2+}$, which exists as an equilibrium mixture with $[Ru(bpy)_2(CO)(OH)]^+$ in weak alkaline solutions. A water molecule ligated to $[Ru(bpy)_2(CO)(H_2O)]^{2+}$ is readily substituted by CO under CO pressures to produce $[Ru(bpy)_2(CO)_2]^{2+}$, which undergoes a nucleophilic attack of OH^- to afford $[Ru(bpy)_2(CO)C(O)OH]^+$. The hydroxycarbonyl complex not only exists as an equilibrium mixture with $[Ru(bpy)_2(CO)_2]^{2+}$ and $[Ru(bpy)_2(CO)(COO^-)]^+$ in alkaline media but also undergoes a decarboxylation reaction at elevated temperatures to give CO_2 and $[Ru(bpy)_2(CO)H]^+$, the latter of which further reacts with H_3O^+ to evolve H_2, regenerating $[Ru(bpy)_2(CO)(H_2O)]^{2+}$. All these species involved in the cycle of the WGS reaction catalyzed by $[Ru(bpy)_2(CO)Cl]^+$ have been isolated or characterized by spectrophotometry.

Chapter 2: The controlled potential electrolysis of CO_2-

saturated H_2O(pH 6.0)/DMF (9:1 v/v) solutions containing [Ru-(bpy)$_2$(CO)$_2$]$^{2+}$ or [Ru(bpy)$_2$(CO)Cl]$^+$ at -1.50 V vs. SCE catalytically produces CO together with H_2. The same electrolysis of a CO_2-saturated alkaline solution, H_2O (pH 9.5)/DMF (9:1 v/v), gives not only CO and H_2 but also $HCOO^-$. The effect of pH on the formation of CO and $HCOO^-$ in the reduction of CO_2 is explained in terms of the generation of an unstable penta-coordinated Ru(0) complex [Ru(bpy)$_2$(CO)]^0 as an intermediate in the irreversible two-electron reduction of [Ru(bpy)$_2$(CO)$_2$]$^{2+}$ or [Ru(bpy)$_2$(CO)Cl]$^+$; the Ru(0) intermediate is added with CO_2 to afford [Ru(bpy)$_2$(CO)-(COO^-)]$^+$, which reacts with protons to produce [Ru(bpy)$_2$(CO)-C(O)OH]$^+$ in weak alkaline conditions. The resulting [Ru(bpy)$_2$-(CO)C(O)OH]$^+$ is further converted to [Ru(bpy)$_2$(CO)$_2$]$^{2+}$ by dehydroxyration in acidic conditions. The [Ru(bpy)$_2$(CO)C(O)OH]$^+$ and [Ru(bpy)$_2$(CO)$_2$]$^{2+}$ complexes thus produced undergo two-electron reduction to afford $HCOO^-$ and CO, respectively, with regenerating [Ru(bpy)$_2$(CO)]^0.

Chapter 3: The selectivity for the formation of $HCOO^-$ in the electrochemical CO_2 reduction catalyzed by [Ru(bpy)$_2$(CO)$_2$]$^{2+}$ in CH_3CN is drastically dependent on the acidity of proton sources used. The selectivity increases with decreasing the acidity of proton sources, and almost selective formation of $HCOO^-$ is achieved by using $(CH_3)_2NH\cdot HCl$ or C_6H_5OH as a proton source in CH_3CN. The selective $HCOO^-$ formation may be explained by the fact that the conversion from [Ru(bpy)$_2$(CO)C(O)OH]$^+$ to [Ru(bpy)$_2$(CO)$_2$]$^{2+}$ does not occur with such proton sources of low

acidities.

Chapter 4: $[RuL_1L_2(CO)_2]^{2+}$ and $RuL_3(CO)_2Cl_2$ (L_1, L_2 = 2,2'-bipyridine (bpy), 4,4'-dimethyl-2,2'-bipyridine (dmbpy), and 1,10-phenanthroline (phen); L_3 = bpy and dmbpy) were synthesized, and the catalytic activity and the product distribution in the electrochemical CO_2 reductions were examined. The equilibria among $[RuL_1L_2(CO)_2]^{2+}$, $[RuL_1L_2(CO)C(O)OH]^{+}$ and $[RuL_1L_2(CO)(COO^-)]^{+}$ are shifted to the former with substitution of a dmbpy ligand to bpy of the catalyst, and the CO generation in the electrochemical CO_2 reductions becomes more predominant. This may be due to a donor property of dmbpy stronger than the bpy ligand. $[Ru(phen)_2(CO)_2]^{2+}$ exhibits a weak catalytic activity compared with $[Ru(bpy)_2(CO)_2]^{2+}$ though these complexes were almost same in the electrochemical properties.

Chapter 5: Electrochemical CO_2 reduction catalyzed by $[Ru(bpy)_2(CO)_2]^{2+}$ in the presence both of $(CH_3)_2NH$ and of $(CH_3)_2NH\cdot HCl$ in anhydrous CH_3CN catalytically produces $HCOO^-$ and N,N-dimethylformamide (DMF) with current efficiency 75.7 and 21.4%, respectively. The formation of the carbamoyl complex, $[Ru(bpy)_2(CO)C(O)N(CH_3)_2]^{+}$, as an intermediate for the DMF generation was confirmed by FT-IR and ^1H nmr spectra.

Chapter 6: A catalytic system composed of $[Ru(bpy)_2(CO)_2]^{2+}$ /$[Ru(bpy)_3]^{2+}$ or $[Ru(phen)_3]^{2+}$/triethanolamine (TEOA) selectively produces $HCOO^-$ from CO_2-saturated N,N-dimethylformamide (DMF) and CH_3CN under irradiation of light ($\lambda > 320$ or 400 nm), where $[Ru(bpy)_2(CO)_2]^{2+}$, $[Ru(bpy)_3]^{2+}$ or $[Ru(phen)_3]^{2+}$, and TEOA function

as a catalyst, a photosensitizer, and an electron donor, respectively. The maximum quantum yield for the formation of $HCOO^-$ attains 16% in the system composed of $[Ru(bpy)_2(CO)_2]^{2+}$ (1.0×10^{-4} mol dm^{-3}), $[Ru(bpy)_3]^{2+}$ (5.0×10^{-4} mol dm^{-3}) and TEOA (2.0 mol dm^{-3}).

Chapter 7: The photochemical CO_2 reduction conducted in H_2O/DMF (1:9 and 3:7 v/v) using 1-benzyl-1,4-dihydronicotinamide (BNAH) as an electron donor in place of TEOA affords CO as a main product together with $HCOO^-$. Quantum yields for the formation of CO and $HCOO^-$ achieve 14.8 and 2.7%, respectively, in H_2O/DMF (1:9 v/v). The predominance of CO to $HCOO^-$ formed in H_2O/DMF (3:7 v/v) is higher than that in H_2O/DMF (1:9 v/v). Not only the alternation of the main product from $HCOO^-$ to CO upon using BNAH as an electron donor in place of TEOA but also the predominant formation of CO to $HCOO^-$ with increasing the H_2O content in DMF may be explained in terms of the acid-base equilibria among $[Ru(bpy)_2(CO)_2]^{2+}$, $[Ru(bpy)_2(CO)C(O)OH]^+$, and $[Ru(bpy)_2(CO)(COO^-)]^+$, which may participate as actual catalysts in the catalytic cycle of the photochemical CO_2 reduction. The present reaction system is the first example for the CO_2 reduction with a model compound of NAD(P)H which is an electron donor in the photosysnthetic systems.

Acknowledgments

The author would like to express his sincerest gratitude to Professor Toshio Tanaka for his kind guidance and hearty encouragement throughout this work. The author would like to thank Professor Katsutoshi Ohkubo for his helpful advice and warm-hearted encouragement. The author is also deeply grateful to Professor Hiroshi Yoneyama, Professor Yasuhiko Shirota, and Professor Masakatsu Nomura for their helpful suggestions.

The author wishes to thank Dr. Koji Tanaka for his continuous advice and valuable discussions. Grateful acknowledges are given also to Associate Professor Gen-etsu Matsubayashi and Dr. Shun-ichi Fukuzumi in Osaka University, and Associate Professor Shigeyoshi Sakaki in Kumamoto university for their helpful suggestions.

Grateful acknowledgments are made to Mr. Hiroaki Tanaka, Mr. Tohru Terada, and Mr. Katsuyuki Fujiki for their helpful collaboration in the course of experiments. Furthermore, the author wishes to thank all members of the Tanaka Laboratory for their occasional discussions, helpful assistances, and friendships.

Finally, the author acknowledges heartwarming encouragement and assistance of his parents Shirou and Tamiko.